



UNIVERSITY OF CAPE TOWN
IYUNIVESITHI YASEKAPA • UNIVERSITEIT VAN KAAPSTAD

Antarctic Sea Ice phytoplankton growth rates and survival mechanisms

Author:

Lisa Kumadiro

Supervisor:

Dr. Tokoloho Rampai

Co-Supervisors:

Dr. Sarah Fawcett

Dr. Susanne Fietz

DISSERTATION SUBMITTED TO THE UNIVERSITY OF CAPE TOWN IN FULFILMENT OF
THE REQUIREMENT FOR THE DEGREE OF MASTER OF SCIENCE IN:

CHEMICAL ENGINEERING

December 2023

The copyright of this thesis vests in the author. No quotation from it or information derived from it is to be published without full acknowledgement of the source. The thesis is to be used for private study or non-commercial research purposes only.

Published by the University of Cape Town (UCT) in terms of the non-exclusive license granted to UCT by the author.

DECLARATION OF AUTHORSHIP

I, Lisa Tatenda Kumadiro, declare that this thesis titled, “Antarctic Sea Ice phytoplankton growth rates and survival mechanisms” and the work presented in it are my own. I confirm that my supervisors have seen my report and any concerns revealed by such have been resolved.

Signed:

Signed by candidate

Lisa Tatenda Kumadiro

30 December 2023

ABSTRACT

Phytoplankton play an important role in the Southern Ocean food web being the primary producers of food, particularly in winter, and partaking in the uptake of CO₂ from the atmosphere via photosynthesis. Despite being photosynthetic organisms, phytoplankton survive at the bottom of sea ice where there is very little irradiance for up to 6 months. Sea ice phytoplankton are understudied. This is mainly because in situ studies on sea ice are not only expensive but logistically difficult. Some researchers have elected to bring sea ice phytoplankton from the Southern Ocean to land-based facilities. This has seen some logistical difficulties as it meant either changing the habitat phytoplankton would have been for transportation, thus changing the species originally found in the Southern Ocean or transporting phytoplankton in ice cores and losing species due to brine drainage or osmotic stress from temperature changes in the core.

The objectives of this study were to optimize a previously designed hybrid tank for the purpose of obtaining and preserving phytoplankton species from the Marginal Ice Zone of the Southern Ocean to land-based facilities. The study also included design of an environmental chamber to be used for housing phytoplankton obtained during experimentation. Responses to temperature and irradiance variation on phytoplankton from the Marginal Ice Zone of the Southern Ocean were then evaluated using the designed environmental chamber.

The solid-liquid hybrid system known as the hybrid tank was successfully optimized by reducing the size of the tank, adding irradiation to the tank, and making improvements to the sampling protocol. The tank was used to obtain ice cores from the Southern Ocean to the University of Cape Town in winter 2022. Post the winter cruise one hybrid tank sample was melted, and microscopic analysis conducted on the sample. In comparison with transportation of phytoplankton in a solid core and in a liquid melt in the dark, the hybrid tank resulted in an increase in phytoplankton cell concentration. Furthermore, the optimized hybrid tank improved preservation of species transported when compared to the initial tank. A desktop environmental chamber made from Perspex and insulated with polystyrene was successfully designed. The environmental chamber offers temperature and irradiation control by making use of a cold plate attached to a chiller and an LED light. Experiments conducted on the diatom species revealed that all the sea ice species were shade adaptive being photo inhibited at irradiances beyond $42\mu\text{molm}^{-2}\text{s}^{-1}$ with the exception of *Navicula spp*, *Cylindrotheca closterium* and the unidentified pennates. The diatom species also preferred warmer environments i.e., 8°C to 5°C.

ACKNOWLEDGEMENTS

First and foremost, I want to extend my deepest gratitude to my primary supervisor, Dr. Tokoloho Rampai, for her invaluable support in opening the doors to this research field through her academic, administrative, and financial assistance. Her patience has been instrumental in my personal and professional growth. I also wish to thank my co-supervisors, Dr. S. Fietz and Dr. S. Fawcett, for their guidance and for addressing my numerous questions.

I am grateful for the support provided by the UCT Oceanography department. My thanks go to Dr. S. Fawcett for permitting me to use her labs, and to Hazel Little-Leighton and Raquel Flynn for their logistical assistance and readiness to help. I also appreciate the technical staff in the Chemical Engineering Electronics lab. Special thanks to Prof. Marcello Vichi for securing funding for my studies. To the captain and crew of the SA Agulhas II during the winter 2022 SCALE cruise, I am thankful for your efforts in helping us achieve our research objectives. The success of sea ice research would not be possible without your presence and courage.

I want to give a special shoutout to Felix Guni, Boitumelo Matlakala, and Tamuka Keche for their academic and emotional support. Our sessions of sharing and venting made us all wiser, and I value the friendship we have developed from colleagues to close friends.

Finally, I am deeply thankful to my mother, Josline Makope, my grandmother, Rosemary Makope (RIP), my grandfather, Joseph Makope, and the rest of my family for their unwavering support and encouraging words throughout this journey. And to my son, Ethan, this achievement is for us.

TO GOD BE THE GLORY

Table of Contents

Declaration of Authorship	i
Abstract	ii
Acknowledgements	iii
List of Figures	vii
List of Tables	xi
1 Introduction	1
1.1 Background	1
1.2 Scope and Limitations	2
2 Literature Review	4
2.1 Background to sea ice and the significance of sea ice on phytoplankton	4
2.2 Ecological importance of phytoplankton.....	7
2.2.1 Categorization of phytoplankton protist groups in sea ice.....	8
2.3 Parameters that affect phytoplankton growth: <i>in situ</i> investigations	9
2.3.1 Nutrient types and availability	9
2.3.2 Temperature, Salinity and irradiance variations	10
2.4 Lab based experiments on Parameters that affect phytoplankton growth	15
2.4.1 Transportation methods of sea ice algae	16
2.4.1.1 Transportation in solid sea ice form	16
2.4.1.2 Transportation in melted sea water	17
2.4.1.3 Hybrid system transportation	18
2.4.2 Simulation of in-situ environmental conditions for laboratory-based experiments on sea ice algae.....	19
2.5 Design considerations for an Environmental Chamber for laboratory-based experiments on sea ice algae.....	22
2.5.1 Material of Construction	22
2.5.2 Environmental controls and regulations	23
2.6 Rationale of study.....	25
3 Research Aims, Objectives and key questions	26
4 Optimization of the hybrid reactor system for transportation of sea ice algae	28
Existing hybrid system as per Hambrock, Rampai and Walker (2021) studies	28
4.1 Improvements to the Hybrid system design and sampling protocol.....	30
4.1.1 Improvement on the sampling protocols.....	31

4.1.2	Number and size of the hybrid tank.....	34
4.1.3	Irradiance input and measurement.....	37
4.2	Results of optimization	38
4.2.1	Quantification of phytoplankton.....	39
4.2.2	Microscopy findings	39
4.2.3	Is the hybrid tank optimized?	46
5	Environmental chamber design considerations.....	49
5.1	Materials and Methods	49
5.1.1	Aquariums within the EC.....	51
5.1.2	Cooling of the EC.....	51
5.1.3	Lighting within the EC	53
6	Phytoplankton Based Experiments using the designed EC	56
6.1	Experimental protocol and method of analysis.....	56
6.2	Experimental Results.....	61
6.2.1	Baseline experiments.....	61
6.2.2	Irradiance variation	65
6.2.3	Temperature variations	68
7	Overall Discussion	71
8	Conclusions and Recommendations	75
8.1	Conclusions.....	75
8.2	Recommendations	75
	References	78
	Appendices	89
	Appendix A: Optimization of the Hybrid Tank	89
A1:	Determination of daylight hours	89
A2:	Additional images and figures.....	91
	Appendix B: Environmental Chamber	94
B1:	Insulation calculations for the EC.....	94
B2:	Temperature and Light mapping within the EC.	96
B3:	Additional drawings and pictures of the EC.....	99
	Appendix C: Nutrient solution.....	102
	Appendix D: Phosphate measurement protocol	104
	Appendix E: Phytoplankton based experiments	107
Experiments	carried out at 8°C	107

Experiments carried out at 5°C111

LIST OF FIGURES

Figure 2-1: A) Consolidated Ice in the Southern Ocean at 59° 30 615S; 00° 24 997°W on the 22 nd of July 2022 B) Pancake ice in the Southern Ocean at 59° 09 320°S; 00°52 298°E on the 19 th of July 2022	5
Figure 2-2: Highly idealized illustration of a) pack ice and b) land-fast ice showing the location of algal communities (Thomas and Dieckmann, 2009).....	6
Figure 2-3: An illustration of the Antarctic food web (Learnz, 2021).....	7
Figure 2-4: Measured spectral irradiance at the Wandel Sea through the snow cover and under sea ice and the corresponding attenuation coefficients (K_d). (a) Profile of PAR (error bars are C.V); (b) profile of $K_{d,PAR}$; (c) $E(\lambda)$ at different depth in the snow cover (see figure legend); and (d) correspond $K_{d(\lambda)}$ (data represent lower depth). (e) $E(\lambda)$ under the sea ice (purple) and 0.35 m above in the snow (lowest good measure) and (f) correspond $K_{d(\lambda)}$. Surface PAR of $750\mu\text{mol photonsm}^{-2}\text{s}^{-1}$ (Hancke et al., 2018).	12
Figure 4-1: I Hybrid system assembly schematic as per A) initial design by Hambrock, Rampai and Walker (2021) and B) optimized hybrid system design	30
Figure 4-2: Sea ice conditions (A) on the 24 th of July 2022 59.16485S, 0.85777E (B) on the 22 nd of October 2019, brash ice showing algae (discoloration) floating in the Southern Ocean (Hambrock, Rampai and Walker, 2021)	33
Figure 4-3: Diatom concentration from extraction in the marginal sea-ice zone in the Southern Ocean to UCT labs using the different forms of transportation.	41
Figure 4-4: Unidentified diatoms all grouped unidentified pennates.....	42
Figure 4-4: Unidentified diatoms all grouped unidentified pennates.....	42
Figure 4-5: Dominant pennates: (A) <i>Cylindrotheca</i> (B) <i>Pseudo-nitzschia</i> (C) <i>Navicula</i> sp. (D) <i>Fragilariopsis kerguelensis</i> (E) <i>Striatella unipunctata</i>	42
Figure 4-5: Dominant pennates: (A) <i>Cylindrotheca</i> (B) <i>Pseudo Nitzschia</i> (C) <i>Navicula</i> sp. (D) <i>Fragilariopsis kerguelensis</i> (E) <i>Striatella unipunctata</i>	42
Figure 4-6: Centrics identified: (A) <i>Dactyliosolen</i> sp. (B) <i>Chaetoceros</i> sp. (C) <i>Thalassiosira</i> sp. (D) <i>Dactyliosolen</i> sp. (E) <i>Chaetoceros</i> sp. (F) <i>Eucampia antarctica</i> sp.	43
Figure 4-7: Empirically suggested logistic growth trend for cell growth in hybrid tanks during transportation.....	45
Figure 4-8: Taxonomic distributions illustrating fractional change of taxonomic groups through intra-sample comparisons of the fractions, for all modes of transportation.	46

Figure 4-9: Change in cell count in comparison to baseline species for the optimized hybrid tank	47
Figure 4-10: Change in cell count in comparison to baseline species for the initial hybrid tank (Hambrock, Rampai and Walker, 2021)	48
Figure 5-1: (A) EC view from the top with the lid open showing cooling plate(red) light and aquariums, (B) Sketch to show positioning of aquariums, par sensors and light in EC.	50
Table 5-1: Cost analysis for designing a temperature environmental chamber	50
Figure 5-2: Cooling plate fitted within the EC.	51
Figure 5-3: Temperature mapping for the aquariums within the EC, when chiller temperature is set to 5°C.	52
Figure 5-4: Temperature mapping for the aquariums within the EC, when chiller temperature is set to 8°C	53
Figure 5-5: Par readings for the par sensors with aquariums filled with milli q water sitting on top of them and for a par sensor with no aquaria sitting on top of it.....	55
Figure 6-1: Chlorophyll A in Vivo measurements for experimental aquarium 1 at 5°C and 200 $\mu\text{molm}^{-2}\text{s}^{-1}$	58
Figure 6-2: Phosphate measurements for experimental aquarium 1 at 5°C and 200 $\mu\text{molm}^{-2}\text{s}^{-1}$	58
Figure 6-3: Pictorial view of the pennate taxa: (A) Navicula species (B) Cylindrotheca closterium (C) Fragilariopsis kerguelensis (D) Unidentified pennates (E) Proboscia.....	59
.....	60
Figure 6-4: Pictorial view of the Centric taxa: (A) Chaetoceros (B) Unidentified centrics	60
Figure 6-5: Cell concentration per ml in aquarium 1 before and after experimentation at 5°C and 200 $\mu\text{molm}^{-2}\text{s}^{-1}$	60
Figure 6-6: Cell concentration per ml difference in aquarium 1 at 5°C and 200 $\mu\text{molm}^{-2}\text{s}^{-1}$	61
Figure 6-7: The different pennate and centric taxa in the baseline before experimentation	62
Figure 6-8: Chlorophyll A In Vivo measurement on the three different aquaria.	62
Figure 6-9: Phosphate concentrations over a period of six weeks	63
Figure 6-10: Cell count at the end of the baseline experiments	64
Figure 6-11: Chlorophyll A in Vivo measurements for high (200 $\mu\text{molm}^{-2}\text{s}^{-1}$), middle (42 $\mu\text{molm}^{-2}\text{s}^{-1}$) and No (0 $\mu\text{molm}^{-2}\text{s}^{-1}$) irradiance variations at 5°C in aquarium 2	65
Figure 6-12: Phosphate concentrations for high (200 $\mu\text{molm}^{-2}\text{s}^{-1}$), middle (42 $\mu\text{molm}^{-2}\text{s}^{-1}$) and No (0 $\mu\text{molm}^{-2}\text{s}^{-1}$) irradiance variations at 5°C.....	66
Figure 6-13: Before and after cell concentration difference for a 6-week experiment to determine adaptability of species to irradiance 0 $\mu\text{mol}/\text{m}^2/\text{s}$, 42 $\mu\text{mol}/\text{m}^2/\text{s}$ and 200 $\mu\text{mol}/\text{m}^2/\text{s}$ 5°C.	67

Figure 6-14: Chlorophyll A in Vivo measurements for experimentation on phytoplankton species in the dark at 8°C and 5°C	68
Figure 6-15: Phosphate concentrations for experimentation in the dark at 8°C and 5°C	70
Figure 6-16: Species cell count before and after experimentation difference In the dark at 8°C	70
Table A. 1: Calculation of Daylight hours at sampling sites	89
Figure A. 1: On deck coring of pancake	91
Figure A. 2: Setup of hybrid tank with open insulation during transportation.....	91
Figure A. 3: Unidentified pennates as per Hambrock, Rampai and Walker (2021) studies.....	93
Figure A. 4: Bray Curtis Dissimilarity for all modes of transportation in comparison with baseline count.....	94
Figure B. 1 : illustration of heat transfer for the EC.....	95
Figure B. 2: Temperature mapping within EC at 5°C focusing on the cooling plate.	96
Figure B. 3: Temperature mapping at 5°C within EC focusing on the EC walls	97
Figure B. 4: Temperature mapping at 8°C within the EC focusing on the cooling plate	97
Figure B. 5: Temperature mapping at 8°C within the EC.....	97
Figure B. 6: Par readings for light mapping in the EC when a shade filter is applied	98
Figure B. 7: Par readings for light mapping in the EC when a shade filter is applied	98
Figure B. 8: Front view of EC with its dimensions.....	99
Figure B. 9: Top view of EC and its associated dimensions making use of key given in front view figure.....	100
Figure B. 10: Front pictorial view of the EC	100
Figure B. 11: Side pictorial view of EC to show perforation.	101
Figure E. 1: Chlorophyll A in Vivo for experiments carried out at 8°C for an irradiance of 0 $\mu\text{mol}/\text{m}^2/\text{s}$	107
Figure E. 2: Phosphate measurements for experimentation at 8°C with an irradiance of 0 $\mu\text{mol}/\text{m}^2/\text{s}$	107
Figure E. 3: Cell concentration per ml before and after experimentation for aquarium 1 at 8°C and with an irradiance of 0 $\mu\text{mol}/\text{m}^2/\text{s}$	108
Figure E. 4: Cell concentration per ml before and after experimentation for aquarium 2 at 8°C and with an irradiance of 0 $\mu\text{mol}/\text{m}^2/\text{s}$	108
Figure E. 5: Cell concentration per ml before and after experimentation for aquarium 3 at 8°C and with an irradiance of 0 $\mu\text{mol}/\text{m}^2/\text{s}$	109
Figure E. 6: Chlorophyll A in Vivo for experiments carried out at 8°C for an irradiance of 42 $\mu\text{mol}/\text{m}^2/\text{s}$	109

Figure E. 7: Phosphate measurements for experimentation at 8°C with an irradiance of 42 $\mu\text{mol}/\text{m}^2/\text{s}$	110
Figure E. 8: Cell concentration per ml before and after experimentation for aquarium 1 at 8°C and with an irradiance of 42 $\mu\text{mol}/\text{m}^2/\text{s}$	110
Figure E. 9: Cell concentration per ml before and after experimentation for aquarium 2 at 8°C and with an irradiance of 42 $\mu\text{mol}/\text{m}^2/$	111
Figure E. 10: Cell concentration per ml before and after experimentation for aquarium 3 at 8°C and with an irradiance of 42 $\mu\text{mol}/\text{m}^2/\text{s}$	111
Figure E. 11: Chlorophyll A in Vivo for experiments carried out at 5°C for an irradiance of 0 $\mu\text{mol}/\text{m}^2/\text{s}$	112
Figure E. 12: Phosphate measurements for experimentation at 5°C with an irradiance of 0 $\mu\text{mol}/\text{m}^2/\text{s}$	112
Figure E. 13: Cell concentration per ml before and after experimentation for aquarium 1 at 5°C and with an irradiance of 0 $\mu\text{mol}/\text{m}^2/\text{s}$	113
Figure E. 14: Cell concentration per ml before and after experimentation for aquarium 2 at 5°C and with an irradiance of 0 $\mu\text{mol}/\text{m}^2/\text{s}$	113
Figure E. 15: Cell concentration per ml before and after experimentation for aquarium 3 at 5°C and with an irradiance of 0 $\mu\text{mol}/\text{m}^2/\text{s}$	114
Figure E. 16: Chlorophyll A in Vivo for experiments carried out at 5°C for an irradiance of 42 $\mu\text{mol}/\text{m}^2/\text{s}$	114
Figure E. 17: Phosphate measurements for experimentation at 5°C with an irradiance of 42 $\mu\text{mol}/\text{m}^2/\text{s}$	115
Figure E. 18: Cell concentration per ml before and after experimentation for aquarium 1 at 5°C and with an irradiance of 42 $\mu\text{mol}/\text{m}^2/\text{s}$	115
Figure E. 19: Cell concentration per ml before and after experimentation for aquarium 2 at 5°C and with an irradiance of 42 $\mu\text{mol}/\text{m}^2/\text{s}$	116
Figure E. 20: Cell concentration per ml before and after experimentation for aquarium 3 at 5°C and with an irradiance of 42 $\mu\text{mol}/\text{m}^2/\text{s}$	116

LIST OF TABLES

Table 4-1: Variables for the materials used.....	36
Table 5-1: Cost analysis for designing a temperature environmental chamber.....	50
Table 6-1: Sea ice sampling stations for the SCALE 2019 spring cruise	56
Table A. 1: Calculation of Daylight hours at sampling sites	89
Table A. 2: Day length definitions defined by the position of the sun with respect to the horizon (Forsythe et al., 1995).....	90
Table A. 3: Additional information on cores collected during the SCALEWIN 2022 in the marginal sea ice zone of the Southern Ocean	92
Table A. 4: Microscopic cell concentration per mL for all taxonomic groups for the different transport systems.....	92
Table A. 5: Microscopic cell concentration per Hambrock, Rampai and Walker (2021) studies for hybrid tank 1 sampled -59.3248S, 0.066617E in the marginal ice zone of the Southern Ocean	93
Table D. 1: Phosphate concentrations and appropriate volumes used	105

1 INTRODUCTION

1.1 Background

In polar regions, the cooling of seawater below the freezing point initiates the formation of sea ice. A significant aspect of this process involves the extraction of phytoplankton from the seawater, concentrating them within the sea ice (Thomas and Dieckmann, 2009). Phytoplankton are photosynthetic organisms that play a crucial role in mitigating climate change. CO₂ drawdown in the Southern Ocean is by a large part via phytoplankton photosynthesis and transportation of the sequestered carbon to the deep ocean (the biological pump) (Le Quéré *et al.*, 2007). The world's oceans are estimated to take up between 25 and 30% of the carbon dioxide (CO₂) released in the atmosphere. Of this, up to 40% is estimated to be from the Southern Ocean. Research estimates that 10% of the 40% uptake from the Southern Ocean is via the biological pump (Deppeler and Davidson, 2017).

In addition to the biological pump, phytoplankton also partake in increasing reflectance of solar radiation as a result of cloud nucleation. Dinoflagellates, a type of phytoplankton, synthesize dimethylsulfoniopropiothetin (DMSP), forming dimethylsulfide (DMS) upon enzymatic cleavage. Oxidation of DMS in the atmosphere results in the formation of sulfate aerosols leading to cloud nucleation (Charlson *et al.*, 1987). Alongside reducing the effects of climate change, phytoplankton are part of the primary production in the Southern Ocean and, are at the base of the food chain. The majority of phytoplankton are grazed by micro heterotrophs or degraded by bacteria (Kohlbach *et al.*, 2017).

Before comprehending the impact of climate change on the ecological dynamics of phytoplankton, it is essential to grasp the current operational characteristics of phytoplankton communities. Despite being photosynthetic organisms, phytoplankton exhibit the ability to endure extended periods of darkness during winter, particularly within ice environments, an intriguing phenomenon that remains shrouded in mystery (McMinn, Martin and Ryan, 2010). Research indicates that phytoplankton productivity approaches zero in winter, possibly due to diminished light availability. However, even in ice-free zones during summer, where ample light and nutrients are presumed to be present, there is reported low phytoplankton productivity (Smith *et al.*, 2000). Several studies propose that during summer, nutrient availability declines, and deep vertical mixing diminishes the exposure of phytoplankton to light, consequently impeding their growth rate (McMinn, Martin

and Ryan, 2010). Noteworthy is the observation of a substantial phytoplankton bloom in spring, attributed to the vertical stability facilitated by melting ice and the provision of optimal light conditions (Smith *et al.*, 2000). The responses of different phytoplankton species to variable environmental conditions are species-specific and largely unexplored. Understanding these responses, mostly unknown at present, holds significance for estimating the bio-productivity of the Southern Ocean.

In situ monitoring of phytoplankton, though well-established is expensive, relies on the safety of humans, and is mostly limited by equipment. Additionally, *in situ* monitoring has to be undertaken in calm and stable conditions, which is not always possible in the Southern Ocean. Recognizing these challenges, it is therefore necessary for phytoplankton species to be transported to land facilities and investigated. Hambrock, Rampai and Walker (2021) designed a hybrid system, composed of sea ice and seawater to simulate environmental conditions phytoplankton species would have lived in, when being transported to land facilities. Though some preliminary success was realized with the hybrid system, there are aspects of the initial design that need optimization to better simulate environmental conditions for the sea ice algae, thus preserve the community compositions. Therefore, the focus of this study was on developing and/or optimizing techniques, equipment and methodologies for land based experiments with Antarctic sea ice algae/phytoplankton from the Marginal Ice Zone (MIZ) of the Southern Ocean.

1.2 Scope and Limitations

The scope of this work was limited to 3 main technical developments; 1) to optimize the existing hybrid system, 2) design an Environmental Chamber (EC) that will allow controlled conditions for these specific algae, and 3) develop preliminary methodologies and protocol for experimentations with sea ice algae in the designed environmental chamber. Optimization of the hybrid tank excluded environmental conditions such as snow cover, wind and turbulence as these could not be investigated due to logistical or timeline limitations. It should be noted that the optimization of the hybrid system is dependent on the availability of the SA Agulhus II to the MIZ, and this was beyond the control of the researchers as it is a national infrastructure and, the COVID pandemic limiting number of possible research expeditions. The design of the EC was limited to temperature, irradiance and humidity as these, in addition to nutrients, were identified as the most important factors in sea ice algae growth. This was also due to the limited time for this project.

These preliminary factors can further be supplemented with introduction of ice in the aquaria and agitation to the system. Lastly, the experimental protocol and investigation for sea ice algae in the environmental chamber were also largely focused on what the technical limitations of the EC were and what the working parameters were. Some preliminary conclusions on how the sea ice algae are affected by irradiance and temperature could be drawn, however, these are subject to the limitations of the EC. Moreover, the sea ice algae experimented on in the EC were from the Southern Ocean Seasonal Experiment (SCALE) spring cruise of 2019. This was due to that; these were the available cultures when the project commenced. In 2022 winter, the researchers had an opportunity to use the optimized hybrid system to collect more sea ice algae, however, since these communities were different from those already experimented on, the researchers continued with the spring 2019 cultures as restarting the investigation would extend the project to unreasonable timelines. The winter 2022 cultures were used for the subsequent project that focused on optimizing the limitations of the EC, and protocols, designed in this project.

2 LITERATURE REVIEW

2.1 Background to sea ice and the significance of sea ice on phytoplankton

Cooling ocean waters to below the freezing point of water i.e. -1.8°C for the Antarctic salty waters, results in the formation of sea ice (Timco and Weeks, 2010). Sea ice can be visualized as a thin blanket covering the ocean surface because of interactions between heat flux, moisture, and momentum across the atmosphere-ocean interface. The polar region with Arctic waters sees the formation of the Arctic sea ice, while the southern region with the Southern Ocean forms the Antarctic sea ice (Thomas and Dieckmann, 2009). The Arctic is characterized as an ocean basin mostly enclosed by land, whereas the Antarctic is a continent encircled by the ocean. The current understanding of sea ice primarily pertains to the Arctic and is not directly applicable to the Antarctic due to variations in environmental conditions (Timco and Weeks, 2010).

The formation of sea ice begins with the development of ice crystals known as frazil ice. In calm conditions, such as those found in the Arctic, these crystals conglomerate to form a thin layer of sea ice called nilas, which continues to grow as water molecules bind to the ice surface under freezing conditions. In contrast, under strong wave and wind action, particularly in the Southern Ocean's Marginal Ice Zone, frazil crystals coalesce into a sludge-like structure referred to as grease ice (Ackley and Sullivan, 1994). As this grease ice thickens, it forms larger masses with rounded edges, known as pancake ice, which eventually consolidate into ice sheets (Weeks and Ackley, 1986).

When ice formation exceeds 30 to 40% in the Southern Ocean and freezing temperatures persist, a fully consolidated frazil-dominated ice sheet develops. Due to the proximity of this advancing ice sheet to the open ocean, wave fields can penetrate the ice cover as a result of the surface-wind interface (Ackley and Weeks, 1990). Continuous winds lead to the rafting of pancake ice, creating new patches of open water. Waves further infiltrate these open areas until the energy is insufficient to cause additional rafting, typically reached when pancake floes attain a thickness of 0.4 to 0.6m. The formation of pancake ice is a critical process at the advancing ice edge in the Southern Ocean (Ackley and Weeks, 1990; Convey, 2006).

As sea ice formation progresses, consolidated ice sheets develop into columnar ice. This columnar ice extends from the lower margin of the ice into the water column. The lower portion of the columnar ice, which is highly porous, maintains a temperature just below the freezing point of water and is referred to as the skeletal layer (Figure 2-2) (Thomas and Dieckmann, 2009).



Figure 2-1: A) Consolidated Ice in the Southern Ocean at 59° 30 615S; 00° 24 997°W on the 22nd of July 2022 B) Pancake ice in the Southern Ocean at 59° 09 320°S; 00°52 298°E on the 19th of July 2022

Sea ice provides a platform for which sea ice algae can be suspended in the upper ocean where there is sufficient light for growth (Thomas and Dieckmann, 2009). In the Southern Ocean, sea ice formation begins in autumn (Louw, Walker and Fawcett, 2022). Surface waters consist of substantial microbial populations from the prior spring. This is such that when frazil ice forms, microalgae, protists, and bacteria are scavenged from the water, being incorporated into the ice as crystals rise to the surface (Garrison, Close and Reimnitz, 1989). Weeks and Ackley (1982) suggest that a high concentration of organisms is found in young ice because frazil ice crystals form on suspended particles. These particles adhere to the ice crystals as they rise to the surface. In some instances, young frazil ice has been found to consist of over 50 times particle concentrations than the underlying seawater with diatoms mostly observed (Thomas and Dieckmann, 2009). Eicken (1992) suggests that raphe-containing species such as diatoms might be favored during frazil ice formation due to cells being inherently sticky.

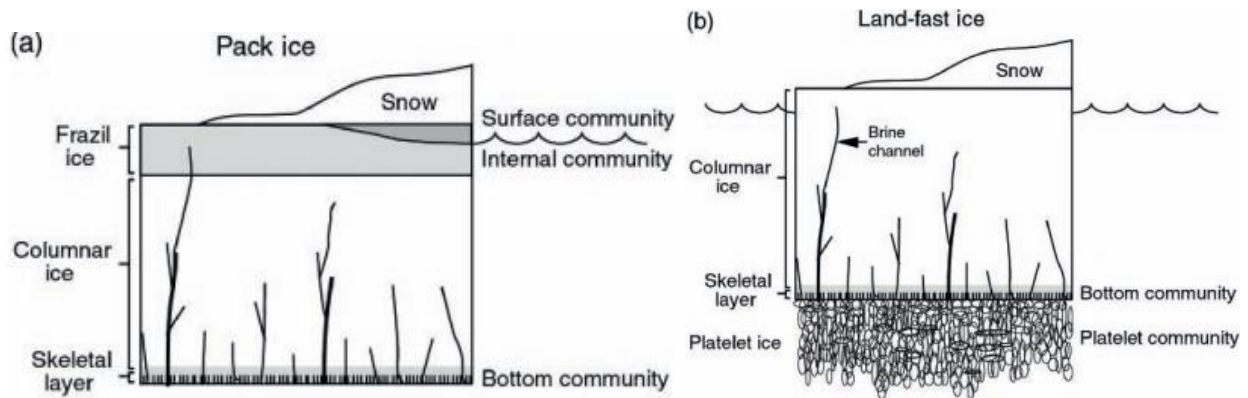


Figure 2-2: Highly idealized illustration of a) pack ice and b) land-fast ice showing the location of algal communities (Thomas and Dieckmann, 2009)

After initial sea ice formation, the biodiversity of sea-ice biota is likely to resemble that of the water they were recruited from. Thereafter dominance of species such as psychrophilic bacteria are likely to develop. Species that reside in sea ice (specifically diatoms) increase after the ice age (Arrigo, 2016). Ice algae communities can be categorized according to the three segments namely: surface, interior, and bottom ice layers (Horner *et al.*, 1992). The greatest portion of sea ice microalgae resides in the bottom 0.2m of the ice sheet. This is where environmental conditions are stable and favorable for growth (Kaartokallio *et al.*, 2006) and is in close proximity to underlying surface water containing essential nutrients for algal growth (Arrigo, 2016). This is the bottom ice community which mostly resides in the skeletal layer (Arrigo and Sullivan, 1992).

Microalgae have also been found and collected from the upper 1-1.5m of sea ice in McMurdo Sound (Kottmeier and Sullivan, 1988). This is known as the internal community and is subjected to large environmental fluctuations (Lizotte and Sullivan, 1991). Although these communities have sufficient light availability, nutrient availability is often restricted. Nutrients are often provided by seawater infiltrating the freeboard layer of the ice (Kattner *et al.*, 2004). The supply of nutrients to algae depends on the porosity of the surrounding ice. For algae growing at the snow interface, surface flooding because of snow loadings results in the supply of nutrients (Wadhams, Lange and Ackley, 1987). Snow cover reduces the amount of light available for algal growth however it is partially responsible for providing nutrients to the surface community (Arrigo *et al.*, 1997). Phytoplankton community organization in sea ice is related to the extinction of light (Margalef, 1978). Distribution of phytoplankton in ice is controlled by brine-salinity characteristics in the ice interior and the availability of nutrients (Figure 2-2) (Arrigo and Sullivan, 1992; Louw, Walker and Fawcett, 2022; Van Leeuwe *et al.*, 2018).

2.2 Ecological importance of phytoplankton

Phytoplankton blooms occur in the ice zones and are said to contribute to total primary productivity in the Southern Ocean. The Southern Ocean sustains high populations of krills, sea birds, and seals (Nelson and Smith, 1986). Krill spawn during the summer months, specifically from December to March, and their larvae rely on ice algae as a food source, grazing beneath ice floes during the winter (Smetacek, Scharek and Nöthig, 1990).

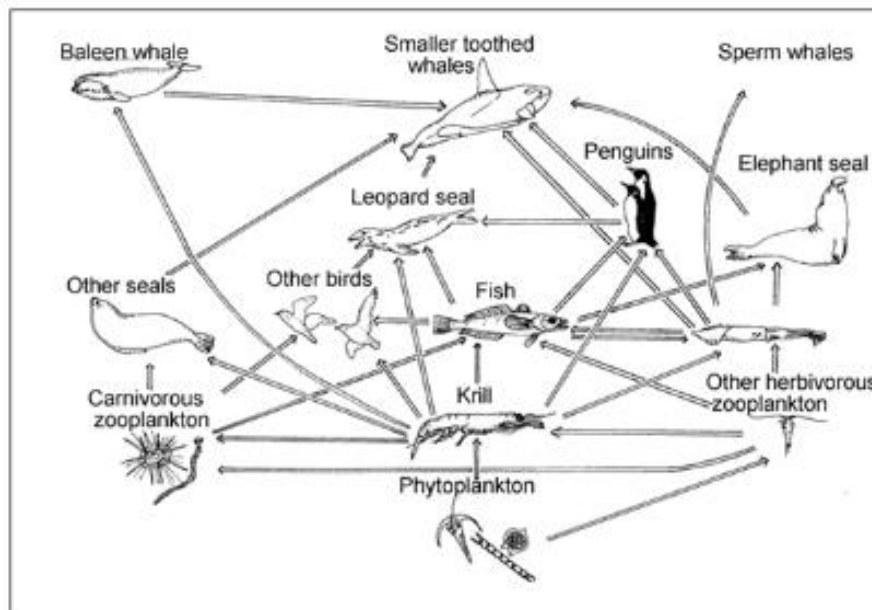


Figure 2-3: An illustration of the Antarctic food web (Learnz, 2021)

The transfer of carbon from phytoplankton to primary carnivores (krill) is estimated to be 30%. Nelson and Smith (1986) have suggested that at least 10% of carbon produced by phytoplankton is consumed as krill by seals and other carnivores. Phytoplankton are therefore at the base of the food chain, feeding krills which subsequently provide food to larger carnivores (Figure 2-3). Kohlbach *et al.* (2017) highlight that the Antarctic krill, *Euphausia superba*, is regarded as one of the Antarctic's invaluable primary food sources considering its ecological importance in providing a large magnitude of dietary carbon to fish, marine mammals, and seabirds. Global silicon budgets suggest that the ecological and geochemical impact of phytoplankton productivity is greater in the Southern Ocean than in other oceanic systems (Nelson and Smith, 1986).

Sea ice algal assemblies are virtually fixed spaces that can be revisited repeatedly as opposed to studying planktonic systems. Within the sea ice, the incident irradiance, temperature, and salinity are relatively constant and losses due to grazing appear to be minor (Cota and Smith, 1991). This gives ice algae an advantageous edge when looking into the ecology of the polar regions.

Sea ice algae concentrations in ice are up to 80 times those found in the water column. Sea ice algae are important as they provide a carbon export pathway from surface waters to the deep ocean. It is approximated that up to a quarter of human activity-related carbon dioxide is absorbed by the oceans. Of this absorbed carbon dioxide, 12% is attributed to the polar regions with sea ice algae and sea ice processes accounting for 0.9% of global carbon fixation (Le Quéré *et al.*, 2016).

2.2.1 Categorization of phytoplankton protist groups in sea ice

The protist groups in sea ice are predominantly photoautotrophic i.e., they capture energy from light via photosynthesis. Studies show that in the Southern Ocean, diatoms make up > 90% of the photosynthetic organism diversity in sea ice. In both the Antarctic and the Arctic, diatoms show a wide range of species (Lizotte, 2003). Their frustules (readily preserved cell walls), made up of silicon have been attributed to them being described in detail. Sea ice also harbors dinoflagellates, amoebas, and ciliates (Lizotte, 2003).

In general, phytoplankton species abundance is said to be in the bottom ice communities as opposed to top ice. Diatoms are observed to dominate interior ice communities confined to brine channel networks beneath ice covers, while flagellates dominate the brackish waters of surface melt ponds (Mundy *et al.*, 2011). Diatoms vary in size but generally represent the predominant portion of the 'larger phytoplankton size fraction' in marine surface water communities. (Huisman and Sommeijer, 2002). In the Southern Ocean, pennate diatoms comprise of up to 90% of the ice flora, being the most abundant microalgae in sea ice (Petrou *et al.*, 2011). Species of pennate genera *Nitzschia*, *Fragilariopsis*, and *Navicula* are generally observed forming both long chains or large unicellular cells (>20µm) (Arrigo, 2016; Louw, Walker and Fawcett, 2022). Large blooms of centric diatoms i.e., *Porosira* and *Thalassiosira* have also been observed in the Antarctic (Lizotte and Sullivan, 1992; Louw, Walker and Fawcett, 2022). In sea ice assemblages, centric diatoms occur under specified conditions, an example is the entrainment of *Chaetoceros* which

is seen in newly formed ice in autumn (Arrigo, 2016). Centric diatoms dominate young ice while pennate diatoms dominate old ice (Kauko *et al.*, 2018; Lizotte, 2003; Thomas and Dieckmann, 2009). Centric diatoms also outcompete pennate diatoms under nutrient-deplete-high light conditions (Campbell *et al.*, 2018).

2.3 Parameters that affect phytoplankton growth: *in situ* investigations

The factors influencing the growth and biomass productivity of phytoplankton in the Southern Ocean remain insufficiently understood. While some argue that radiation primarily governs phytoplankton growth, others propose that the nutrient iron serves as a limiting factor for phytoplankton in this region (Smith Jr, *et al.*, 1996). Arrigo *et al.* (1997) contend that, in sea ice, primary productivity is low, and nutrient uptake is regulated by light availability. The Southern Ocean's limited research has led to incomplete knowledge, contributing to inaccuracies in depicting ecological communities and their significance (Chapman *et al.*, 2020).

2.3.1 Nutrient types and availability

Sea ice phytoplankton obtain their nutrients from the brine channels and, in the channels, nutrients are supplemented by surface flooding on the ice (Gradinger, 2009). As algae use the organic and inorganic nutrients in the brine channels and pockets, limitations of algal growth within the ice are foreseen during periods of peak production (Meiners and Michel, 2016). Nutrient exchange for phytoplankton in ice is a function of surface flooding and ice porosity (Gradinger, 2009). The distribution of nutrients in the brine channels is determined by the local composition of seawater. While the bulk salinity of sea ice is relatively low compared to the underlying water, resulting in lower bulk concentrations of nutrients within the sea ice, the concentrated nutrients within brine channels create an environment for sea ice algae with higher nutrient concentrations than those found in the water column (Meiners and Michel, 2016).

Phytoplankton growth relies on carbon, nitrate, phosphate, and for diatoms, silicate. These nutrients are primarily available in inorganic forms in seawater (Thomas and Dieckmann, 2009). Studies indicate that while Antarctic waters are typically rich in nutrients, Silicate is often the

primary limiting factor for diatom growth during the later stages of a bloom (Thomas and Dieckmann, 2009). Hayes *et al.* (1984) found that nutrient availability—including Nitrate, Phosphate, Silicate, trace metals, and vitamins—does not significantly control phytoplankton abundance south of the Polar Front. However, Smith Jr. *et al.* (1996) highlighted that the relationship between silicic acid and chlorophyll *a* underscores the importance of nutrients in phytoplankton growth, suggesting the need for further research. Meiners and Michel (2016) noted that the lack of macronutrients, particularly Nitrate and Silicic acid, can adversely affect sea ice algae communities, particularly impacting diatom growth. Additionally, Massom and Stammerjohn (2010) and Arrigo (2017) identified nutrients, especially the micronutrient iron, as the primary factor limiting growth in pack ice communities, including surface and interior microhabitats.

In Arctic waters, nitrate depletion is reported to drive shifts from diatom-dominated to flagellate-dominated phytoplankton assemblages (Ardyna *et al.*, 2011). High NO_3^- and low Si(OH)_4 waters, i.e., having a $\text{NO}_3^- : \text{Si(OH)}_4$ molar ratios >1 can drive assemblage shifts from diatom to *Phaeocystis* dominance in sea ice-covered areas (Ardyna *et al.*, 2020). The C: N ratio between different phytoplankton varies much less than either C: Si or C: P ratios, as such diatoms can likely grow to greater biomass on the same N inventory than other taxa, and thus both winter water Si(OH)_4 and PO_4^{3-} concentrations, and $\text{Si(OH)}_4 : \text{NO}_3^-$ and $\text{NO}_3^- : \text{PO}_4^{3-}$ drawdown ratios, are good predictors of bloom magnitude (Ardyna *et al.*, 2020). It is thought that diatoms flourish in upwelling regions as they can outcompete other phytoplankton for newly upwelled NO_3^- (Dugdale and Wilkerson, 1991), with Malone (1980) first linking the success of large phytoplankton ($>20 \mu\text{m}$) in upwelling regimes specifically to nitrate utilization.

2.3.2 Temperature, salinity and irradiance variations

Microorganisms residing within sea ice are exposed to pronounced gradients in temperature, salinity, and irradiance. In the brine channels of ice, temperatures can range from -2°C to -8°C (Duncan and Petrou, 2022). In contrast, the ice-water interface, specifically the skeletal layer, provides relatively mild and stable conditions for algae, with temperatures around -1.8°C that remain consistent throughout the spring. Fluctuations in brine channel temperatures are critical in shaping the communities of sea ice algae in the Antarctic region (Duncan and Petrou, 2022).

In situ, studies have revealed that some Antarctic sea ice algae can photosynthesize below -8°C and at 110psu in autumn. Notably, the centric diatom *Chaetoceros* demonstrated resilience by thriving at temperatures as frigid as -17°C and in saline conditions reaching 196psu (Mock and Thomas, 2005). The diatoms *Nitzschia frigida* and *Thalassiosira antarctica* grew rapidly between -4°C and -6°C (Aletsee and Jahnke, 1992). It is noteworthy that the responses of these sea ice algae to varying temperature and salinity conditions are distinctly species-dependent, as highlighted in the study by Mock and Thomas (2005). This diversity in reactions underscores the adaptability of Antarctic sea ice algae to extreme conditions and emphasizes the importance of considering species-specific dynamics in understanding polar marine ecosystems.

Furthermore, phytoplankton species from both polar and temperate regions often exhibit optimal growth temperatures that are significantly higher than the mean annual temperatures of their habitats (Yan *et al.*, 2019). Previous research indicates that most ice diatoms are capable of tolerating temperatures up to 8°C (Yan *et al.*, 2019; Fiala and Oriol, 1990). This finding suggests that while sea ice algae can endure harsh conditions, their growth potential may be limited by temperature constraints, thereby influencing community composition and productivity in sea ice environments.

Salinity levels in Antarctic sea ice typically range from 5 to 70psu, often exceeding three times that of the surrounding surface waters (Torstensson *et al.*, 2019). Notably, salinity values of up to 173psu have been recorded in McMurdo Sound Bay (Arrigo, 2017). The salinity of brine is generally much higher than that of seawater due to the thermodynamic equilibrium between pure ice and brine at the ice temperature. Consequently, temperature and salinity in sea ice can reach extreme levels and may fluctuate significantly over short time periods (Ewert and Deming, 2013). As a result, microalgae within sea ice must acclimate to these dynamic environmental conditions, and some species may struggle to survive and thrive in these habitats. This can lead to notable differences in algal composition between sea ice and adjacent seawater (Yan *et al.*, 2022).

The Antarctic has close to 6 months of winter. The light levels are very low during this time and the presence of sea ice cover further exacerbates the light levels such that phytoplankton receive < 1% of surface irradiance (McMinn, Martin and Ryan, 2010, Hancke *et al.*, 2018). Studies have shown that phytoplankton can survive for long periods of darkness, resuming photosynthesis within 24 hours after experiencing darkness for 6 months. However, chlorophyll a levels suggest that the quantity of phytoplankton able to survive these conditions is low. The surviving

phytoplankton is however important in seeding phytoplankton bloom in spring (McMinn, Martin and Ryan, 2010).

In ice, light levels are not equal from the top to the bottom of the ice. Studies have shown that, for under-ice algae communities, bloom can begin at irradiances as low as $0.17 \mu\text{mol m}^{-2} \text{s}^{-1}$. At this irradiance the chlorophyll a was detected to be 0.001 mg/m^2 and par transmittance was $< 1\%$. Increasing light attenuation was observed at wavelengths $> 500 \text{ nm}$ and $< 750 \text{ nm}$ (e) (Hancke et al., 2018).

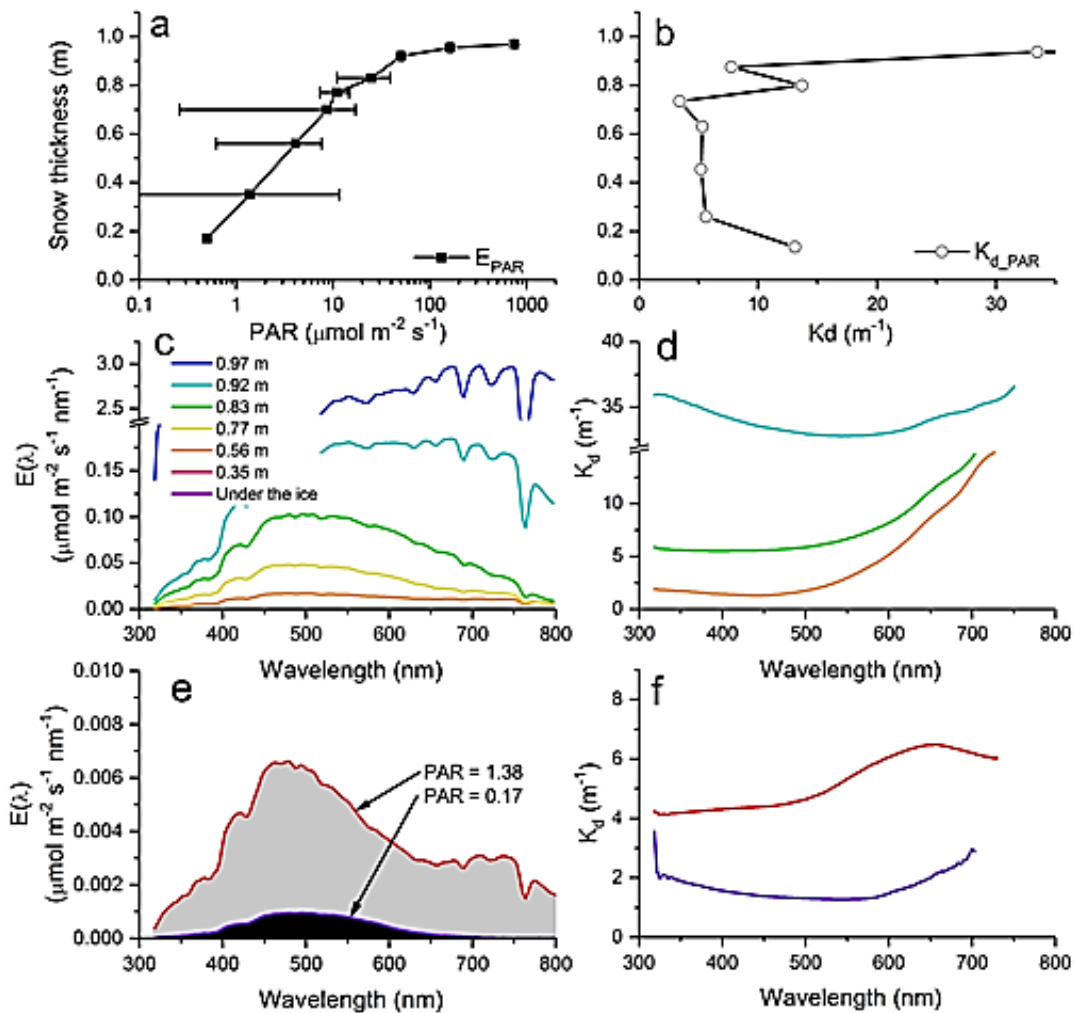


Figure 2-4: Measured spectral irradiance at the Wandel Sea through the snow cover and under sea ice and the corresponding attenuation coefficients (K_d). (a) Profile of PAR (error bars are C.V.); (b) profile of $K_{d,PAR}$; (c) $E(\lambda)$ at different depth in the snow cover (see figure legend); and (d) correspond $K_{d(\lambda)}$ (data represent lower depth). (e) $E(\lambda)$ under the sea ice (purple) and 0.35 m above in the snow (lowest good measure) and (f) correspond $K_{d(\lambda)}$. Surface PAR of $750 \mu\text{mol photons m}^{-2} \text{s}^{-1}$ (Hancke et al., 2018).

Studies in the MIZ of the northwestern Weddell Sea have shown that enhanced primary production is usually during ice melting of a vertically stable upper layer of ice resulting in the

production of meltwater and subsequent seeding. Melt ponds allow light to reach phytoplankton (Lancelot *et al.*, 1993). The phytoplankton bloom appears to be initiated when vertical stability is imparted in austral spring. Studies conducted by investigating the relationship between chlorophyll a and particulate carbon showed that increasing irradiances are associated with increasing photosynthetic biomass (Horvat *et al.*, 2022; Smith *et al.*, 2000). Arrigo *et al.* (1997) observed that an increase in light availability in the Southern Ocean in November (spring) increased phytoplankton biomass production. The increase is attributed to increased light levels for phytoplankton cells and the creation of a vertically stable environment while the removal of sea ice is ongoing.

Arrigo *et al.* (1997) showed that phytoplankton production in the Southern Ocean mostly occurs from October to February and annual primary production was 27 times more in first-year sea ice when compared to multiyear sea ice. Lancelot *et al.* (1993) showed that deep-mixed sea ice free zones are not exceptionally phytoplankton productive despite high nutrient availability. After leaving the sea ice habitat, phytoplankton species either continue to grow in sea water or disappear from the water column over time (Mundy *et al.*, 2011). In summer, Arrigo *et al.* (1997) observed that algal growth is limited, and suggested that this was a result of a decrease in availability of nutrients. Smith Jr *et al.* (2000) suggested that, in addition to nutrient limitation, deep vertical mixing in ice free zones limits the total assemblage of irradiance on phytoplankton thus reducing daily growth. High phytoplankton concentrations are often associated with hydrographic features such as the presence of sea ice (Hayes, Whitaker and Fogg, 1984). It is now well understood that vertical stability is a necessity to initiate phytoplankton ice edge bloom however not a sufficient condition to sustain high biomass development (Lancelot, *et al.*, 1993).

Mangoni *et al.* (2009) found that when bottom ice algae communities that are acclimatized to low light levels i.e., $7-9\mu\text{molm}^{-2}\text{s}^{-1}$, are subjected to high irradiances, they incur significant photo damage. There were notable substantial differences in the adaptability of different algae to environmental change (Mangoni *et al.*, 2009). Additionally, Palmisano *et al.* (1985) noted that some Antarctic sea ice species become photo-inhibited at irradiances which are more than $25\mu\text{molm}^{-2}\text{s}^{-1}$ confirming the shade adaptive nature of bottom ice algae communities. Other diatom species, however, needed time to adapt from low to high irradiances ($100-800\mu\text{molm}^{-2}\text{s}^{-1}$). Phytoplankton species with a high ability to generate the non-photosynthetic quenching (NPQ) parameter can cope with greater irradiances as transition from spring to summer occurs. NPQ

reflects the ability of a species to dissipate excess light energy generated during photosynthesis. It is these species that become commonly found after winter (McMinn, Martin and Ryan, 2010).

When temperatures decrease in February (in the Southern Ocean), productivity in sea ice decreases as ice porosity decreases to below the threshold required for nutrient exchange (Arrigo *et al.*, 1997). Smith Jr *et al.* (2000) observed that in the Southern Ocean, carbon assimilation decreased rapidly in austral autumn and approached zero when ice formed. As the amount of light decreases, organisms must acclimate to such light conditions. Extreme low acclimation is accomplished by an increase in photosynthetic efficiency of organisms (Smith Jr *et al.*, 2000). This is achieved by increasing accessory photosynthetic pigments. Accessory photosynthetic pigments are increased relative to the main photosynthetic pigment, chlorophyll a, to allow the cell to enhance light harvesting at the wavelengths of light penetrating the ice. Diatoms are also observed to acclimate to low radiance by increasing the number of photosynthetic units per cell (Thomas and Dieckmann, 2009).

In sea ice environments, significant fluctuations occur in key abiotic factors, including temperature (~ -20°C to -1.8°C; Petrich and Eicken, 2017), salinity (ranging from 25 to 170psu; Arrigo *et al.*, 2010), and light availability (0 to 1000 $\mu\text{molm}^{-2}\text{s}^{-1}$; Galindo *et al.*, 2017). These variations can significantly influence the photosynthetic efficiency of ice algae. Importantly, these abiotic parameters are not independent; rather, they often interact as multiple co-stressors, which can complicate their individual effects on algal physiology (McMinn *et al.*, 2017). Understanding these dynamics is crucial for elucidating the resilience and adaptability of ice algal communities in response to changing environmental conditions.

2.3.3 Sympagic environment and symbiotic relationships

Changes in sea-ice biochemistry, influenced by high sea-ice algae biomass, partly determine the composition of algae species communities. These changes affect sea-ice brine chemistry, including nutrient availability, salt concentrations, and pH levels (Arrigo and Thomas, 2004). A robust biological community can further alter the surrounding sympagic environment through increased photosynthesis. Primary production and high algal biomass change brine channel chemistry by increasing oxygen levels, depleting CO₂ levels, and making the environment more alkaline (can increase to a pH of 10) (Thomas and Dieckmann, 2002). Other expected changes

include higher ammonium levels, increased dissolved particulate organic matter (POM), and lower nutrient concentrations (Thomas and Dieckmann, 2002). While environmental factors such as pH, CO₂ concentration, and UV radiation are often not investigated due to their perceived limited effects (Arrigo *et al.*, 2017), the increasing input of anthropogenic CO₂ into the atmosphere poses serious implications for marine ecosystems, particularly in polar regions where adverse effects are likely to be more pronounced (Torstensson *et al.*, 2015).

The Southern Ocean ecosystems contain a microbial assemblage of algae, protozoans, and bacteria which serve as the primary energy source for Antarctic organisms (Andreoli *et al.*, 2000). In the spring, when sea ice is still near its maximum extent, algae form distinct, banded assemblages within the ice matrix. As these algal blooms develop, bacterial growth within the ice accelerates. Many sea-ice bacteria are epiphytic and depend on the organic matter produced by algae (Bowman and Demming, 2017). However, sea ice bacteria and algae interact both synergistically and antagonistically, depending on resource availability and the specific stressors of the sea ice environment. The study of bacterial production (BP) in sea ice has been limited by the temperature sensitivity of indigenous bacteria, many of which are psychrophiles that cease growth well below room temperature (Junge *et al.*, 2002). Despite these challenges, a synthesis of existing data on BP and primary production reveals that while BP in sea ice shows a poor correlation with primary production, it has a strong and variable relationship with chlorophyll a levels. Specifically, there is a positive correlation with chlorophyll a concentrations below 50 mg m⁻³ and a negative correlation above this threshold (Bowman and Ducklow, 2015).

2.4 Lab based experiments on Parameters that affect phytoplankton growth

In situ monitoring of sea ice algae, however established, presents several challenges which in turn suggest the need for laboratory experimentation. The harsh winter climate experienced in the Southern Ocean renders it largely inaccessible, particularly over long periods, and costly for field sampling. Oxygen monitoring methods (Miller *et al.*, 2015) as well as diving-assisted subsampling methods (McMinn and Hegseth, 2007) are restricted by their lack of vertical and horizontal measurement accuracy, respectively. Deployment of these methods is also very reliant on calm and stable conditions for the safety of scientists and considering the limitations of

equipment on and underneath the ice. This makes *in situ* monitoring challenging for studies on sea ice algae bloom where the ice has substantially melted as well as on pancake ice.

Vancoppenolle and Tedesco (2016) noted that laboratory-based experimentation on sea ice algae behavior is lacking, but it can aid in reducing the uncertainty of the current biogeochemistry sea-ice models, and consequently earth system models. In addition, they noted that sea ice algae are understudied and this limits confidence in estimations of overall sea ice productivity. To conduct these investigations as robustly as possible, two factors need to be undertaken with care; 1) transportation of the sea ice algae and 2) careful control of the environment in which these experiments are conducted. Ryan *et al.* (2011) emphasize that most studies involve releasing algae from ice and measuring their stress responses in artificial culture techniques which potentially damages cells thus algae must be studied *in situ*. However, certain claims about species behavior can only be made when the number of variables is reduced and isolated species are experimented on. Overlap between liquid cultures and *in situ* algae behavior needs to be proven and discrepancies noted. Considering the vastly differing weather conditions in the Antarctic, it may be challenging to relate liquid culture behaviors to specific locations, hence, Vancoppenolle and Tedesco, (2016) and Ryan *et al.* (2011) also advocate for *in situ* studies.

2.4.1 Transportation methods of sea ice algae

During the transportation of sea ice algae, the survival of phytoplankton is dependent on keeping the conditions similar to their *in situ* conditions. Currently, there are three ways of transporting sea ice phytoplankton from the polar regions to land, and these are discussed below.

2.4.1.1 Transportation in solid sea ice form

One way of transporting phytoplankton to land is in the solid sea ice form as obtained from the Ocean. Transportation of an ice core was done from the Sea of Okhotsk. Post-coring, the sampled cores were immediately covered with polyethylene bags to prevent light penetration to the core during transportation/storage in a freezer for three weeks. The temperature of the core immediately after coring was -4.7°C at the top to -1.87°C at the bottom of the core (Yan *et al.*, 2020). The core was stored at -5°C as the threshold for fluid permeability in sea ice is said to be at -5°C for sea ice with a bulk salinity of 5psu (Ewert and Deming, 2013). Lower temperatures are therefore assumed to cause much more cell death when there is long transportation or storage.

Transporting the core at a higher temperature may lead to loss of brine due to brine drainage in solid form (Cox and Weeks, 1986).

Sea ice has a non-uniform temperature profile. The sea ice directly in contact with sea water will approximate that temperature, while sea ice closer to the surface approximates the temperature of snow or the surrounding air. Quick changes to the temperature of an ice core result in changes to the brine salinity thus introducing osmotic stress to ice algae. Osmotic stress has been directly linked to the death of ice algae affecting species differently, but least affecting diatoms (Thomas, 2017). Cooling the core to a uniform temperature, rather than a temperature gradient found *in situ*, may lead to the degradation of community species. Kauko *et al.* (2018) noted that species sensitive to osmotic stress frequently inhabit the lower segments of the sea ice where the temperature is warmer. The top and bottom of a sea-ice core typically have higher bulk salinities than the centre of the core, resulting in salinity profiles often being C-shaped (Thomas, 2017). The top and bottom of the ice core also contain the largest fraction of ice algae (Ackley and Sullivan, 1994; Thomas, 2017).

Hambrock, Rampai and Walker (2021) presented an opposing view to Cox and Weeks (1986) investigation that salinity within an ice core does not change once the core reaches a storage temperature of -20°C , suggesting that brine drainage still occurs in the ice cores during transportation. Hambrock, Rampai and Walker (2021) also suggest that storing ice at any temperature where brine exists results in deformation of the brine profile, and storing cores at -5°C for three weeks will cause many changes to the ice community as at -5°C , sea ice is permeable (Golden, Ackley and Lytle, 1998). Transportation as solid sea ice is advantageous as there is no initial processing time and the only requirement is maintaining temperature the same when ice cores are transported between ship and land storage facilities.

2.4.1.2 Transportation in melted sea water

Transportation of algae in melted sea water requires a much higher processing time when compared to transportation in solid sea ice. However, it offers an opportunity for immediate experimentation of algae and allows for access of algae to light, nutrients, and air. Sea ice samples are melted immediately after extraction for transportation and, direct melting provides a potential for osmotic stress resulting in degradation of algae. Grant and Horner (1976) and Dawson *et al.* (2020) both employed immediate post-sampling melting of their sea ice. Campbell

et al. (2019) developed methods to limit the osmotic stress algae experience. This means immediate experimentation can be done, however more preparation beforehand is required.

Miller *et al.* (2015) note the lack of consensus in the scientific community when melting ice samples. Campbell *et al.* (2019) highlight that within the scientific community, the melting of ice cores is consistently done in the dark to avoid light stress on the shade acclimated algae; however, melt procedures vary in the temperature and duration of melt. Rintala *et al.* (2014) melted samples at room temperature and at 4°C. No significant difference in algal activity was detected and it was therefore recommended that rapid melting be conducted to avoid the influence of biological impacts such as the growth of bacteria. In contrast, Mikkelsen and Witkowski (2010) showed that melting ice samples at room temperature resulted in a low abundance of the non-diatom cells concluding that rapid melting of ice samples at more than 4°C should be avoided.

Overall, while transporting algae in melted seawater can expedite experimentation, it requires careful planning and execution to mitigate the potential for osmotic stress and to maximize the reliability of the results obtained. Balancing the immediacy of experimentation with the need for careful processing remains a key consideration in this approach.

2.4.1.3 Hybrid system transportation

Transportation of phytoplankton involves either a solid medium only or a liquid medium only i.e., transportation is either within sea ice or within melted sea ice. Transportation in the solid medium only faces challenges of brine loss, thus algal loss and fluctuations in the temperature of the core. This means immediate experimentation on algae cannot be done as they must adapt to new environmental conditions which may lead to change in the algal communities (Thomas, 2017; Yan *et al.*, 2020). Transportation in the liquid form may result in significant alteration in the community composition resulting from post-melting production of algae which is linked to osmotic stress (Grant and Horner, 1976). As such, a hybrid system was designed by (Hambrock, Rampai and Walker, 2021) to alleviate some of the disadvantages of both these transportation methods. The aim of the method was to preserve phytoplankton species compositions while increasing the algae concentrations during transportation from the Southern Ocean to land based facilities for lab based experiments (Hambrock, Rampai and Walker, 2021). The designed hybrid system explored the ability to simulate the ice-ocean dynamics within the designed system. This was done by

immersing collected cores in the filtered sea water from the same location in a specially designed reactor that allows the filtered sea water to remain liquid and the sampled ice core to remain solid and maintain the temperature gradient of the core. This closely mimics the conditions phytoplankton have been living in, to improve survivability of species during transportation. This method of transportation/storage was used only for the biologically active layer of the sea ice (bottom 0.2m) and over longer periods (3 months). The hybrid system showed some preliminary initial successes in maintaining algal community compositions while increasing their concentrations, however, had some shortcomings regarding simulation and control of irradiation, temperature control as well as introduction of nutrients to the system (Hambrock, Rampai and Walker, 2021).

2.4.2 Simulation of in-situ environmental conditions for laboratory-based experiments on sea ice algae

Fiala & Oriol (1990) conducted investigations of temperature and light intensity on separated Antarctic diatoms in a plant incubator. They cultured 7 species of diatoms (some ice-algae) found in the Southern Ocean and found that optimal growth of the species occurred at $220\mu\text{molm}^{-2}\text{s}^{-1}$ and between 3°C and 5°C . The study however did not indicate how much, if any, adaptation time the diatoms needed. Fiala and Oriol (1990) also note that the growth rate of the tested species must be less than what is seen at $220\mu\text{molm}^{-2}\text{s}^{-1}$ as they receive less than this amount *in situ*, due to their rapid movements under turbulence. A combined effect of temperature and light was noted as one of the limitations of Antarctic phytoplankton growth (Fiala and Oriol, 1990). Additionally, Juhl and Krembs (2010) demonstrated that the diatom, *Nitzschia frigida*, can acclimate to irradiances of up to $110\mu\text{molm}^{-2}\text{s}^{-1}$.

Studies conducted on sea ice algae in liquid cultures are mostly above 2°C and, sea ice algae taxa cultured in liquid form demonstrate optimal growth at temperatures between 2°C and 6°C (Torstensson *et al.*, 2019; Schlie and Karsten, 2016). Sugie *et al.* (2020) demonstrated that higher temperatures, increasing from 3°C to 5°C , enhanced the growth of most sea ice phytoplankton traits, in particular diatoms. A lower salinity however has marginal effects on most phytoplankton species (Sugie *et al.*, 2020). In ice melt incubations, centric diatoms especially, *Thalassiosira spp.* dominated the sea ice phytoplankton community while the pennate diatoms died. It was observed that, in liquid incubations, the growth rate of pennate diatoms is 3.5 times slower than that of

centric diatoms (Yan *et al.*, 2020). Smith Jr, Nelson and Mathot (1999) hypothesize that some sea ice diatoms are adapted to low temperatures and are therefore genetically adapted to certain maximum growth rates that cannot be exceeded.

The physiological activity of sea ice algae is sensitive to changes in ambient salt concentrations. Photosynthetic capacity decreases as salinity moves away from sea water conditions. Antarctic surface water in the Atlantic sector has a salinity of 34psu (Giuseppe Aulicino *et al.*, 2018). When exposed to extreme salinities, sea ice algae exhibit closure of photosystem reaction centers when radiation is applied. Acclimation to either high or low salinity values is possible although the first 3 days of the experiment are characterized by a reduction in biomass and growth rates (Thomas and Dieckmann, 2009). Ryan, Ralph and McMinn (2004) suggest that when experimenting on sea ice phytoplankton, the ratio of the melted ice to filtered seawater should be at least (1:2).

Sea ice diatoms can maintain relatively high growth rates within a wide range of salinity i.e., 10 to 50psu, with maximum photosynthetic rates typically found at salinities comparable to ocean surface water (Grant and Horner, 1976). An example of this was the culturing of the diatom *Nitzschia lecointei* in nutrient-replete conditions and simultaneously increasing the temperature from -1.8°C to 3°C while lowering salinity from 35 to 10psu. This resulted in increased cell abundance (Torstensson *et al.*, 2019). Table 2-1 gives a summary of the effect of salinity on sea ice algae. The table gives a list of previous studies showing that most sea ice algae can maintain normal photosynthesis and growth within a salinity range of 20-50psu (Yan *et al.*, 2020). Nevertheless, if not given enough time to acclimate to changes in salinity, sea ice algae are susceptible to osmotic shock (Ryan *et al.*, 2004).

Table 2-1: A summary of the effect of salinity on photosynthesis and growth of ice algae in previous studies.

Diatoms used	Culture temperature (°C)	Culture Salinity (psu)	Salinity with almost no decrease in algal growth (psu)	Salinity with no photosynthetic growth (psu)	References
Ice algal community dominated by <i>Fragilariopsis curta</i>	2	10 to 30	28-30	None	Ryan <i>et al.</i> , 2004
Ice algal community dominated by <i>Nitzschia stellate</i> and <i>Fragilariopsis curta</i>	-0.7	16, 21, 35, 51 and 65	35 and 51	None	Ralph <i>et al.</i> , 2007
<i>Nitzschia frigida</i>	-8 to -4	73, 109, 145	73	None	Aletsee and Jahnke, 1992
Ice algal community	-3	0, 12, 24 and 36	24 and 36	None	Ryan <i>et al.</i> , 2011
Ice algal community dominated by <i>Nitzschia stellata</i>	-6, -2 and 6	0 to 100	30 to 50	100	Arrigo and Sullivan (1992)

Barcelos e Ramos *et al.* (2017) conducted lab-based experiments on nutrient-specific responses on phytoplankton communities in the North Atlantic Gyre. Single and combined nutrient pulse enrichments were done on phytoplankton collected from sea water and, their responses were

measured. Experiments were conducted in 1.5L bottles. The bottles were placed randomly such that they were all exposed to an approximate temperature of 20°C and a light intensity of $2500\mu\text{molm}^{-2}\text{s}^{-1}$ (Barcelos e Ramos *et al.*, 2017). It is important to note, however, that the setup of the bottles to receive light from the sun and have approximately the same temperature, does not give confidence that light and temperature did not deviate within the bottles, any deviation in temperature or light affects the algae. Aeration was also not considered in the experiment and thus it can be assumed that lack of aeration altered the results of the experiments.

Experiments conducted in an incubator offer control over parameters such as temperature and light, this enhances the confidence of results as one could change only one variable at a time to decouple the effects of specific variables from the observed behavior. It is therefore vital that, for laboratory-based experiments on sea ice algae, incubators such as environmental chambers be utilized in order to make sound conclusions on algae species behavior in response to environmental changes.

2.5 Design considerations for an Environmental Chamber for laboratory-based experiments on sea ice algae

Environmental chambers are usually used when studying the impact the environment has on animals or plants. The most commonly controlled variables are temperature, humidity, and air flow (Lefcourt, Buell and Tasch, 2001). Temperature is an important phenomenon as most biological processes are temperature-dependent. Humidity affects rates of heat transfer thus respiration in plants and air flow is of critical importance in cases where gas fluxes must be measured (Franklin, 1998). Lighting is also an important variable that can be adjusted in an environmental chamber as light intensity directly affects plants (Lefcourt, Buell and Tasch, 2001).

2.5.1 Material of Construction

Assembly of most environmental chambers involves a casing fitted with insulation. Lefcourt, Buell and Tasch (2001) designed a 10.5m long x 7.4m wide x 3.4m high environmental chamber which had 10.2cm thick aluminum panels as the casing and contained injected foam insulation in the interior. The environmental chamber was constructed to investigate the effect of environmental

conditions on gaseous emissions. Ezike *et al.* (2018) designed a 210mm x 260mm x 360mm environmental chamber with a 1mm thick aluminum sheet casing and expanded polystyrene as the insulation. A low-cost and low-energy consuming chamber was constructed to be used in laboratories with a scarce power supply. Aluminum is chosen as material of construction for the casing due to it being relatively cheap and resistant to corrosion (Ezike *et al.*, 2018). Expanded polystyrene was chosen as it is a good thermal insulator with a low weight, low thermal conductivity, and low cost (Franklin, 1998). Foam-filled panels have also been used to construct an environmental chamber. The rigid and durable polyurethane foam-filled panels make use of galvanized sheets as the casing providing both structural support and insulation to the chamber (Lifferth, 2009). This is advantageous as paneling ensures durability and polyurethane has significantly higher insulating values, but is more costly and harder to install (Installed Building Contacts, 2017). Industrial-type chambers are commonly made of steel casing due to its durability and insulated with fiberglass or mineral wool due to it being fire retardant and non-corrosive (IQS Manufacturer Directory, 2019). The door of the environmental chamber should be fitted such that it incurs minimal heat losses. Ezike *et al.* (2018) had rubber fitting on the front wall of the chamber to create an airtight door that had minimal heat losses. A wooden bar was also used to reinforce the door of the chamber.

2.5.2 Environmental controls and regulations

2.5.2.1 Temperature control

Air flow regulation within an environmental chamber depends on the size of the chamber. Walk in chambers make use of ceiling ducts and exhaust ducts to allow for entry and exit of air (Lefcourt, Buell and Tasch, 2001). Franklin (1998) notes that air flow must be decided when designing environmental chambers and air movement that maintains optimum growth of the plant in the chamber should be used. Morse and Evans (1962) suggest an air flow rate of between 0.3 and 0.7ms⁻¹ in a plant growth chamber. Air movement within a chamber can be easily increased by the use of fans or blowers but this depends on the size of the chamber (Franklin, 1998).

Environmental chambers employ two distinct methods for temperature control, each tailored to specific operational requirements. For maintaining ambient room temperature, compressed air systems are utilized, effectively sustaining temperatures within the range of 20-21°C (Darehshouri

et al., 2020). In contrast, for cooler temperature requirements, Peltier elements are commonly deployed in smaller environmental chambers. These thermoelectric coolers are particularly advantageous for achieving precise temperature control in compact units (Greenspan *et al.*, 2016). For larger chambers, heat exchangers integrated within refrigeration cycles are employed, allowing for the maintenance of significantly lower temperatures. (Darehshouri *et al.*, 2020). In most walk-in chambers heat exchangers operate with water or ethylene glycol depending on the desired temperature, to cool the chambers (Franklin, 1998). An example of employing a refrigeration cycle in humidity chambers is the Rankine refrigeration cycle. In this system, the moisture present in the incoming air is utilized to lower the surface temperature of the evaporator heat exchanger. By reducing the temperature to the point where the dew point of the room air is reached, the air is effectively cooled. This cooling process not only condenses moisture but also cools the condenser unit before the air is reheated prior to re-entering the chamber. The result is processed air that is drier but at a higher temperature than its initial state. Consequently, this method presents a challenge for temperature control within the chamber, as the chamber's overall temperature may not be easily regulated in this configuration (Huang, Liao, and Kuo, 2007).

Lefcourt, Buel and Tasch (2001) designed a walk-in chamber that made use of a 20-ton cold water chiller to cool the room to 2°C. The chiller made use of a mixture of propylene glycol and water as the coolant. The primary control mechanism for both temperature and air flow in the walk-in chamber was a simple Proportional, Integral Differential (PID) feedback loop control subroutine. The input for the subroutine is a known setpoint together with its controlled variable while the output is a process control variable (Lefcourt, Buell and Tasch, 2001). Franklin (1998) suggests that temperature deviations of about 10°C inside an environmental chamber should trigger an alarm so that the chamber is turned off quickly before irreparable damage occurs.

2.5.2.2 *Lighting within an Environmental Chamber*

Light Emitting Diodes (LED) have a spectral output of 620 to 680nm thus making them useful for plant irradiation in chambers (Franklin, 1998). Ezike *et al.* (2018) makes use of 40W filament bulbs in their desktop environmental chamber. It is important to note, however, that the chamber was solely for materials testing using light as a heat source (Ezike *et al.*, 2018). In heating chambers, infra-red lamps are used as a source of light and as a heat source within the chamber (Darehshouri *et al.*, 2020). The type of lighting used in a chamber is dependent on the size and use of the chamber. Particular importance is placed on the spectral range of the light and its

corresponding Photosynthetically active Photon Flux Density (PPFD) if the chamber houses plants (Franklin, 1998).

2.6 Rationale of study

The ecological and geochemical impact of phytoplankton productivity is said to be greater in the Southern Ocean than in any other oceanic system, yet sea ice phytoplankton (most prevalent in the Southern Ocean) is understudied. Studying of the ice phytoplankton *in situ* poses challenges. Firstly, it is dependent on prevailing environmental conditions which can fluctuate unpredictably. Secondly, there is a need to use equipment that can withstand harsh weather conditions, which is expensive and can become easily damaged. Furthermore, routine safety checks need to be conducted before any fieldwork can take place, which can create logistical difficulty and can be time-consuming and ultimately costly. Lastly, access to the Marginal Ice Zone (MIZ) of the Southern Ocean is only for a limited time and conditions are often too harsh which limits long-term observation and measurements. Thus, there is a need to utilize land-based facilities for laboratory experiments where variables can be decoupled and controlled, and long-term measurements can be conducted at a relatively lower cost and with better safety conditions.

To experiment on the different sea ice phytoplankton communities on land, transportation which ensures the preservation of the algae communities' compositions is an essential consideration. In addition to this, increasing the algae concentrations is ideal to allow multiple repeats of experiments. The designed hybrid system for transportation of phytoplankton to land-based facilities, though successfully implemented needs further optimization to ensure better input and simulation of irradiance and nutrient supply.

Additionally, for diverse sea ice algae behaviours to be investigated under certain environmental conditions, there is a need for an Environmental Chamber (EC) to be specially designed. This EC will be used to carefully control the variables; temperature and irradiation, and document algae behaviour.

3 RESEARCH AIMS, OBJECTIVES AND KEY QUESTIONS

The aim of this study is to design and/or optimize systems and equipment that will facilitate the laboratory experimentation of sea ice algae from the Marginal Ice Zone (MIZ) of the Southern Ocean (SO). This involves, first, the optimization of an existing hybrid system used to obtain sea ice algae from the Antarctic, and secondly, designing, commissioning, and testing of an Environmental Chamber that will allow controlled temperature, humidity, and irradiance while experimenting on the sea ice algae on a land-based laboratory.

The objectives that emulate this aim are therefore to:

- Optimize the existing hybrid transportation system's irradiance, temperature control, and nutrient supply system to preserve the composition of the sea ice algae community as sampled *in situ* from the SO's MIZ.
- Optimize the existing hybrid transportation system's irradiance, temperature control, and nutrient supply system for possible increases in sea ice algae concentrations from the MIZ of the SO.
- Design an Environmental Chamber that will precisely control temperature, humidity, and irradiance to the targeted levels for experimentation on the sea ice algae.
- Investigation and implementation of protocols in investigating the effect of irradiance on the behaviour of the phytoplankton community from the MIZ of the SO.
- Investigation and implementation of protocols in investigating the effect of temperature on the behaviour of the phytoplankton community from the MIZ of the SO.

3.1 Hypothesis

1. This study hypothesizes that optimizing the irradiance, temperature control, and nutrient supply in a hybrid transportation system will enhance the preservation and concentration of sea ice algae from the Marginal Ice Zone of the Southern Ocean to land based facilities.
2. Laboratory experiments conducted in a specially designed Environmental Chamber will reveal that controlled variations in temperature and light intensity significantly influence

the physiological responses and community composition of sea ice phytoplankton from the Southern Ocean, allowing for a better understanding of their ecological roles and adaptations compared to in situ conditions. This hypothesis suggests that by isolating and manipulating specific environmental variables, researchers can identify key factors that affect phytoplankton growth and survival.

4 OPTIMIZATION OF THE HYBRID REACTOR SYSTEM FOR TRANSPORTATION OF SEA ICE ALGAE

Testing of the hybrid systems was conducted via obtaining ice cores and filtered sea water from the Marginal Ice Zone (MIZ) of the Southern Ocean, then incorporating these into the hybrid system tanks as described in Sections 4.1 and 4.2. The transportation of the hybrid system, and the ice cores, was thus carried out onboard on the SA Agulhas II for the duration of the research cruise after coring and stored in laboratory-based facilities before experimentation commenced. The initial hybrid system was tested during the 2019 Southern Ocean Sesaonal Experiment (SCALE) spring cruise in (Hambrock, Rampai and Walker, 2021). The optimized hybrid tank was tested during the 2022 SCALE winter cruise. The two variations of the hybrid system were therefore tested during different seasons. During the 2022 winter cruise, ice cores were only obtained from one station due to logistical difficulties presented by highly windy conditions, low sea ice extents and concentrations, in addition to a short-scheduled cruise time (3 weeks). In contrast, the 2019 spring cruise allowed for collection of cores from four stations as the conditions were calmer, and due to longer cruise times (6 weeks) there was opportunity to sail to areas of high sea ice coverage and overboard coring. The two cruises also explored different locations thus ice samples obtained from each cruise are from different locations. During the winter 2022 cruise, ice cores were obtained from a pancake (mostly abundant during winter in the MIZ), whereas during the spring 2019 cruise ice cores were obtained from consolidated ice and brash ice. This also meant the ambient temperature and irradiance was different when considering both geographical locations and ice type.

Existing hybrid system as per Hambrock, Rampai and Walker (2021) studies

The initial hybrid system satisfies control over two known parameters that affect algae namely temperature and access to nutrients. The Hybrid system utilised filtered sea water from the site the ice cores were obtained from. This filtered water together with the sampled sea ice core (bottom 20 cm), are placed in the hybrid tank, see Figure 4-1. The sea water temperature is

controlled by heating the bottom of the tank, while the ice core remains solid due to its exposure to the sub-zero atmospheric temperature in the laboratory housing the hybrid system. In addition, there is allowance for the addition of the modified f/2 medium (henceforth referred to as nutrient solutions) prepared as outlined by Hallegraeff, Anderson and Cembella (2004).

The hybrid system consists of a polymer tank wherein the ice core and sea water can be stored, insulation to ensure heat exchange from the sides of the tank does not take place, and an electronic control system to maintain the temperature of the water above freezing temperatures of the sea water. The tank is made from Perspex and insulated with isotherm. The tank sits on top of polystyrene sheets to insulate the tank from the surface it is placed on (Figure 4-1). The design of the hybrid tank ensures that ice temperature is maintained at the atmospheric lab temperature, while water temperature below the sea ice is maintained at -1.8°C (seawater freezing point) or slightly above. The temperature of the water is maintained by an electrical, resistance-based, heating cable at the lower tank wall. This is controlled through a relay attached to a temperature probe immersed in the ocean filled level of the tank. When the water temperature falls below the programmed set point, -2°C , the heating circuit activates and deactivates when the water temperature reaches 0°C . Excessive cooling from the sides and bottom of the tank is prevented through insulation and the heating applied at the lower part of the tank. Solid ice, is therefore, exclusively maintained at the top of the tank, exhibiting a vertical temperature profile.

In the initial hybrid system, Figure 4-1A, three “hybrid tubes” made of polyvinyl chloride, 95 mm in diameter and 400 mm in length, were placed inside the tank. These “hybrid tubes” were placed inside the tank so that they could house each individual ice cores so that the ice cores would not break as ice core diameter was much smaller than diameter of the tank. Breakage would typically occur on the ship under high turbulent weather conditions when the ice cores were still free-floating in the filtered sea water, before a uniform ice forms at the top due to the lab temperatures. The hybrid system was successful in improving survivability of algae and increasing some algae species during transportation. There were some changes in algae communities' composition, this was attributed to notable differences between the hybrid system and *in situ* environments. Radiation could have been one of the major factors that resulted in algae community changes as the light control on the hybrid system was not accounted for appropriately. Initially, the ice cores in the tank were exposed to ambient light of the lab, there was no control over exposure time, intensity and wavelength of the lab lights. Furthermore, no PAR measurements were taken during transportation, rather estimated settings from the lights were used.

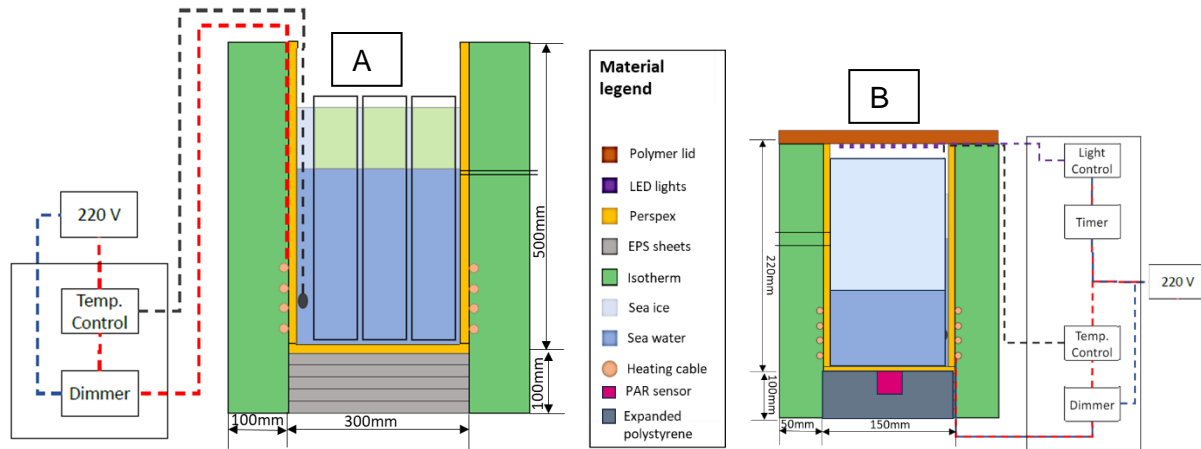


Figure 4-1: I Hybrid system assembly schematic as per A) initial design by Hambrock, Rampai and Walker (2021) and B) optimized hybrid system design

The other limitation that was identified to affect the limitations in algae growth and community compositions is the periodic incorporation of the nutrient solution into the hybrid system, through one small, localized channel drilled through the ice to the filtered ocean water level. Lastly, placing the ice cores into the “hybrid tubes” could have been a limitation. This could have presented a challenge as the temperature probe that controls the relay is in the larger tank and the water temperature in the larger general tank may not be the same as in the localized individual “hybrid tubes”. In addition, due to the hybrid tank being large and the temperature regulation system relying on one localized temperature sensor, ice melted and refroze irregularly at the bottom of the tank as the variation in temperature is large in a larger tank. Considering that phytoplankton mostly inhabit the bottom of the ice cores, constant melting and refreezing of ice would likely result in some phytoplankton species dying due to the osmotic shock.

4.1 Improvements to the Hybrid system design and sampling protocol

Optimization of the hybrid system considered irradiance, size and number of tanks, and insulation to the tanks; this was supplemented by improvements to the sampling protocol of the ice cores for targeted control over the existing and optimized parameters. Other parameters such as materials of construction and temperature control system were not changed. In addition, to evaluate the extent of effectiveness of the hybrid system over the conventional transportation methods, solid and liquid transportation, was also investigated to affirm the effectiveness of the

hybrid system. The solid and liquid transportation methods were prepared and subjected to conditions as outlined by researchers in literature rather than the same conditions as the hybrid tank. This was done in this manner to compare methods largely used currently by researchers and the hybrid method. It is noted, however, that if parameters such as irradiance control (in both solid and liquid transport) and nutrients incorporation (in solid transportation) were introduced to all transport systems, the reported results would be different.

4.1.1 Improvement on the sampling protocols

During the 2019 spring cruise, cores were obtained primarily from consolidated ice, and the bottom 20cm of the core was isolated for incorporation into the hybrid system. Each 20cm core section was further segmented vertically into two hemispheres. The one half was introduced into the hybrid tank while the other was melted for immediate preservation to serve as a “baseline sample” for the algae concentrations and community composition *in situ*. Nutrients were introduced in the hybrid tank every 7 days after being sampled, until melting in land-based laboratories. After the cruise concluded the contents of the hybrid system tanks were melted and stored in a fridge at 5°C. The liquid culture was stored in 250ml and 500ml glass bottles and nutrient concentrations readjusted regularly. The glass bottles had a continuous supply of air providing gases and agitation (Hambrock, Rampai and Walker, 2021).

During the winter 2022 cruise, five cores were obtained from a pancake per station. One core was segmented vertically into two hemispheres. One hemisphere was immediately melted in the dark at 5°C and stored under the same conditions for the duration of the cruise. The second hemisphere was stored in a black plastic core bag and stored at -10°C for the duration of the cruise. The second ice core was tested for temperature and salinity measurements, with the bottom 20cm of the core also sampled and preserved for a “baseline sample” for the algae concentrations and community composition *in situ*. The top of the core had an average temperature of -2.05°C while the bottom had a temperature of -1.9°C. The lab in which the hybrid tanks were was -10°C, a vastly different temperature from their natural conditions. Three cores were introduced into the hybrid system tanks (bottom 18cm), to account for the size of tanks and considering the phytoplankton community profile vertically along the core. Sampling and testing of more than one core increased the reliability of results as discussed in Section 4.1.2. For testing of the optimized hybrid tank, cores were obtained on the 24th of July 2022 from one station, -59.16485S, 0.85777E. Two pancakes were lifted at the station and cored using a 9cm Kovacs

Mark II ice corer, on the ship deck. Cores used in the hybrid systems reported in this work were obtained from one of the pancakes which had a 1cm snow layer on top of the pancake.

During pancake lifting, a 20L bucket was used to collect sea water from the location of the pancake before lifting. A rope was tied to the bucket, and the bucket was thrown overboard and then lifted using a pulley system. Hybrid tanks were set up in a lab with an ambient temperature of -10°C. The hybrid tanks were filled to 4cm with the collected and filtered sea water then left open awaiting cores. Cores obtained from the pancake were segmented with a circular saw and introduced into the hybrid system tanks within 30 minutes of extraction to limit the degree of brine loss.

Figure 4-2 shows sea ice conditions on the day the pancake was lifted and cored on deck, versus one of the days sampling was done for the initial hybrid system. Unlike in spring where discoloration is seen in the ice (Hambrock, Rampai and Walker, 2021), to show the presence of blooming phytoplankton, the ice in winter is clear. In addition, observations of the state of the sea ice in the hybrid system tanks during transportation to land revealed discoloration for the 2019 spring cruise (Hambrock, Rampai and Walker, 2021) and nothing to that effect in the 2022 winter cruise. This was expected as the collection had been of winter samples, and it was not expected to see discoloration as phytoplankton would not have started blooming.

Every 3-day cycle, the hybrid tanks were supplemented with nutrients prepared a month before the cruise. The Synthetic Ocean Water and the major nutrients were stored in a 5-degree fridge while the vitamin stock solution was frozen. The lid of the tanks was opened, and the lights turned off. Three equidistant holes across the tank center were drilled through the ice to the filtered sea water level, and nutrients (Appendix C) were injected through these holes using a milli Q rinsed pipette. In the 2019 spring cruise nutrients were injected through one hole, this was changed to ensure nutrients were concentrated more evenly in the tank. Transfer of nutrients was conducted within 7 minutes of opening the lid of the tank in all cases to prevent long exposure to variable light and prevent the nutrient solution from freezing due to exposure to the sub-zero temperatures in the lab.

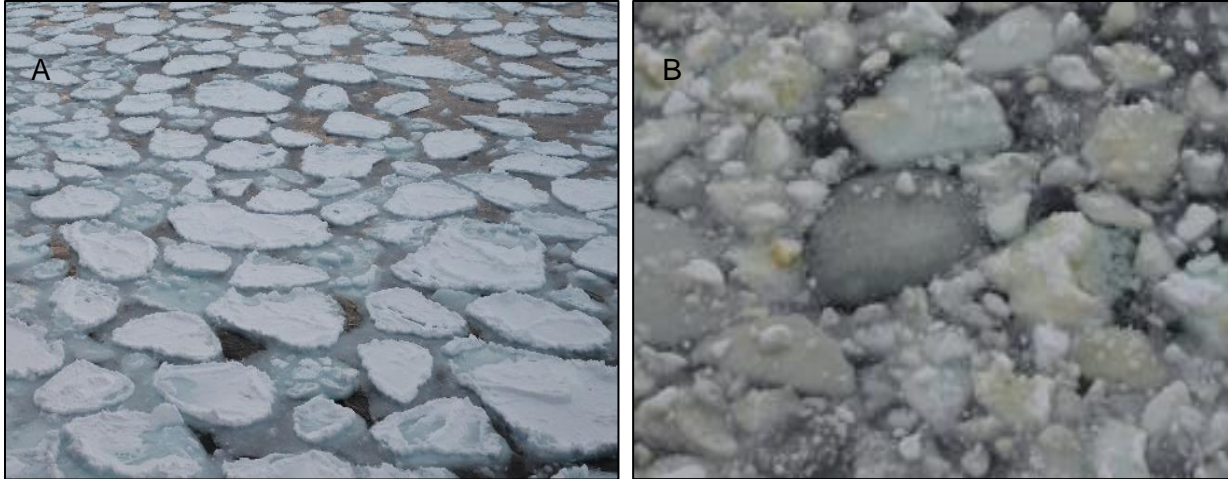


Figure 4-2: Sea ice conditions (A) on the 24th of July 2022 59.16485S, 0.85777E (B) on the 22nd of October 2019, brash ice showing algae (discoloration) floating in the Southern Ocean (Hambrock, Rampai and Walker, 2021)

Upon conclusion of the winter cruise, hybrid tanks were transported to a -20°C freezer for latter experiments and investigations. One hybrid tank (Hybrid tank 1), reported in this report, was melted a week after the cruise (2 weeks of transportation) by placing it in an environmental chamber under controlled irradiation as on the ship and a constant ambient temperature of -1.8°C. Melting at -1.8°C, instead of 5°C as in the initial hybrid system, was to ensure gradual temperature change in the system thus not shocking the phytoplankton. Three samples, from different levels and locations of the tank, were taken from the meltwater and mixed with Lugol's solution. The first sample was taken from the top of the tank, the second sample at the 500ml point i.e., the middle of the tank, and the third sample was obtained 20ml from the bottom of the tank. The melted solutions, kept in the Perspex hybrid system tank, were later transferred to a 5-degree fridge and were gently stirred with a glass rod previously rinsed with milli Q water and supplemented with nutrients regularly. These samples are kept in the dark and utilized for subsequent experiments. The core transported as a solid, was also melted in the environmental chamber at -1.8°C. Sub-samples were taken from the melt as done for the hybrid tank and fixed with Lugol's solution, the same was done for the core transported as a liquid.

The second hybrid tank (Hybrid tank 2) was to be melted exactly 6 weeks after the cruise and the last hybrid tank (Hybrid tank 3) was to be melted 12 weeks after the cruise. However, the lab was impacted by loadshedding multiple times a day for a few weeks. This resulted in sub-optimal functionality of the heating and light systems, thus compromising the comparability of these tanks to the hybrid system tank melted immediately after the 2022 winter cruise. Hambrock, Rampai and Walker (2021) proved that increased hybrid tank incubation time increased cell concentration

and hybrid tanks were to be melted in increasing time increments to show that this is true for all hybrid tanks. In Hambrock, Rampai and Walker (2021) studies, hybrid system samples were melted 29 to 39 days after collecting them.

4.1.2 Number and size of the hybrid tank

Perspex was maintained as the material of construction due to its flexibility for the tank in the hybrid system. Perspex also does not introduce trace elements that may contaminate the nutrient solution. Additionally, Perspex is transparent, allowing for ease of visual inspection during transportation (Maizey Engineering Plastic Products, 2021). The aspect ratio and the circular shape of the tanks were maintained to lower the risk of wall fracture when sea ice expands (Grenfell and Perovich, 1981). A smaller tank size, from 30L to 3L, was chosen to allow for better temperature sensing and control (Figure 4-1B), this only allowed one ice core in the tank. To supplement for, three tanks were utilized in order not to lose the quantity of samples collected. Multiple tanks allowed for redundancy if a system failure occurs in one of the hybrid systems. In addition, a study on the variables changed during storage can be undertaken by changing one variable per tank for multiple tanks in one station. Most importantly, smaller tanks offer more control over the temperature variation in the filtered water at the bottom of the tank. Reducing the surface area over which the relay system covered, meant the temperature probe measurements from inside the tank were more representative of all the water at the bottom of the tank. This eradicated the melting and refreezing of the ice at the ice-ocean interface. This may largely be due to the heat capacity of the system coupled with the insulation around the tanks and lids reducing airflow on the sea-ice surface. Maximum ice depth fluctuations were 15mm, a massive reduction from the maximum of 100mm the initial hybrid system experienced. The utilized “hybrid tubes” from the initial design were discarded as the diameter of the optimized hybrid system was sufficient to prevent the breakage of the cores as explained previously, the “hybrid tubes” also interfere with the monitoring of the ice cores during transportation (Figure 4-1A).

Due to a change in dimensions of the tank, thickness of the insulating material had to be reevaluated. Isotherm was maintained as the choice of insulation, insulating the sides of the tank and expanded polystyrene insulating the base of the tank. A top-down cooling approach is required to imitate growth of sea ice in the Southern Ocean. Thus, all cooling from the sides and the bottom is undesired. To combat this, insulation is used on the sides and at the bottom of the tank. Isotherm has an absorption capacity of 2% by mass of moisture making it hydrophobic (Brits

Nonwoven, 2020) and thus suitable for use in the laboratory where moisture accumulates. Isotherm was wrapped with black plastic sheeting to prevent light from entering the tank through the sides. Expanded polystyrene was chosen as insulation for the bottom of the tanks as it is water repellent and sufficiently rigid to support the hybrid system tank and its contents (Cumulus Insulation, 2019). The side insulation was reduced by 50mm to better fit and function in the optimized hybrid system tanks with smaller dimensions as justified below:

Williams (1963) describes the net heat flux from natural water surfaces as Equation 4-1,

Equation 4-1

$$Q_a = Q_c + Q_{lw} + Q_e - Q_{sw}$$

Where Q_a is the net heat flux, Q_c is convective heat loss, Q_{lw} is long wave radiation, Q_e is evaporative heat transfer and Q_{sw} is short wave radiation. For the cylindrical tank, heat loss from the base and the walls also has to be included and the modified equation is as in Equation 4-2, where Q_w is heat loss from the walls and Q_{base} is heat loss from the base.

Equation 4-2

$$Q_a = Q_c + Q_{walls} + Q_{base} + Q_{lw} + Q_e - Q_{sw}$$

The hybrid system was utilized indoors thus incoming short-wave radiation and long wave radiation were assumed to be zero. Since ambient temperature is below the freezing point, evaporative heat transfer can be assumed to be zero. The simplified equation is as below:

Equation 4-3

$$Q_a = Q_c + Q_{walls} + Q_{base}$$

It is desired that convective heat loss be much greater than conduction i.e., $Q_c \gg \gg \gg Q_{walls} + Q_{base}$

Equation 4-4

$$Q_c = h_o A (T_w - T_a)$$

Equation 4-5

$$Q_{walls} = \frac{kA(T_w - T_a)}{l}$$

Equation 4-6

$$Q_{base} = \frac{kA(T_w - T_a)}{l}$$

Where h_o is the bulk heat transfer coefficient and A is the surface area while T_w and T_a refer to wall temperature and ambient temperature respectively. k is the thermal conductivity and l is insulation thickness, for this study the values used can be found in Table 4-1.

Table 4-1: Variables for the materials in Figure 4-1 considered for insulation of hybrid system tank contents form the atmospheric conditions.

	Material	Thickness (mm)	Thermal conductivity (Wm⁻¹K⁻¹)	Reference
Tank	Perspex	5	0.18	(Maizey Engineering Plastic Products, 2021)
	Isotherm	50	0.0552	(Brits Nonwoven, 2020)
Insulation	Expanded polystyrene	100	0.035	(Cumulus Insulation, 2019)

Ashton (1989) suggested that bulk heat transfer coefficient is $10\text{Wm}^{-2}\text{s}^{-1}$ for calm conditions and $30\text{Wm}^{-2}\text{s}^{-1}$ for high wind conditions. Forced cooling occurs in the cold lab as a fan is used to promote air flow, inherently increasing heat transfer rate, thus the high value can be assumed to be the bulk heat transfer coefficient.

It is assumed that the thermal conductivity R is given by $R = \frac{k}{L}$ Where L is the thickness of each layer. The thickness of the Perspex tank is 5mm while thickness of the insulation was 50mm, Figure 4-1B. The total value of R is determined as $R_1 + R_2 + \dots + R_n$ and found to be $42.552\text{Wm}^{-2}\text{K}^{-1}$. Determining k , where L is for the insulation on the walls and $k = \frac{l}{R}$, the value is found to be $0.00235\text{Wm}^{-1}\cdot\text{K}^{-1}$. $Q_c \gg \gg \gg Q_{walls}$ is sufficed as $30A(T_w - T_a) > 0.0235A(T_w - T_a)$. When calculated for the base, the same conclusion is reached and thus convective heat loss at the ice-atmosphere surface is said to be 1 500 times greater than heat loss through the tank walls. Insulation massively reduces heat loss from tank walls and tank base. Furthermore, to prevent ice formation

completely to the bottom of the tank, heating coils are placed at the bottom 50mm of the tank as in the initial hybrid system.

4.1.3 Irradiance input and measurement

Irradiance was also considered in the optimization of the hybrid system. Irradiance affects algae species and is considered one of the main parameters to affect algae growth, thus, the optimized hybrid system incorporated careful control of irradiance with community survival and preservation in mind. LiCOR 191 PAR sensors, connected to a Campbell CR5000X datalogger were used to determine PAR under the pancake on the day of coring. PAR at the bottom of the pancake was determined to be an average of $1.05\mu\text{molm}^{-2}\text{s}^{-1}$. Light intensity for the tanks was adjusted in accordance with these measured values. In addition, there was consideration for the lack of snow and decrease in the height of the ice sheet when transferring to the hybrid system tanks.

Cool white 4000K LED strip lights were attached to a flexible polymer lid that covers the hybrid tank. The LED lights offered a full photomorphogenic plant response with a spectrum of 380-450nm. The PPFD of the LED lights ranged from 0-250 $\mu\text{molm}^{-2}\text{s}^{-1}$, which is ideal considering the light experienced by phytoplankton at the bottom of ice sheets. The lights system was set up such that all three tanks from a single coring station will receive light from a single strip light, of the same intensity. The strip of lights also works with a dimmer to adjust light intensity as desired, this allowed for different light intensities for every coring station as per the *in situ* condition of the sea ice algae. PAR sensors were positioned at the bottom of every hybrid system tank for the monitoring and logging of light intensity during transportation, Figure 4-1B.

For the optimized hybrid setup, CS310 Campbell par sensors which work with Campbell CR3000X datalogger were used. The CS310 par sensors can measure light of up to 4000 $\mu\text{molm}^{-2}\text{s}^{-1}$. The Campbell CR3000X datalogger records light intensity measurements every 5 seconds with values being averaged over 150 seconds. These PAR sensors operate over a temperature range of -40°C to +70°C which made them suitable for this application. The datalogger, however, had to be insulated from the sub-zero conditions of the lab as it is not water resistant and was specified to be operational at room temperature.

The control of turning lights on and off as per estimated daylight hours was operated manually, this was not ideal and merits incorporation of an automated system, however, this was sufficient

for the purpose of this study. To calculate the amount of time between sunrise and sunset, the modified version of the CBM model as developed by Schoolfield (1982) was used still (Forsythe *et al.*, 1995). The model calculates day light hours depending on location, time of the year, and chosen definition of day length. The modified model achieves a maximum error of 7 minutes for a day between 30°S and 60°N, making it sufficiently accurate for any conventional ecological purpose. The modified CBM model is as in Equations 4-7 to 4-9.

Equation 4-7

$$\theta = 0.2163108 + 2 \arctan(0.9671396 \tan(0.00860(J - 186)))$$

Equation 4-8

$$\varphi = \arcsin(0.39795 \cos\theta)$$

Equation 4-9

$$D = 24 - \frac{24}{\pi} \arccos\left(\frac{\sin \frac{p\pi}{180} + \sin \frac{L\pi}{180} \sin\varphi}{\cos \frac{L\pi}{180} \cos\varphi}\right)$$

" θ " denotes the revolution angle of the sun (in radians), "J" the day of the year, " φ " the sun's declination angle (in radians), "L" the latitude, "p" the day length coefficient (in degrees) and "D" the amount of daylight in hours (Forsythe *et al.*, 1995). Based on the latitude and date of sampling, daylight hours were estimated to be 7 hours. Despite the usage of only the bottom 18cm and lack of snow cover added to the samples in the hybrid system tanks, daylight hours were kept at 7 hours to facilitate bloom during transportation without significantly changing environmental conditions to which phytoplankton were exposed to.

4.2 Results of optimization

Bearing in mind the differences in season and location when considering the optimization of the hybrid system, below are the results of the optimized system and the differences from the initial system.

4.2.1 Quantification of phytoplankton

In addition to ship-based sampling protocols, further protocol optimization was considered for the analytical methods used to measure sea ice algae growth.

Quantification of phytoplankton communities was done via microscopy. For each sample, 50ml was poured into a settling chamber and left over 24 hours to allow for the settling of phytoplankton. Single wellled slides, with a diameter of 26mm and a depth of 5.0mm, with a volume of 2.7ml were utilized. Counting and identification of phytoplankton were conducted.

Phytoplankton were counted within single transect passes under 400X magnification with an inverted Zeiss Axiovert.A1 microscope using a quicksilver lamp as a light source. The magnification area was measured to be 0.56mm, bringing the transect volume to 0.073ml. A microscope integrated Axiocam 105 color was used to produce images of phytoplankton for classification and documentation purposes. Cell concentrations were calculated by dividing the number of counted cells of each taxonomic group by the transect volume. Due to a limitation in microscope resolution, some algae taxa could not be accurately identified to the species level.

4.2.2 Microscopy findings

Phytoplankton concentrations ranged from 460 to 6 680 cells per ml with a cell length of 10µm as the lower identification boundary due to magnification limitations. Overall, 9 dinoflagellates were counted, with the remainder identified as being diatoms. As such, reporting was solely focused on diatoms.

Figure 4-3 shows the class-specific concentrations for the different methods of transportation to lab-based facilities. “Baseline” is the cut core, that was immediately melted and preserved on the ship after coring, and serves as a baseline for all transport methods; hybrid transport, solid core transport, and liquid transport. Differences between transport mode and Baseline concentrations within a labelled transport system thus show growth or loss of algae during transportation. Overall concentrations can be interpreted from Figure 4-3 as the sum of the pennate and centric concentrations. Liquid transport resulted in the greatest loss of phytoplankton. Total cell concentration was reduced for the sample transported as a liquid. Hybrid tank 1 shows increased

cell concentration while solid transport has some brine losses but tries to maintain the cell concentration. Hybrid tank 1 supports Hambrock, Rampai and Walker (2021) findings which correlate hybrid tank incubation with increased cell concentration.

The liquid transport was stored at 5°C in the dark in a closed Tupperware. The Tupperware was closed as the fridge housed other chemicals being used on the ship. Regular swirling of the Tupperware helped maintain cell suspension. Losses in solid transport can be stipulated to brine loss, however, losses in liquid transport are quite significant and can be due to a lack of aeration and stresses induced on the algae by melting post-coring (Mikkelsen and Witkowski, 2010). Algae also stick to the sides of hybrid tanks (Hambrock, Rampai and Walker, 2021), and as such brine channels in the hybrid tanks and solid transport may have localized nutrients for phytoplankton species when compared to transportation in liquid form. Both solid and liquid transportation did not have supplementation of nutrients. The protocol works well for solid transport as there is not a huge decrease in phytoplankton cells when compared to liquid transportation. However, nutrient availability may have been a concern in the liquid transport method. Therefore, for comparative studies, it is recommended to add nutrients to the liquid transport while keeping it in the dark.

Baseline cell count shows that 67% of the species in ice, were made out of pennate diatoms with the common pennate species, making 20% of the total population, being the *Navicula sp* (Figure 4-3). Louw, Walker and Fawcett (2022) studied the community composition, and distribution in the marginal ice zone of the Southern Ocean during the winter of 2017. From sampling three pancakes, 65°S, and 30°E of the Indian Sector, of the Southern Ocean, the study concluded that diatoms of the pennate genera dominate the sea ice protist community. This is generally anticipated for the Southern Ocean (Hop *et al.*, 2020; Lizotte, 2003; Kauko *et al.*, 2018). Van Leeuwe *et al.* 2018 suggest that the dominance of pennate taxa throughout sea ice profiles is a result of species being able to migrate freely within brine channels.

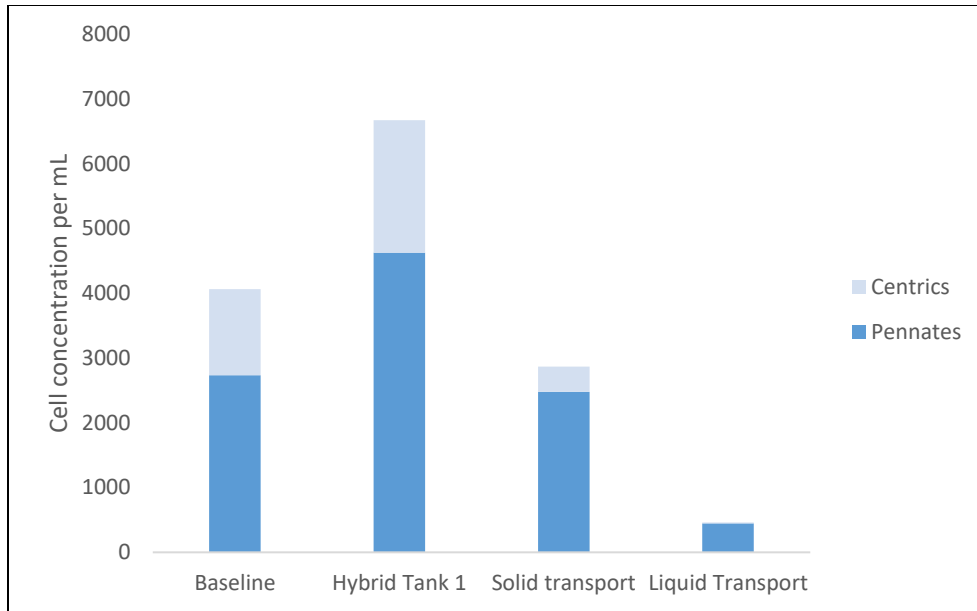


Figure 4-3: Diatom concentration from extraction in the marginal sea-ice zone in the Southern Ocean to UCT labs using the different forms of transportation.

Figure 4-4 shows the unidentified pennates in this study. Debris of the identified taxa was found in all samples but most significant in the hybrid tank. Figure 4-5 shows the most abundant pennate taxa. The largest fraction of the pennates was found to be *Navicula spp* with sizes ranging from 30 to 200µm in length. *Cylindrotheca* also exhibited large size ranges comparable to *Navicula spp*. Figure 4-6 shows the centrics identified in the study. The most abundant centrics were *Dactyliosolen antarctica* and the *Chaetoceros spp*. Debris of *Chaetoceros* cells and *Dactyliosolen* cells were most abundant. Figure 4-6C shows the *Thalassiosira sp.* which came in different sizes ranging from 10 to 40µm in diameter and did not have any debris despite the varying sizes.

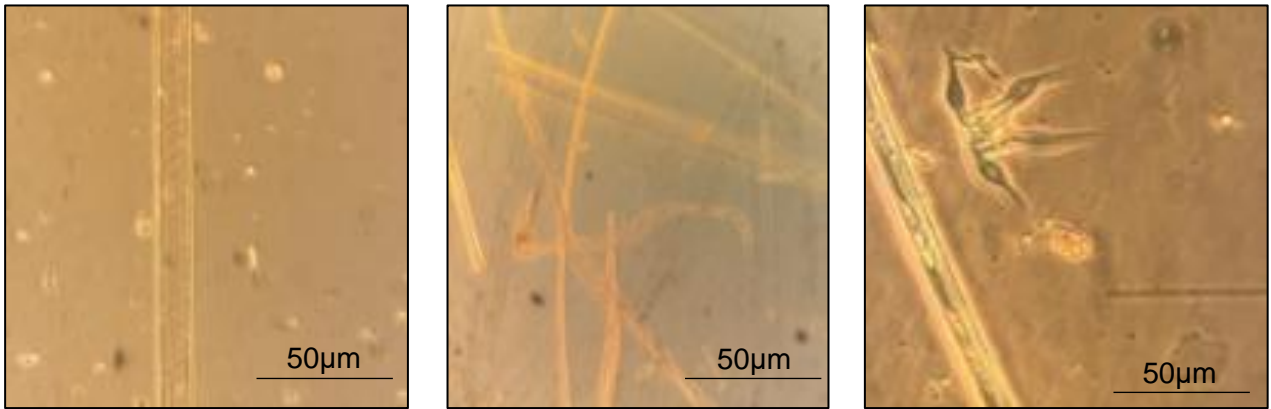


Figure 4-4: Unidentified diatoms all grouped unidentified pennates

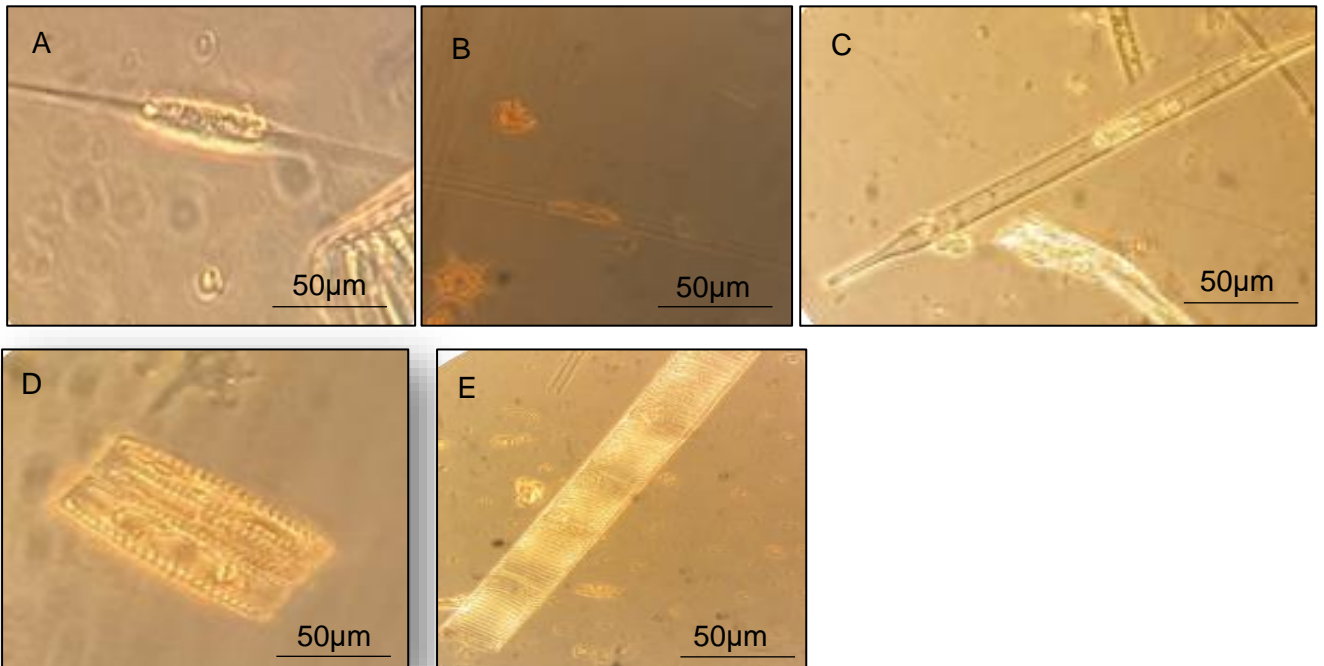


Figure 4-5: Dominant pennates: (A) *Cylindrotheca* (B) *Pseudo-nitzschia* (C) *Navicula* sp. (D) *Fragilariopsis kerguelensis* (E) *Striatella unipunctata*

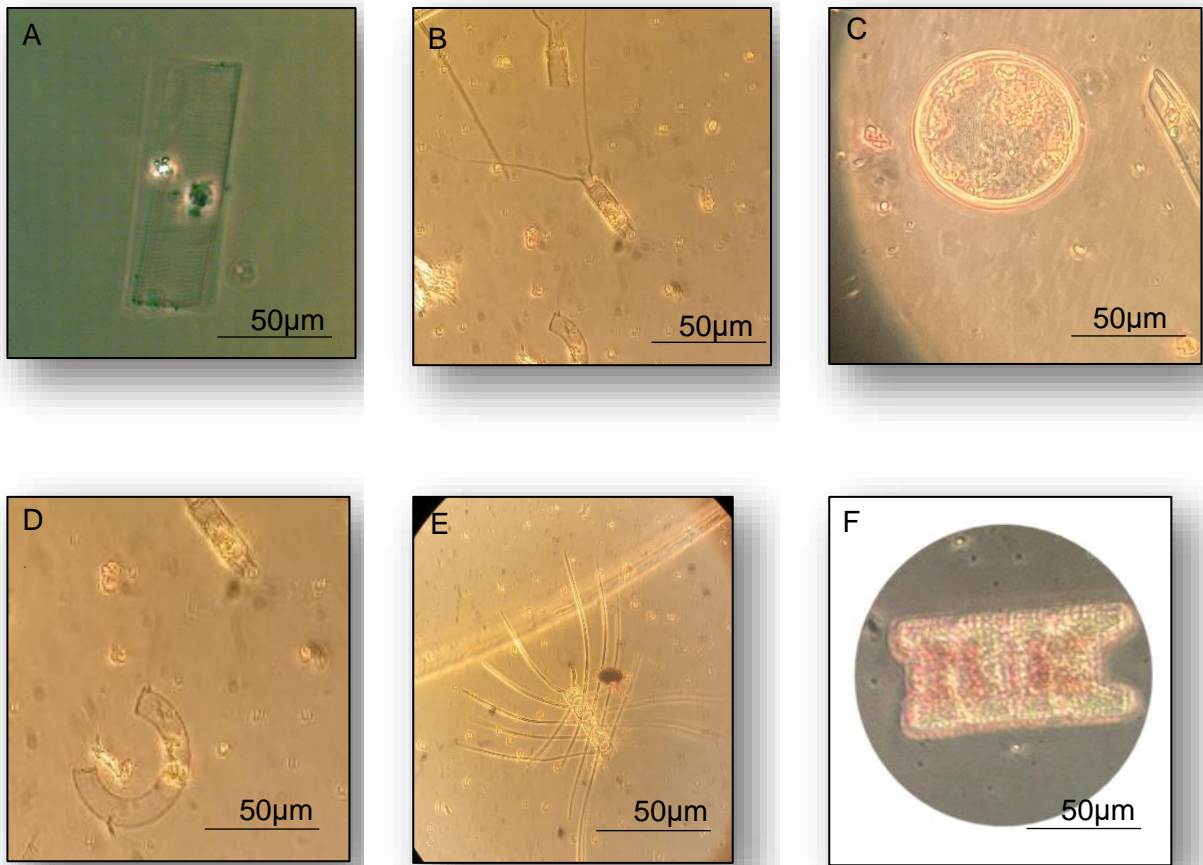


Figure 4-6: Centrics identified: (A) *Dactyliosolen* sp. (B) *Chaetoceros* sp. (C) *Thalassiosira* sp. (D) *Dactyliosolen* sp. (E) *Chaetoceros* sp. (F) *Eucampia antarctica* sp.

The different taxonomic groups in all the modes of transportation are shown in Figure 4-8. Figure 4-8 gives taxonomic distributions that illustrate fractional change of taxonomic groups through intra-sample comparisons of the fractions, for all modes of transportation. Different taxonomic groups show growth or reduction depending on the mode of transport. All taxonomic groups increase in cell concentration in the hybrid tank. Figure 4-9 shows that, in the hybrid tank, except for *Pseudo-nitzschia* and *Dactyliosolen antarctica*, all the other species almost double in cell count, with the unidentified pennates almost tripling. Solid transport particularly shows an increase in *Pseudo-nitzschia* even though all other taxonomic groups show a concentration decrease. *Navicula* spp. and the *Chaetoceros* spp. display great resilience in both the hybrid tank and the solid transport. Yan *et al.* (2020) observed that *Nitzschia* and *Navicula* spp. have a high mortality rate during melting as they are mostly hindered by osmotic stress, thus their abundance is mostly

in solid transport. *Fragilariopsis kerguelensis* shows the most resilience in liquid transport, being the most abundant species. This is well illustrated in Figure 4-8.

A test for normality could not be conducted on the samples as limitations explained earlier resulted in only Hybrid tank 1 being tested, as such normality was not assumed. Bray Curtis Dissimilarity indices for all the transport modes in comparison with the baseline, support the claim that changes during transportation are lower for the hybrid tank and solid transport than those accrued in liquid transport (Figure A4). An empirically derived logistic growth function for overall cell concentrations after transportation is given in Figure 4-7. The logistic growth approach is assumed as hybrid tank simulates growth with limitations of space and nutrient availability. The logistic growth equation is as given in equation 4-10, where a is the population upper boundary, r is a growth rate constant, and b is a determinant for the y-intercept.

Equation 4-10

$$y = \frac{a}{1 + be^{-rx}}$$

Equation 4-10 and the derived parameters, $a = 4\,063$ cells/ml (maximum cell concentration before transportation), $b = 100$ (shift on the x-axis) and $r = 0.0459$ (growth rate per day) can be used to roughly estimate the final concentrations achieved in the hybrid tanks during transportation, for similar ice growth conditions. This is because the correlation coefficient (R^2) achieved is almost 1 suggesting a reasonably good fit. The correlation coefficient may however be slightly less than one as the function under investigation is nonlinear.

The variable in x in the constructed function (Equation 4-10) is unknown. This is because the time of formation of phytoplankton species *in situ* is unknown, and growth conditions *in situ* are assumed to not correspond with growth conditions in the hybrid tanks. The variable in x was therefore assumed to be the transportation time, optimized in conjunction with optimizations for the upper population boundary and the growth rate, by minimizing the squared error in y of the real data relative to the assumed function. Within the first 14 days in the hybrid tank, the phytoplankton cells are assumed to still be in the increasing growth rate phase and will take approximately 150 days to reach carrying capacity.

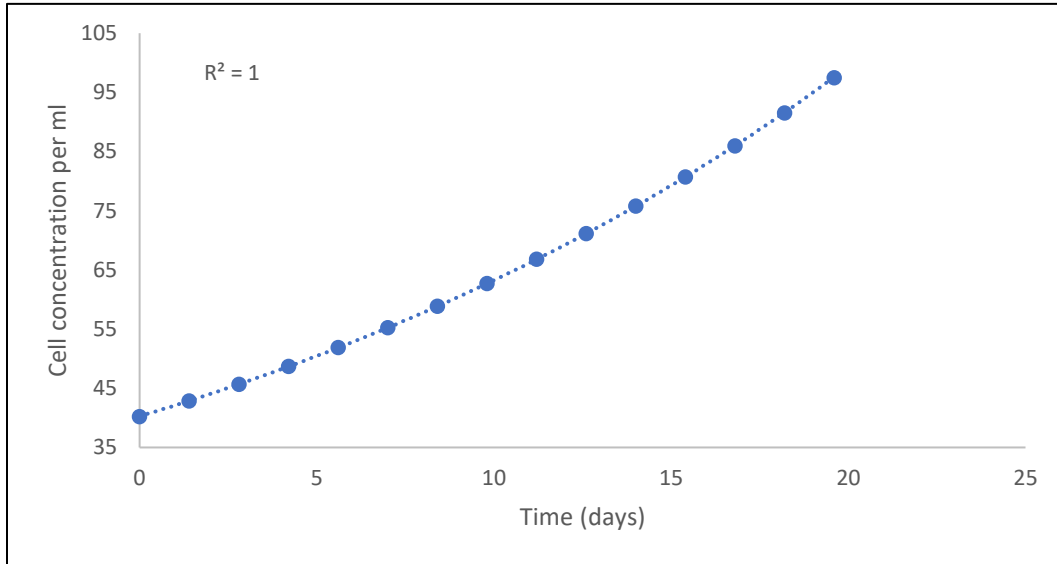


Figure 4-7: Empirically suggested logistic growth trend for cell growth in hybrid tanks during transportation

Even with the lack of results from Hybrid tank 2 and Hybrid tank 3, this data and Hambrock, Rampai and Walker (2021) studies provide strong evidence showing that hybrid tanks promote the survival of phytoplankton species. This is especially important for scientists intending to study ice core communities. The data also shows the potential to increase the cell concentrations with the use of the hybrid tank.

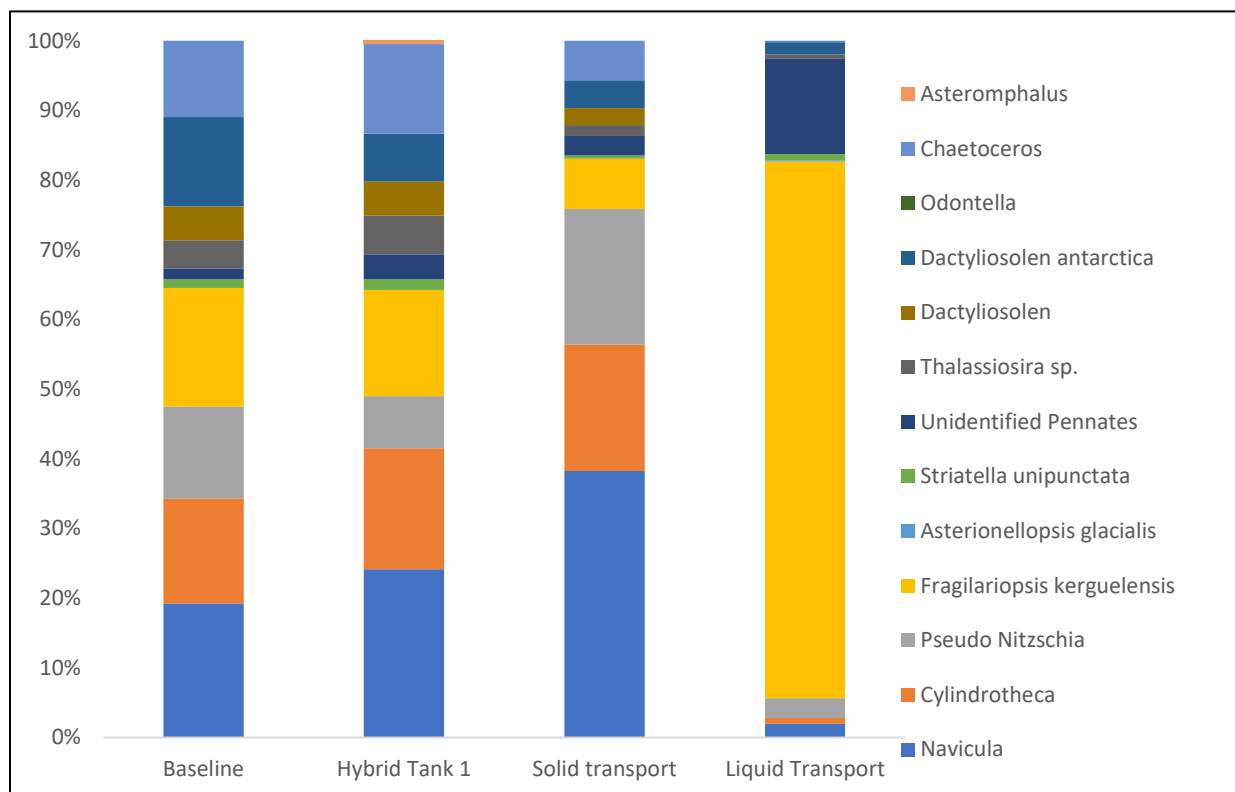


Figure 4-8: Taxonomic distributions illustrating fractional change of taxonomic groups through intra-sample comparisons of the fractions, for all modes of transportation.

4.2.3 Is the hybrid tank optimized?

Even though the initial hybrid tank was used to obtain phytoplankton species in spring and the optimized tank tested in winter, a comparison can be made on community survival in the two tanks. The expected difference in obtained species is the presence of more centrics in the cores obtained in winter when compared to spring. Arrigo (2016) found that centric species are mostly found in newly formed ice, under calm conditions, whereas more diverging conditions such as spring favor pennate species. The majority of the species obtained in the spring 2019 cruise were unidentified pennates and unidentified centrics which are very different from the unidentifiables in this study, which are also not the majority. Sizes of the species obtained in the spring 2019 cruise are comparable to those obtained in the winter 2022 cruise.

In order to fully analyze the extent of the difference before and after transportation, the difference between species composition before and after transportation is calculated and expressed as a percentage of the initial composition before transportation (Figure 4-9 and Figure 4-10).

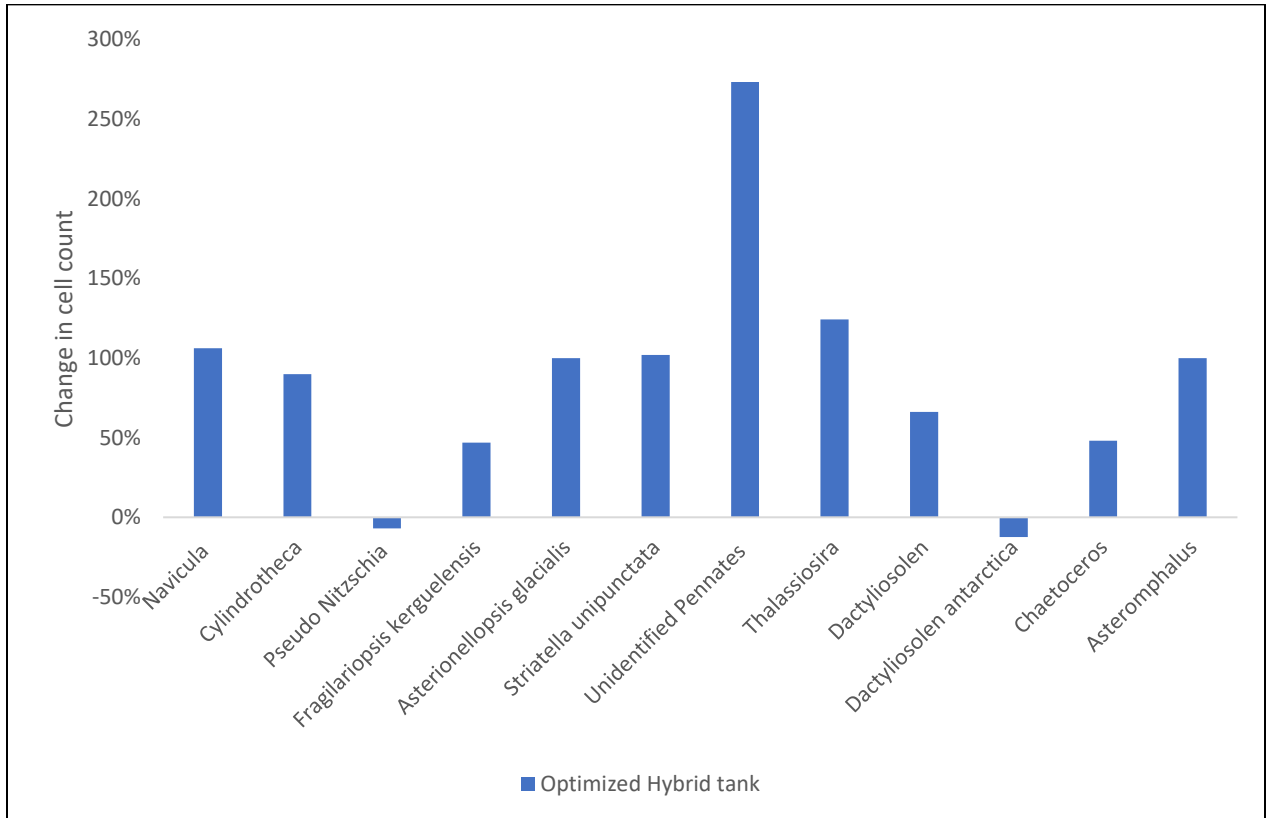


Figure 4-9: Change in cell count in comparison to baseline species for the optimized hybrid tank

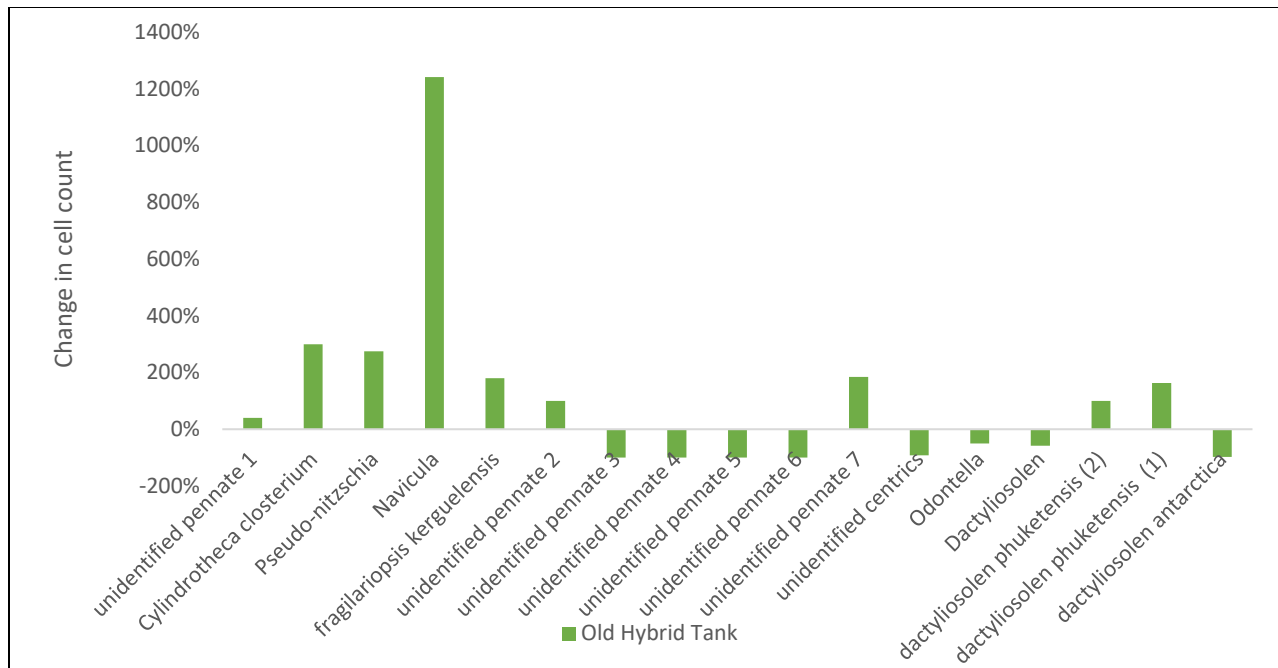


Figure 4-10: Change in cell count in comparison to baseline species for the initial hybrid tank (Hambrock, Rampai and Walker, 2021)

Figures 4-9 and Figure 4-10 show the clear differences in community composition between the initial hybrid tank as per Hambrock, Rampai and Walker (2021), and the optimized hybrid tank. A smaller tank which has more control over the temperature and has dedicated irradiance improves community survival. Except for one pennate species and one centric species, all the other phytoplankton species survived and increased cell concentration in the optimized hybrid tank. Figure 4-10 shows the phytoplankton species resilient to the ice depth fluctuations and rapid change in irradiance in the initial hybrid tank. Unidentified pennates 7 refers to the group of unidentified pennates that was the majority (Appendix A2). The study had many unidentified pennate species due to magnification of the microscope which enabled the determination of only shape but failed to identify specific structures which means correct identification of the species could not be done. The results from Figure 4-10 also show that the community collected had a lot of unidentified species that did not survive whereas in the optimized hybrid tank almost all species survived. The initial hybrid tank had larger increases in cell concentration for the species that survived when compared to the optimized hybrid tank and this is attributed to the high concentration per mL i.e., 46 000 cells per mL that the tank started with when compared to a starting concentration of 4 000 cells per mL in the optimized hybrid tank. The observed difference in the starting concentrations is a result of samples being collected in spring and winter respectively.

5 ENVIRONMENTAL CHAMBER DESIGN CONSIDERATIONS

When designing environmental chambers, careful consideration must be put into construction and operating costs. Dynamic characteristics that control variables must be satisfied (Lefcourt, Buell and Tasch, 2001) The one environmental effect to be considered when experimenting on phytoplankton is temperature thus a temperature environmental chamber is to be designed.

5.1 Materials and Methods

A temperature Environmental Chamber (EC) has been constructed to control temperature when experimenting on phytoplankton. A benchtop EC has been designed to allow for small-volume experimentation of phytoplankton. The EC has internal dimensions of 730 x 550 x 510mm, giving it an internal volume of 204 liters. The external dimensions of the EC are 840 x 560 x 520mm making the total volume of the chamber 245L. The base of the chamber houses 4 aquariums placed along its length. The dimensions of the EC were therefore chosen to give equal spacing between aquariums during experimentation, as well as equal spacing of aquarium from the cooling plate and the light fixture (Appendix B3).

Fabrication of the EC was done using perspex sheets 5mm thick, as the casing of the EC. In addition to being relatively cheap, perspex is light and relatively strong which makes it easy when transporting the EC (Maizey Engineering Plastic Products, 2021). The EC is fitted with expanded polystyrene 50mm thick which acts as insulation (Appendix B1). The polystyrene foam at the bottom plate of the EC has a thickness of 60mm and is built such that three par sensors of diameter 26mm and height 36mm, can be inserted in it. Expanded polystyrene is a good thermal insulator having a thermal conductivity of $0.035\text{W m}^{-1} \text{K}^{-1}$. It is also very light and relatively cheap (Cumulus Insulation, 2019).

The EC has been fabricated such that the top perspex sheet and polystyrene foam (top plate) are detachable making the door of the EC. The door of the EC has also been made such that a light fixture 1 000mm long attaches to it, giving a perforation to the EC which allows gaseous exchange within the EC (Figure 5-1A: Appendix B3). It is advised that there be a beaker with water in the EC during the conduction of experiments to provide humidity in the air.

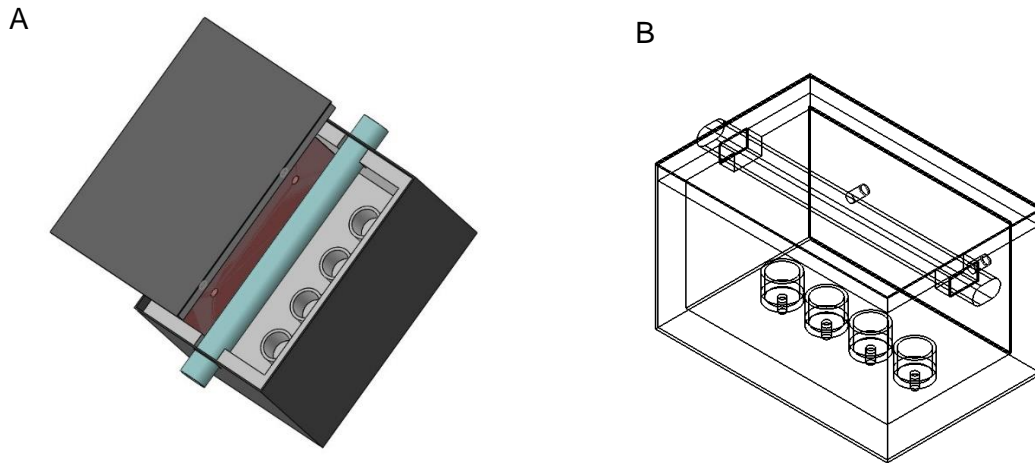


Figure 5-1: (A) EC view from the top with the lid open showing cooling plate (red) light and aquariums, (B) Sketch to show positioning of aquariums, par sensors and light in EC.

The constructed and functional temperature environmental chamber is as shown in Figure 5-1, (Appendix B3). Table 5-1 below outlines the cost of material used in the fabrication of the EC. The major costs arise from the specialized par sensors, the specialized light, and the chiller. Unlike the cost of conventional chambers, this EC is reasonably fabricated.

Table 5-1: Cost analysis for designing a temperature environmental chamber

Material	Specification	Quantity	Total Price
Perspex sheets	5mm thick		R2 552
Expanded polystyrene foam		6 cuts	R322
Aquarium Perspex sheets	5mm thick		R 650
Chiller	600W	1	R41 975
Light	200W	1	R10 850
Par sensors	CS 310 Quantum sensors	4	R64 500
Coolant	Ethylene glycol 5L		R300
Copper sheets	1mm thick		R1 700
Labor			R2 500
Grand total			R 125 349

5.1.1 Aquariums within the EC

Aquariums inside the EC are placed equidistant from each other, the heat source, and the walls. Aquariums are made from perspex sheets. Perspex has been proven to not introduce foreign substances that may alter nutrient concentrations for the algae thus interfering with the experiments (Maizey Engineering Plastic Products, 2021) The aquariums are 1.2L in volume having a diameter of 100mm and a length of 150mm.

5.1.2 Cooling of the EC

The EC has been fitted with a cooling plate which runs of a coolant provided by a 600W chiller. The cooling plate is as shown in Figure 5-2. The cooling plate is made of copper, with copper tubing's fitted within it. Copper has been chosen as it is a good conductor of heat and relatively cheap. The chiller, which is water-cooled and measures 400mm in height and 80mm in width, supplies the necessary coolant for the system.

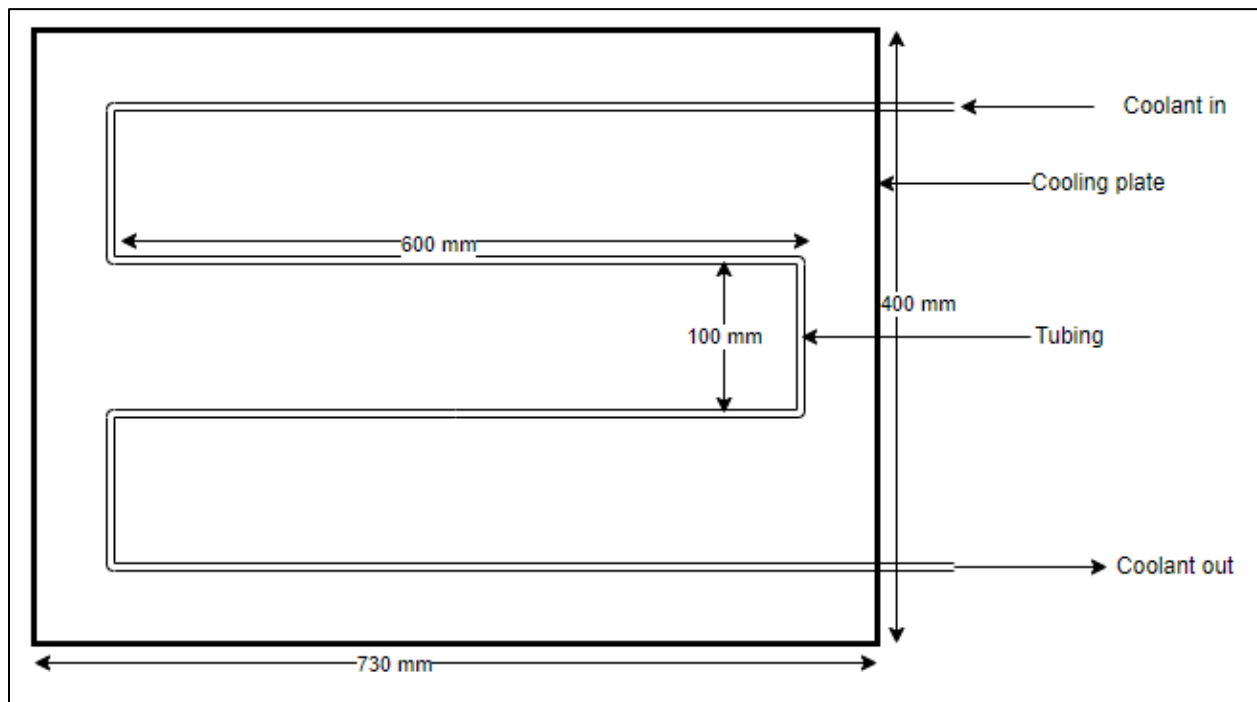


Figure 5-2: Cooling plate fitted within the EC.

The temperature control mechanism employs a basic PID (Proportional-Integral-Derivative) feedback loop. This control system takes as inputs the actual temperature of the coolant and the desired temperature setpoint. If the chamber temperature exceeds the setpoint, the system decreases the coolant temperature and activates the chiller until the chamber temperature returns to the setpoint. Conversely, if the temperature drops below the setpoint, the chiller is turned off until the desired temperature is achieved.

After its construction, the Environmental Chamber (EC) was tested and calibrated to verify its temperature regulation capabilities during experiments. The EC was placed on a benchtop in a laboratory set to a room temperature of 18°C. During testing, the chiller was set to 5°C. Aquariums 1, 2, and 3 were filled with milli-Q water. Class A PT100 temperature probes (with an accuracy of $\pm 0.15^\circ\text{C}$) were positioned on the cooling plate, on the wall opposite the cooling plate, and inside the aquariums. Data was collected over a 12-hour period. The temperature probes were connected to a Campbell Scientific CR5000 datalogger, which recorded temperature readings every 6 seconds and averaged them over 150 seconds. The recorded temperature measurements were the average of 25-second intervals.

Figure 5-3 illustrates that the aquaria within the Environmental Chamber (EC) take approximately 8 hours to reach the desired temperature, while the EC itself requires about 2 hours to stabilize. When the chiller is set to 5°C, the temperature in the aquaria adjusts to between 5.3°C and 5.85°C. The cooling plate maintains the set temperature of $\pm 5^\circ\text{C}$, whereas the temperature on the EC wall opposite the cooling plate ranges from 6°C to 5.3°C, depending on the coolant flow direction from the exit to the entrance (see Appendix B2). The chiller was subsequently adjusted to 8°C, and the resulting data is provided below.

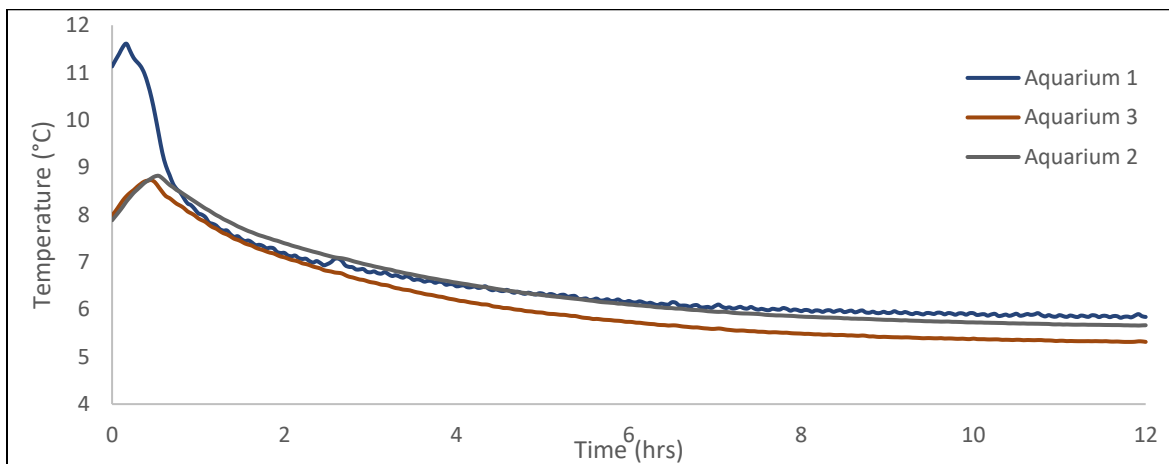


Figure 5-3: Temperature mapping for the aquaria within the EC, when chiller temperature is set to 5°C.

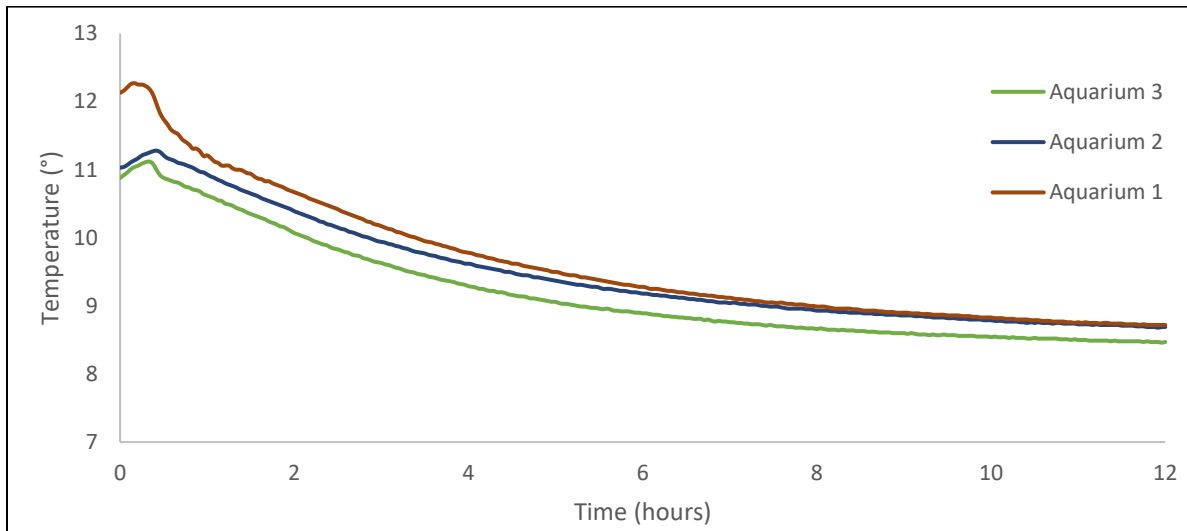


Figure 5-4: Temperature mapping for the aquariums within the EC, when chiller temperature is set to 8°C

For a set temperature of 8°C on the chiller, the aquaria regulate to between 8.5°C and 8.7°C (Figure 5-4). The cooling plate regulates to 8°C while the EC wall opposite the cooling plate regulates between 8.3 and 9.0°C (Appendix B2). The data shows that once temperature is regulated within the aquaria, it is not subjected to fluctuations. Overall, the temperature variation within the EC is + 1.0°C suggesting that the chamber could perform optimally as a temperature-regulated chamber. The EC together with the aquaria setup needs to be switched on for 8 hours to acclimatize before an experiment is considered started.

5.1.3 Lighting within the EC

The light fixture attached to the top plate of the Environmental Chamber (EC) is a 200W Wide Growth Spectrum light with a dimmer, designed to support full photomorphogenic plant responses. It has a spectrum range of 450-650nm and can achieve a Photosynthetic Photon Flux Density (PPFD) of up to 3500 $\mu\text{molm}^{-2}\text{s}^{-1}$. The dimmer allows for adjustable light intensity. This fixture is well-suited for measuring chlorophyll a, as it operates within the relevant wavelengths of 400-500nm and 600-700nm. Additionally, it provides a full range of PPFD similar to natural light conditions in the Antarctic.

Light received by the phytoplankton in the aquariums will be measured by the CS310 quantum sensors, sitting below the aquariums. The self-powered, full spectrum sensors are able to

measure a PPFD of up to $4000\mu\text{molm}^{-2}\text{s}^{-1}$. The dome-shaped sensors are 2.4cm in diameter and 3.5cm in length and, have an operating temperature range of -40°C to 70°C . The sensors are compatible with a Campbell Scientific CR300 data logger (Campbell Scientific Africa, 2019). Placement of sensors is as shown in the front view of the EC in (Appendix B3) i.e., at the bottom of the aquariums in the middle.

The light fixture provides a very high PPFD, giving light of up to $3500\mu\text{molm}^{-2}\text{s}^{-1}$. Dimming the light to 10% gives the results as in Figure 5-5. When the testing was conducted, placeholders 1, 2 and 3 had aquariums 1-3 on top of the par sensors, while position 4 was left bare. The aquariums had 1L of milli Q water in them. Par 4 readings thus give the light data in the EC while Par 1-3 readings show how light is filtered when there is milli Q water in the aquariums. Par 4 readings are superimposed on par 2 readings suggesting that the par sensor in position 2 sits such that it receives exactly the same light as when there is no aquaria on it. The milli q therefore does not filter any light. Seeing as the light covers the whole aquarium, all aquariums are said to be receiving the same amount of light. Slight variations in PAR sensor readings are attributed to their positions within the EC, though these differences are minimal.

The par readings all note that the light needs up to 2 hours to acclimatize before the experiment can officially begin. Milli Q water filters very little light as shown by the par readings. The experiment was repeated with the light fixture dimmed to 10% and covered by a shade filter. The results followed the same trend, with detailed outcomes provided in Appendix B2.

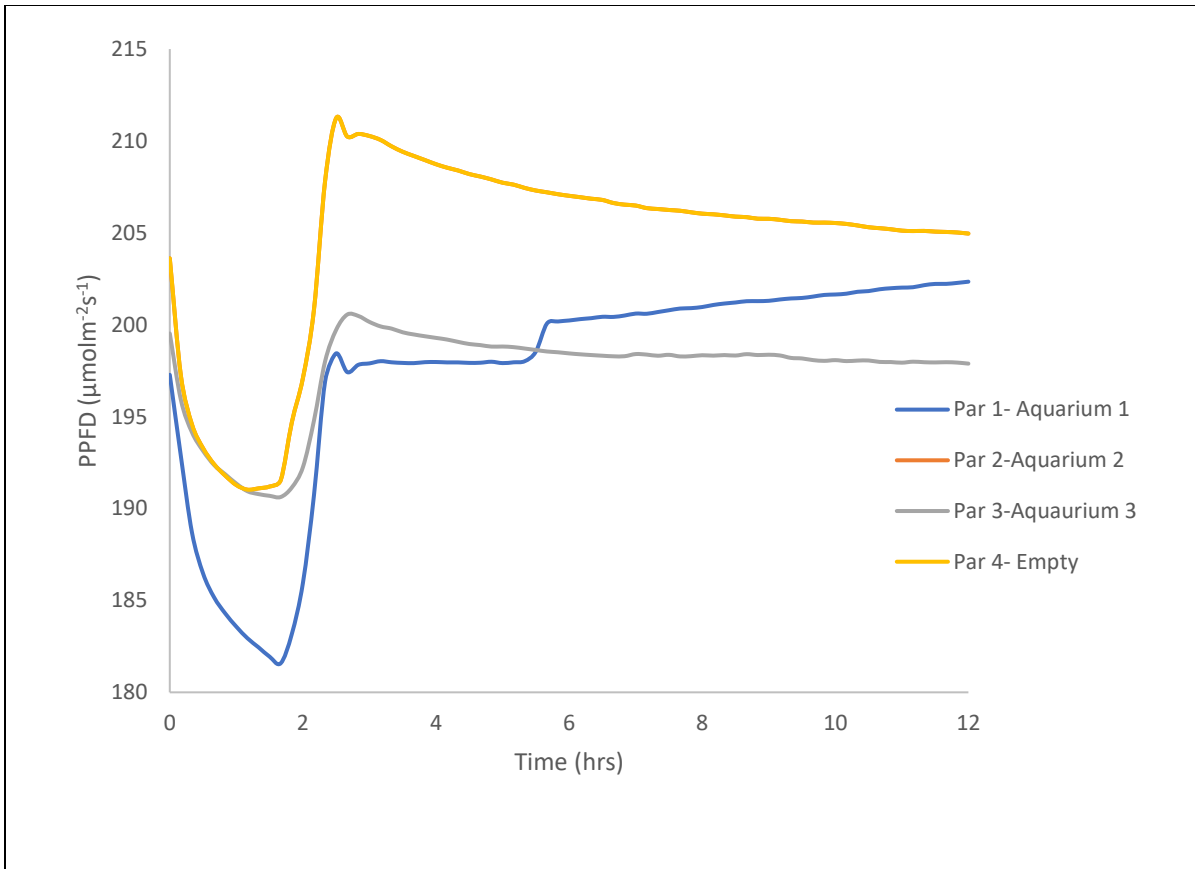


Figure 5-5: Par readings for the par sensors with aquariums filled with milli q water sitting on top of them and for a par sensor with no aquaria sitting on top of it.

6 PHYTOPLANKTON BASED EXPERIMENTS USING THE DESIGNED EC

6.1 Experimental protocol and method of analysis

The aim of the research conducted in this study was to ensure the suitability of the designed EC for phytoplankton experimentation. To achieve this aim, only variations in irradiance and temperature were examined. As stated in the scope of this dissertation, phytoplankton species utilized in this study were obtained from ice cores retrieved from the Marginal Ice Zone in the Southern Ocean during the SCALE spring cruise in 2019. Detailed information regarding the sampling stations is provided in Table 6-1 (Hambrock, Rampai and Walker, 2021).

Table 6-1: Sea ice sampling stations for the SCALE 2019 spring cruise

Station Type	Date	Latitude [N]	Longitude [E]
Consolidated	24 October 2019	-59.3248	0.066617
Consolidated	24 October 2019	-58.9833	0.011883
Consolidated	29 October 2019	-59.3645	8.158917
Consolidated	30 October 2019	-59.4726	10.88933

After sampling and transporting the initial hybrid systems to the UCT labs, hybrid systems were melted 29-39 days post the 2019 spring cruise. Melting of the hybrid tanks and storage of phytoplankton are detailed in Chapter 4.1.1. The phytoplankton species transported using the initial hybrid tank on the SA Agulhas II, were determined via microscopy to be diatoms. No individual species were separated from the community for experimentation, to minimize potential stresses on the diatom species due to manipulation during size fractionation or selection. Additionally, no grazers were removed before experimental analysis. Therefore, it was crucial in this study to conduct a baseline experiment to identify and quantify the species within the community before carrying out the relevant experiments.

Phytoplankton diatom species were originally stored at 5°C in glass bottles where they were provided with a continuous supply of air and nutrients. Prior to experimentation, three aquariums

were setup in the EC fabricated in Chapter 5 and designated the experimental aquaria. A nutrient solution was transferred into the experimental aquaria followed by the addition of a 100ml solution containing phytoplankton from the glass bottles into each aquarium. The nutrient solutions utilized in this study contained phosphate, nitrate, and silicate and this is outlined in Appendix C. Artificial sea water was then added to each aquarium to bring the total volume of the solution to 1L, ensuring proper dilution and consistency across all experimental setups. Salinity in the aquaria was maintained at 34psu. A fourth aquarium was filled with milli Q water and placed in the EC to allow for humidity. All aquariums were left open to allow for gaseous exchange to take place.

The temperature within the EC was set to 5°C to ensure consistency with the conditions the phytoplankton had been accustomed to. Additionally, the irradiance level was set to $200\mu\text{molm}^{-2}\text{s}^{-1}$. This decision was informed by observations during the 2019 spring cruise, which revealed that the highest irradiance received by ice phytoplankton during ice melting was approximately $200\mu\text{molm}^{-2}\text{s}^{-1}$. The first experiment, termed the “baseline experiment” was run for 6 weeks. During the experiment, samples were taken from the experimental aquaria for chlorophyll A in Vivo analysis, nutrient analysis, and for phytoplankton identification and counting.

Samples were taken for chlorophyll A in Vivo measurements twice every week (Figure 6-1) and, for nutrient analysis once every week (Figure 6-2). Before sample collection, aquariums were gently stirred with a milli Q rinsed glass rod to ensure the suspension of phytoplankton cells within the aquaria. A Trilogy Turner Designs fluorometer was used to measure chlorophyll A in Vivo of the obtained samples. 3.0ml was sampled from each aquarium and measured for fluorescence in the fluorometer. The choice of chlorophyll A in Vivo measurements for the experiments was based on the minimal sample requirement, as only 3ml was needed, thereby allowing for tracking the presence of photosynthetic matter in the aquaria. Additionally, an extra 3.5ml sample was taken from the aquaria to measure phosphate levels in the system, following the protocol outlined in Appendix D.

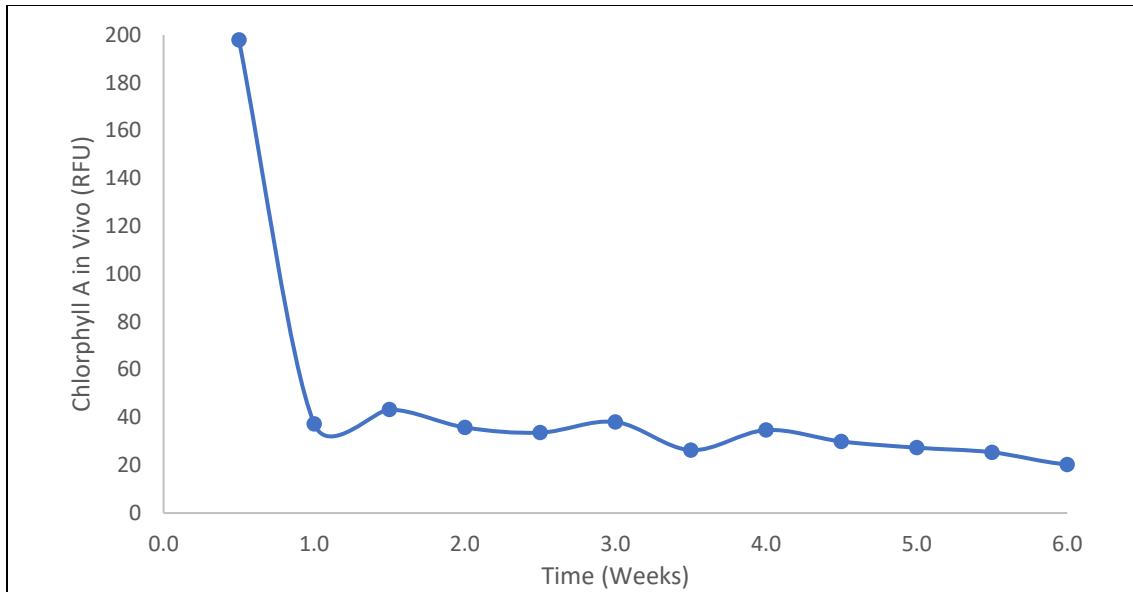


Figure 6-1: Chlorophyll A in Vivo measurements for experimental aquarium 1 at 5°C and 200 $\mu\text{molm}^{-2}\text{s}^{-1}$

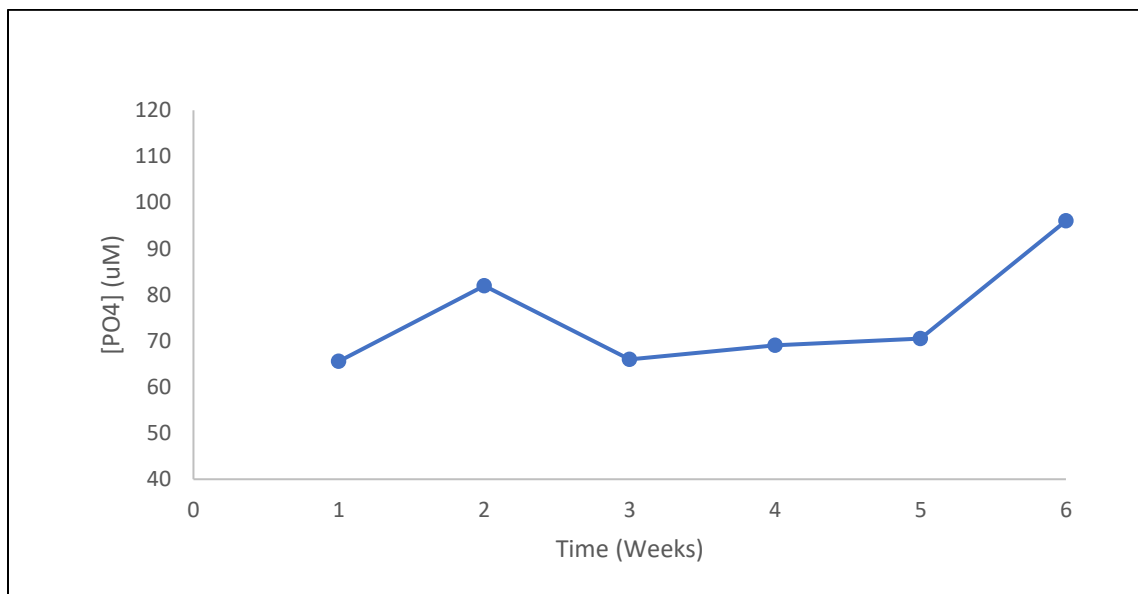


Figure 6-2: Phosphate measurements for experimental aquarium 1 at 5°C and 200 $\mu\text{molm}^{-2}\text{s}^{-1}$

Community quantification in the experimental aquaria was conducted using microscopy. Samples, each measuring 3.5ml, were collected both at the beginning and the end of each experiment. The samples were collected from the top, middle, and bottom of the experimental aquaria. To preserve them, 1% glutaraldehyde was added to each, and they were stored in an 8°C refrigerator until analysis. For each experimental aquarium, a sample was poured into a single-well microscopy slide. Slides were left to rest for about 10 minutes before counting and

identification, to allow for the settling of algae, due to the depth of slides. The wells had a diameter of 26mm and a depth of 5.0mm, totaling a volume of 2.7ml per well. Phytoplankton counting with the microscope was done as discussed in 4.2.1. Identification of phytoplankton species is as seen in Figure 6-3 and Figure 6-4 which illustrate the prevalent pennates and centrics used in this study.

A Bray Curtis dissimilarity between aquaria 1 and 2 and aquaria 1 and 3 showed significant differences in species quantity and type amongst the three aquaria. This is attributed to the fact that source of phytoplankton species in the individual experimental aquaria not from the same location. Aquarium 2 had the most varied species (Figure 6-7), thus only results from aquaria 2 are shown in 6.2.2 and 6.2.3, with aquaria 1 and 3's results documented in Appendix E. Despite the variation of species, the trends within the three aquaria were observed to be the same (Appendix E). Shapiro Wilk tests were conducted on all experiments for the individual species groups, for significance of tests conducted. Only 30% of the groups for a quarter of the experiments were found to be normally distributed. Normality was therefore not assumed. Wilcoxon signed ranked tests were therefore performed, comparing concentrations of a taxonomic group at a certain temperature or irradiance to concentrations of the same group at another temperature or irradiance, to test significance of results.

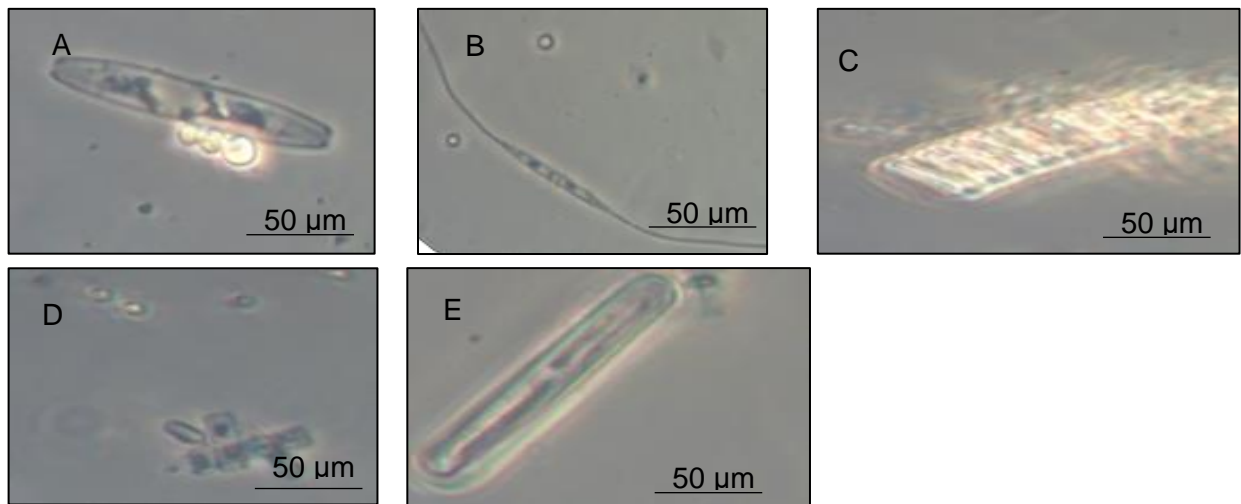


Figure 6-3: Pictorial view of the pennate taxa: (A) *Navicula* species (B) *Cylindrotheca closterium* (C) *Fragilariopsis kerguelensis* (D) Unidentified pennates (E) *Proboscia*

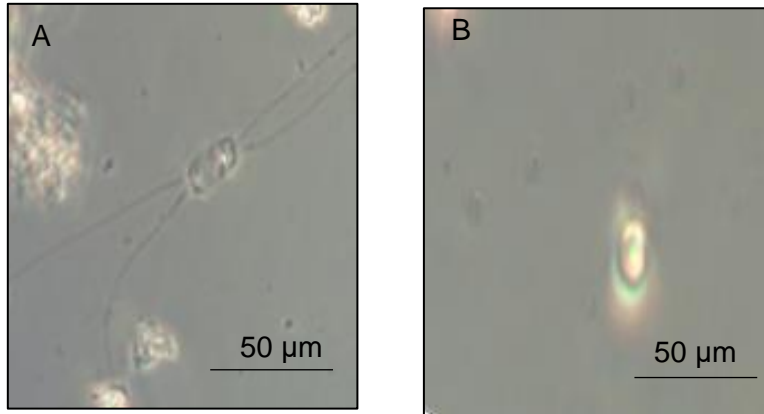


Figure 6-4: Pictorial view of the Centric taxa: (A) *Chaetoceros* (B) Unidentified centrics

Figure 6-5 illustrates how the data is presented in concentration per ml before and after experimentation. In order to fully analyze the extent of the difference before and after experimentation, the difference between species composition before and after experimentation was calculated and expressed as a percentage of the initial composition before experimentation. This is as illustrated in Figure 6-6. Moving forward, only the species percentage difference is presented with the actual cell concentration given in Appendix E.

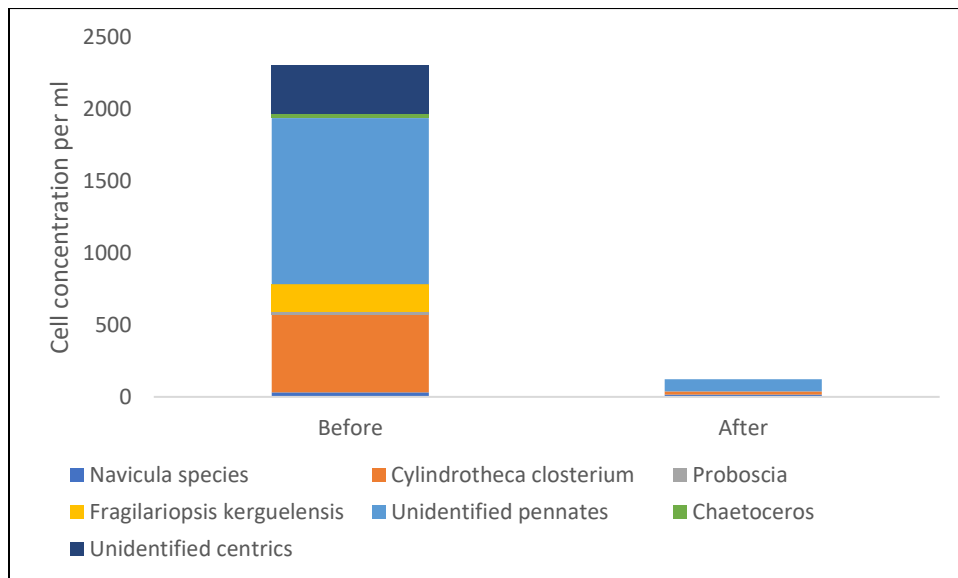


Figure 6-5: Cell concentration per ml in aquarium 1 before and after experimentation at 5°C and 200 μmol m⁻² s⁻¹

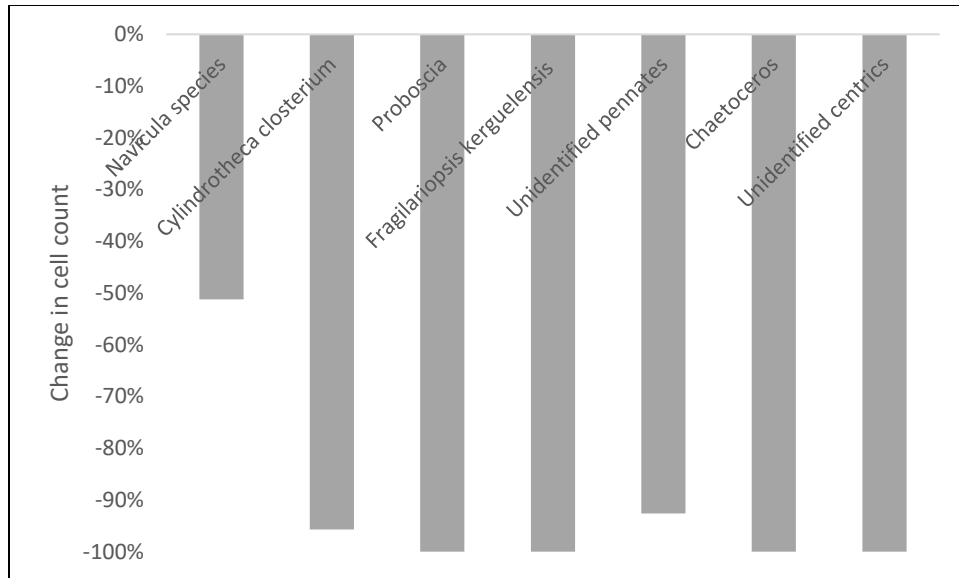


Figure 6-6: Cell concentration per ml difference in aquarium 1 at 5°C and $200\mu\text{molm}^{-2}\text{s}^{-1}$

6.2 Experimental Results

6.2.1 Baseline experiments

Pre incubation in the EC, the three experimental aquaria showed that diatoms were the only phytoplankton present and of these were mostly pennate diatoms, then centrics. The ratio of pennates to centrics was determined to be roughly the same in all three aquaria i.e., 79%:21%. Figure 6-7 shows the different taxonomic groups in the three aquaria. Of note, the *Cylindrotheca closterium*, unidentified pennates and unidentified centrics were common in all three aquaria. The different taxonomic groups varied in each aquarium with the highest cell concentration and the widest range of species found in aquarium 2. A lot of debris was also identified across all aquaria.

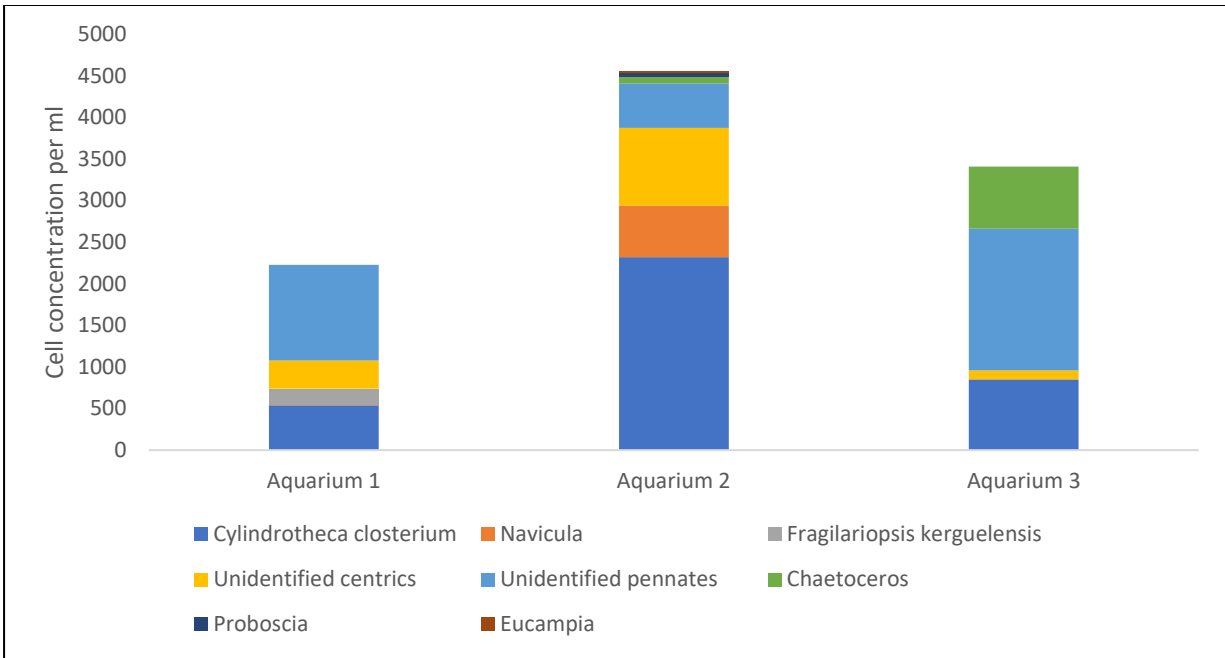


Figure 6-7: The different pennate and centric taxa in the baseline before experimentation

Figure 6-8 gives the chlorophyll A in Vivo measurements for the three different aquaria six weeks. The in Vivo measurements show that phytoplankton had a negative growth rate throughout the six weeks. At the beginning of the experiment, aquarium 1 had the greenest color of the three aquariums giving a noticeable film of phytoplankton. This corresponds with the high chlorophyll A in Vivo measurement of aquarium 1 at the beginning of the experiment. By the end of the experiment, all aquariums showed clear solutions. Aquarium 1 and aquarium 3 showed overall decreasing rates of the phytoplankton species. Aquarium 2 however, showed noticeable variable increasing and decreasing rates of the different phytoplankton species.

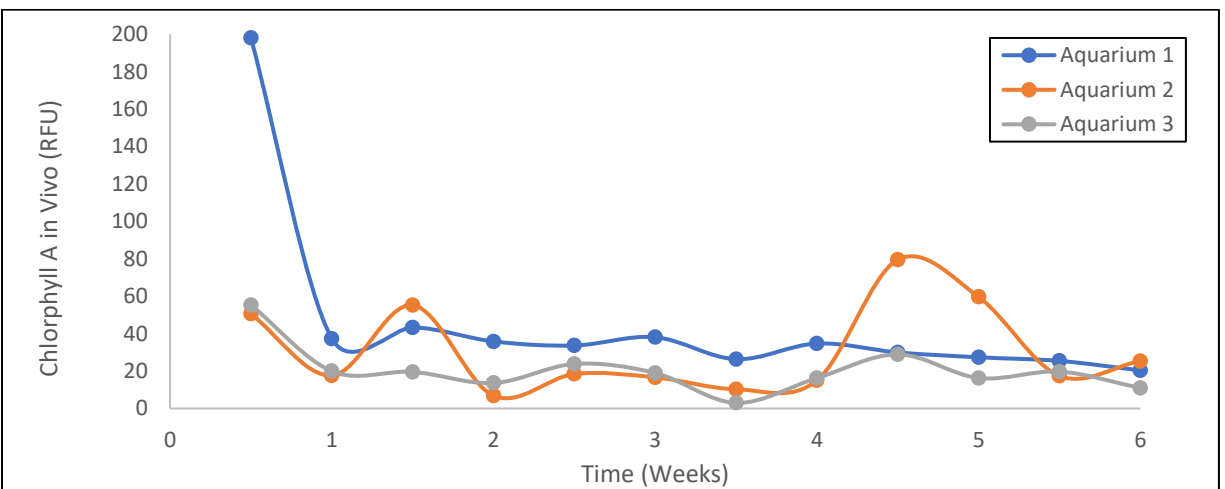


Figure 6-8: Chlorophyll A In Vivo measurement on the three different aquaria.

The chlorophyll A in Vivo measurements are not a true representation of the cell count as the sampled solution might not be homogeneous. A true homogeneous solution can only be acquired by obtaining larger than 3.0ml samples. Chlorophyll A in Vivo measurements will therefore only be interpreted in trends and not the individual points.

Phosphate measurements (Figure 6-9) taken once every week, to determine if phytoplankton were using the nutrients, show that, for the baseline experiment, the phytoplankton did not use the phosphate nutrients. Instead, phosphate concentration in the experimental aquaria increased. The absence of nutrient utilization correlates with the negative growth rate indicated by the in Vivo measurements. Furthermore, the rise in phosphate concentration might be attributed to dying phytoplankton cells releasing phosphate into the solution.

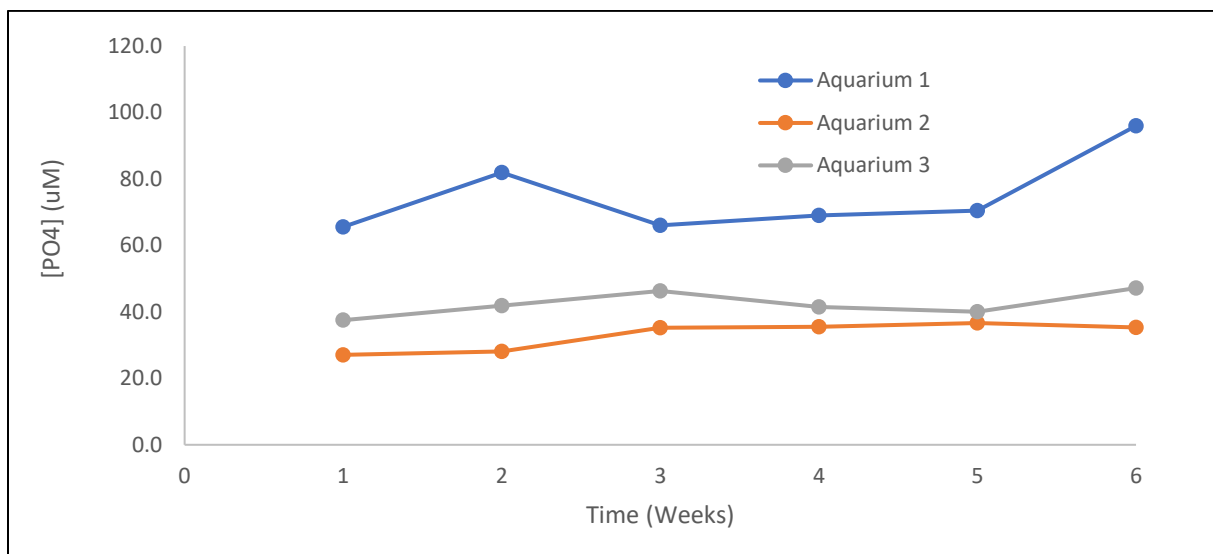


Figure 6-9: Phosphate concentrations over a period of six weeks

An analysis of the cell concentration via microscopy (Figure 6-10) at the end of the six weeks showed that only the *Navicula species*, *Cylindrotheca closterium* and unidentified pennates were present at the end of the six weeks, in very small amounts. Despite the high nutrient concentration as shown by the phosphate levels in Figure 6-9 and, with phytoplankton being subjected to previous storage temperature of 5°C, majority of the phytoplankton species did not survive. In particular all centrics did not survive even though Campbell *et al.* 2018 suggests that centric diatoms thrive when there is high light. Despite the established association between high nitrate

concentrations and diatom proliferation (Ardyna *et al.*, 2020; Dugdale and Wilkerson, 1991), nearly all diatoms failed to survive the baseline experiment, even with the increased nutrient levels. Natarajan (1970) found that in excess NH_4^+ is toxic to phytoplankton as it makes the environment acidic. The decrease in cell concentration was therefore attributed to the high light intensity and possible intoxication of species due to increase in NH_4^+ as a result of death of phytoplankton (Natarajan, 1970).

Although Fiala and Oriol (1990) found that diatoms obtained from the Southern Ocean have optimal growth at irradiances between $115\mu\text{molm}^{-2}\text{s}^{-1}$ and $220\mu\text{molm}^{-2}\text{s}^{-1}$ (Yan *et al.*, 2019; Spilling *et al.*, 2015), this study preliminarily shows that the sea-ice phytoplankton species experimented on, get photo inhibited with light of intensity $200\mu\text{molm}^{-2}\text{s}^{-1}$ and possibly higher. This outcome aligns with observations from the SCALE 2022 winter cruise to the Marginal Ice Zone, which recorded an average under-ice irradiance of $1.05\mu\text{molm}^{-2}\text{s}^{-1}$, with phytoplankton species receiving less than 1% of incident photosynthetically active radiation (PAR). Additionally, these findings are consistent with the observations of Castellani *et al.* (2020), who noted that the highest under-ice PAR levels ranged from 4.5 to $21\mu\text{molm}^{-2}\text{s}^{-1}$ in the central Arctic during summer. Given that most species did not survive exposure to high light irradiance, it was tentatively concluded that this threshold represents the upper limit of irradiance tolerable for the phytoplankton species under investigation.

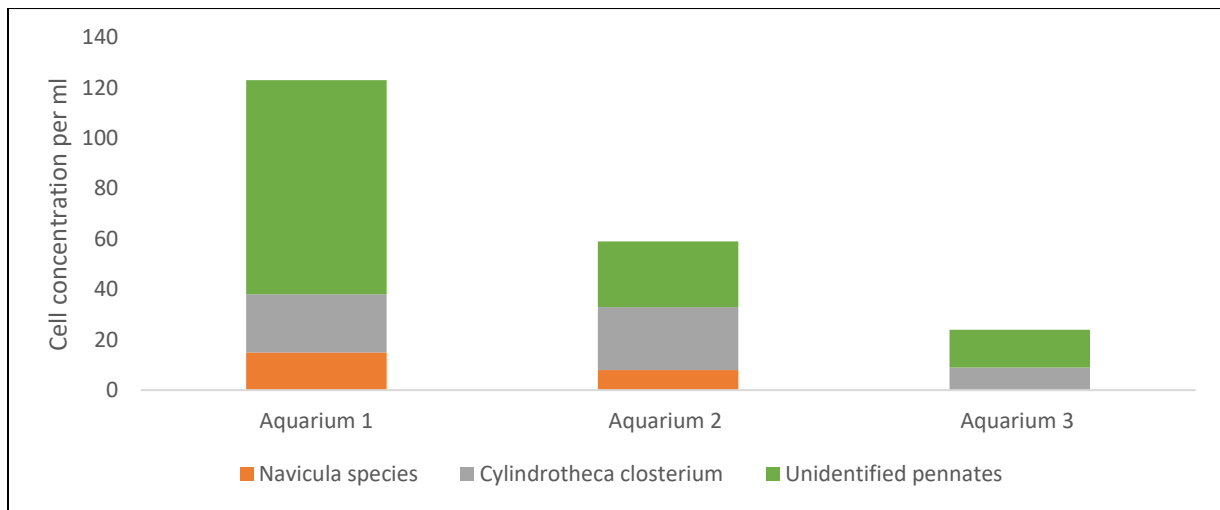


Figure 6-10: Cell count at the end of the baseline experiments

6.2.2 Irradiance variation

With the upper threshold of irradiance being determined to be $200\mu\text{molm}^{-2}\text{s}^{-1}$, a middle-level irradiance was required, and this was achieved by applying a shade filter to the light source. The irradiance was changed to $42\mu\text{molm}^{-2}\text{s}^{-1}$. An experiment was conducted in the EC at 5°C to determine the response of the phytoplankton species to the change in irradiance. The chlorophyll A in Vivo measurements are as shown in Figure 6-11 (Medium light). The data shows a decrease in chlorophyll A in Vivo for the first one and a half weeks indicating adaptation time for the phytoplankton species. Following this period, chlorophyll A levels increased.

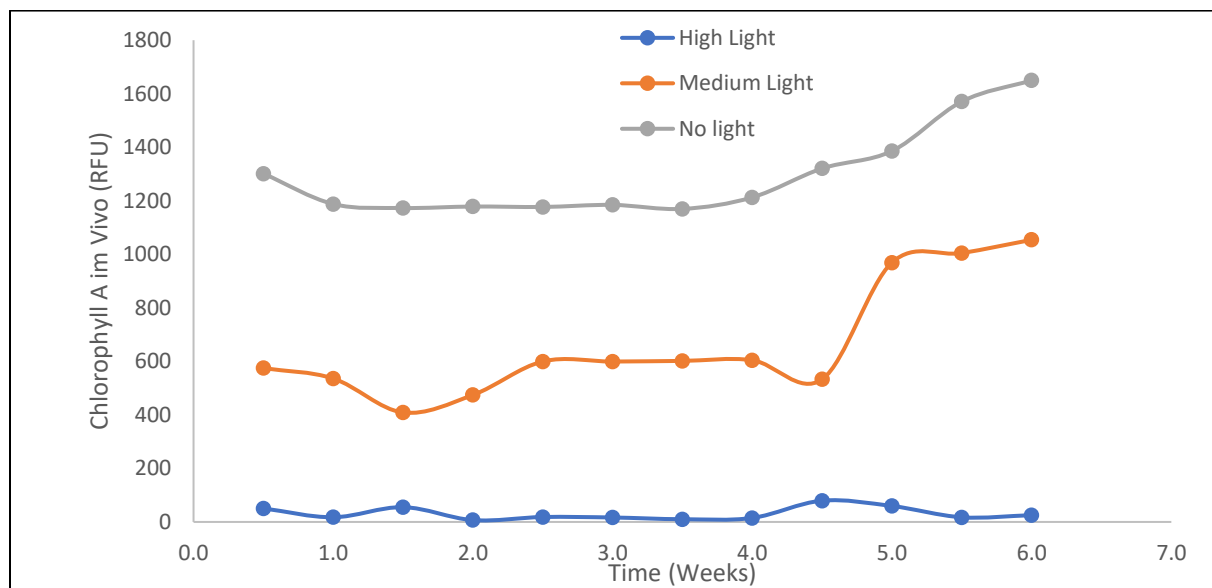


Figure 6-11: Chlorophyll A in Vivo measurements for high ($200\mu\text{molm}^{-2}\text{s}^{-1}$), middle ($42\mu\text{molm}^{-2}\text{s}^{-1}$) and No ($0\mu\text{molm}^{-2}\text{s}^{-1}$) irradiance variations at 5°C in aquarium 2

The phosphate concentrations however indicate that even though chlorophyll A in Vivo measurements start to increase after one and half weeks, some phytoplankton species continue dying beyond two weeks (Figure 6-12; Medium light). Nutrient consumption is only really seen after four weeks. Cell count shows that only the *Navicula spp*, *Cylindrotheca closterium* and the unidentified pennates survived till the end of the experiment, as with high light (Figure 6-13, Figure 6-10, Aquarium 2). This suggests a preliminary conclusion that these three species, in particular, demonstrate an ability to acclimate to a broader range of light intensities. Notably, *Cylindrotheca closterium* is recognized as a common diatom capable of adapting to diverse environmental conditions (Harada, 2016). The absence of vertical stability, such as the presence of ice, may also contribute to the mortality of certain phytoplankton species. Observations revealed that phytoplankton species adhered to the walls of the aquariums, potentially restricting their access

to nutrients. This phenomenon could have resulted in limited nutrient availability, further exacerbating the challenges faced by the phytoplankton populations.

Palmisano and Sullivan (1982) suggests that 0 to $46\mu\text{molm}^{-2}\text{s}^{-1}$ is a good approximation for light intensity phytoplankton under ice receive, and thus, can handle. This study does show that some of the phytoplankton species can handle irradiances of up to $46\mu\text{molm}^{-2}\text{s}^{-1}$. Comparisons between high light and medium light (Figure 6-14) show not much difference in terms of photo adaptability, however. Juhl and Krembs (2010) demonstrated in laboratory experiments that while small increases in light intensity can enhance algal growth, higher irradiances, up to $110\mu\text{molm}^{-2}\text{s}^{-1}$, can suppress growth.

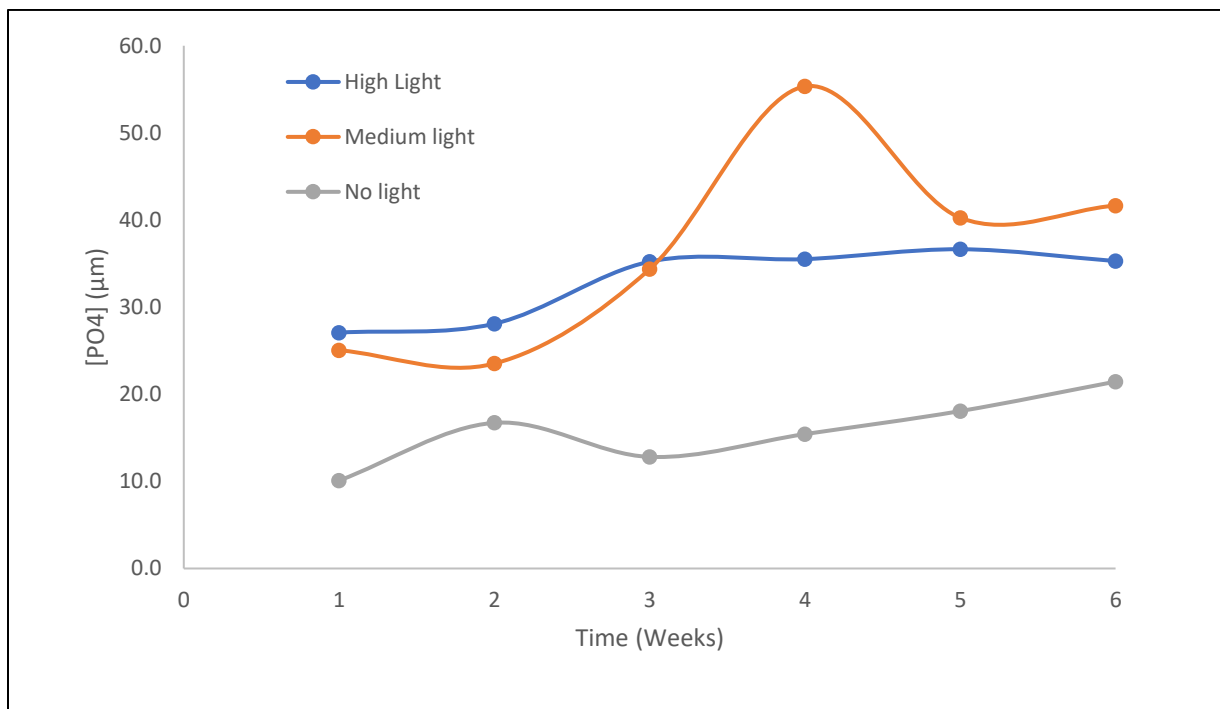


Figure 6-12: Phosphate concentrations for high ($200\mu\text{molm}^{-2}\text{s}^{-1}$), middle ($42\mu\text{molm}^{-2}\text{s}^{-1}$) and No ($0\mu\text{molm}^{-2}\text{s}^{-1}$) irradiance variations at 5°C

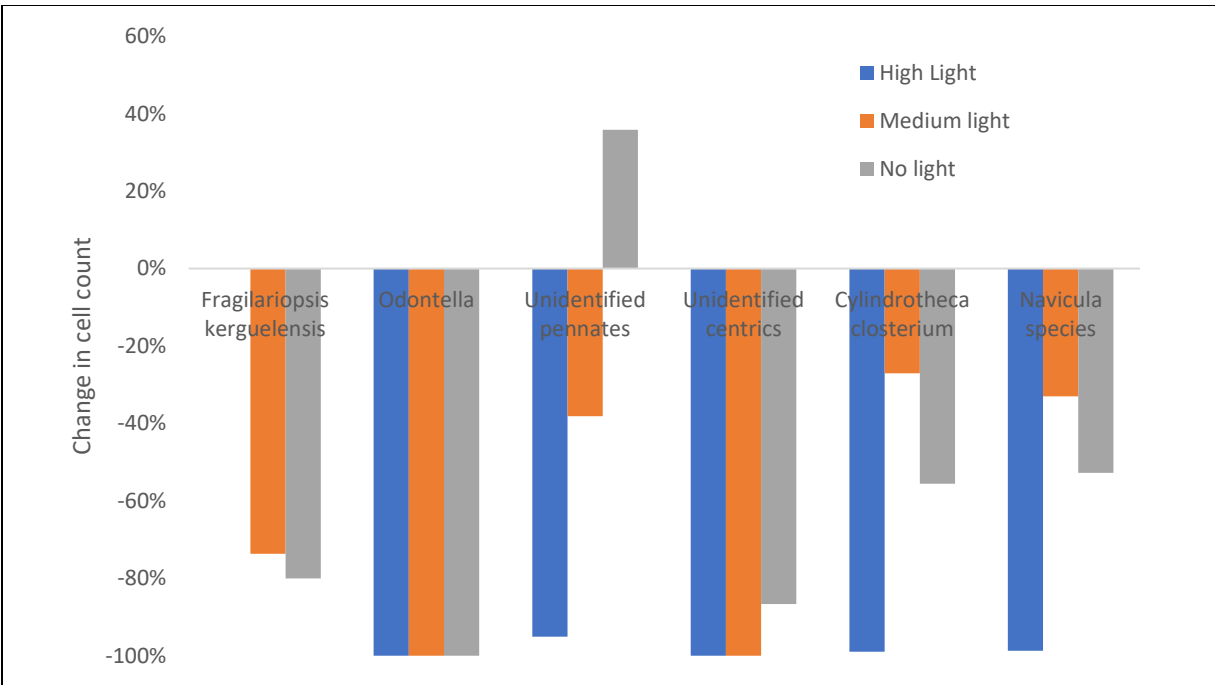


Figure 6-13: Before and after cell concentration difference for a 6-week experiment to determine adaptability of species to irradiance $0\mu\text{mol}/\text{m}^2/\text{s}$, $42\mu\text{mol}/\text{m}^2/\text{s}$ and $200\mu\text{mol}/\text{m}^2/\text{s}$ 5°C .

Phytoplankton species were then experimented on in the dark to determine if growth would occur and possibly increase cell concentrations. The experiment was conducted in the EC at 5°C in the dark. Chlorophyll A in Vivo measurements (Figure 6-11 -No light), indicate that after an adaptation time of two and a half weeks, the phytoplankton species start to grow. Figure 6-12 shows that phosphate amounts increase however, suggesting possible release of nutrients in the system via death of some phytoplankton species. NO_x and NH_4^+ would have been more crucial nutrients to measure in this project, given the significant phytoplankton die-back. The bacteria likely consumed these cells, thereby altering the nitrogen dynamics in the water. Based on these results, it is hypothesized that ammonium levels would have increased as a result, which is less favorable for diatom growth. An analysis of phytoplankton species via microscopy before and after the experiment (Figure 6-13) shows that all species except for the unidentified pennates decreased in cell count.

One tailed paired sample Wilcoxon ranked tests comparing change in the concentrations of the taxonomic groups at high irradiance to concentrations of the same group at medium irradiances were performed to determine statistical significance of the developed trends. The same test was also conducted for comparison between medium irradiance and no irradiance. The null hypothesis of the tests was that concentration changes were the same. For the species outlined in Table 6-

2, Wilcoxon ranked tests show statistically significant growth ($P < 0.05$) for the unidentified pennates under no irradiance and significant reduction for medium and high irradiances, with a rejection of the null hypothesis.

Table 6-2: One tailed paired-sample Wilcoxon signed-rank tests comparing taxonomic group concentrations at different irradiances with $n=3$ for each group.

Taxonomic group	High irradiance vs medium irradiance	Medium irradiance vs no irradiance
	P value	
<i>Cylindrotheca closterium</i>	0.034	0.23
<i>Navicula</i>	0.33	0.32
<i>Fragilariopsis kerguelensis</i>	0.21	0.5
Unidentified pennates	0.1	0.06

6.2.3 Temperature variations

Following observations indicating negative growth among species in darkness at 5°C, it was decided to elevate the temperature to 8°C and conduct further experimentation on the phytoplankton in the absence of light. The increase in temperature resulted in a notable increase in cell concentration across all phytoplankton species.

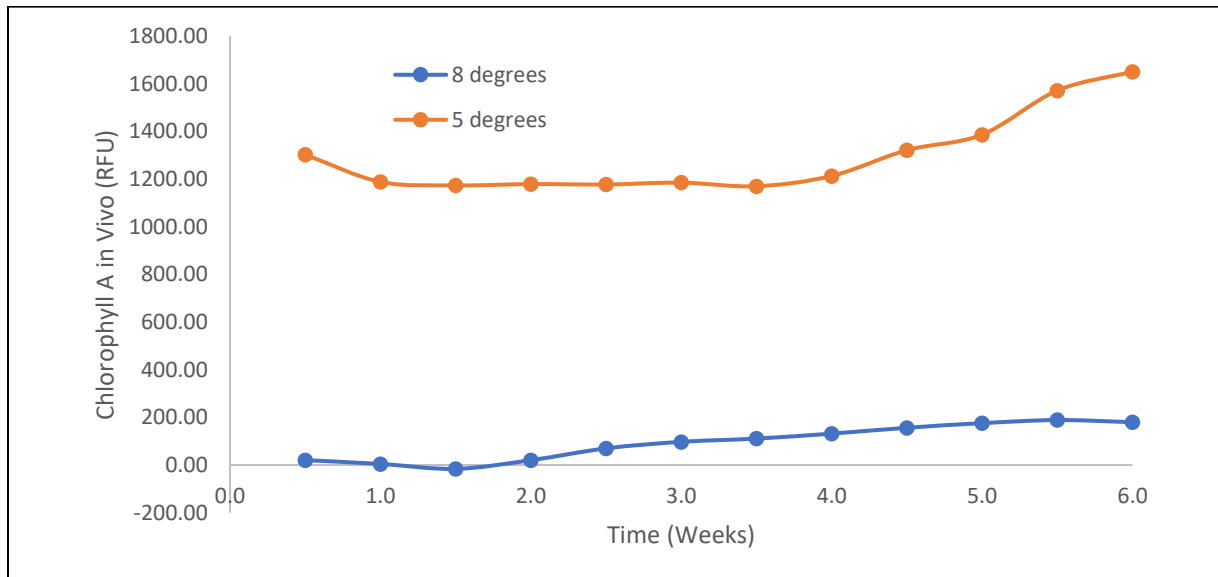


Figure 6-14: Chlorophyll A in Vivo measurements for experimentation on phytoplankton species in the dark at 8°C and 5°C

Figure 6-14 illustrates phytoplankton growth in the aquaria. Interestingly, at higher temperatures, phytoplankton required less time to adapt, as observed in this case, with an adaptation period of only 1.5 weeks. Of all the experiments carried out in this study, Figure 6-15 (8 degrees) demonstrates the highest uptake of nutrients. Noting that sea-ice phytoplankton receive very small amounts of light in their natural habitat, it is therefore expected that all phytoplankton species would increase in cell count in the dark making use of the available nutrients. Figure 6-16 shows the cell concentration per species and of note, the centrics which preliminarily show the most photoinhibition when compared with pennates, thrived in the dark.

All phytoplankton increased in cell concentration and in particular, the unidentified pennates. The size of the unidentified pennates however remained small i.e., 10µm while other species increased in cell size. For instance, *Cylindrotheca closterium* increased in cell size from 30µm to 50µm. One tailed paired sample Wilcoxon ranked tests comparing change in the concentrations of the taxonomic groups at high temperature to concentrations of the same group at low temperature showed statistically significant ($P < 0.05$) increase in cell count for all species in Figure 6-16.

Sugie *et al.* (2020) demonstrated that increases in temperature and dissolved carbon dioxide within a fully liquid environment promote the growth of diatom species such as *Cylindrotheca closterium* and *Pseudo-nitzschia*, while leading to the decline of *Thalassiosira* spp. Similarly, Torstensson *et al.* (2019) found that rising temperatures correlated with enhanced growth rates among diatom species. Additionally, Yan *et al.* (2019) identified that *Nitzschia cf. neglecta*, an ice diatom, exhibited optimal growth rates at 10°C, compared to 2°C, under irradiance levels of 100µmol m⁻² s⁻¹. Although sea ice phytoplankton typically inhabit environments with temperatures around -1.8°C, preliminary results indicate that sea ice species capable of surviving transportation and acclimatizing to experimental conditions displayed improved growth at elevated temperatures, specifically 8°C compared to 5°C.

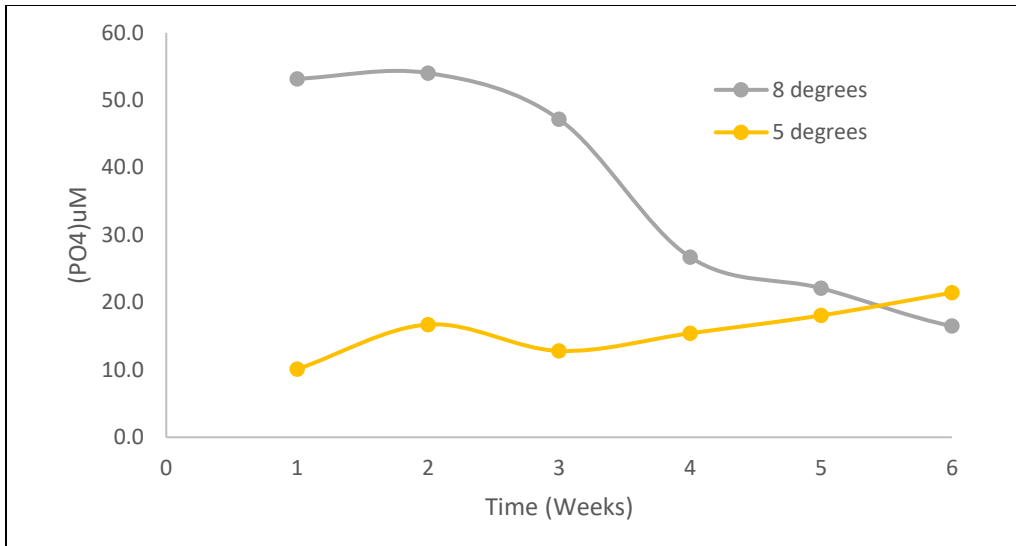


Figure 6-15: Phosphate concentrations for experimentation in the dark at 8°C and 5°C

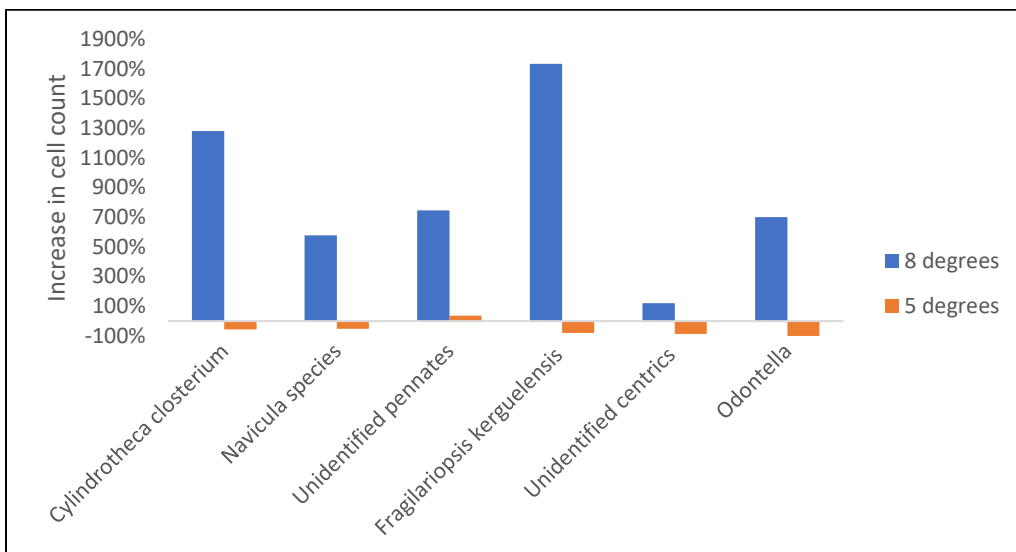


Figure 6-16: Species cell count before and after experimentation difference In the dark at 8°C

7 OVERALL DISCUSSION

Controls of sea ice phytoplankton growth are still not well understood. This study therefore aimed to investigate the response of phytoplankton species to different temperature and light conditions. To do this, firstly a previously designed hybrid tank (Hambrock, Rampai and Walker, 2021) had to be optimized so that it could be used to obtain phytoplankton species from the Marginal Ice Zone in the Southern Ocean. The hybrid tank can hold ice cores and water at its freezing temperature i.e., -1.8°C , by making use of insulation and heating cables. The previously designed hybrid tank as in Figure 4-1A, satisfies control over temperature and access to nutrients for phytoplankton. The hybrid tank however needed to be improved to increase phytoplankton species survival rate during transportation from the Southern Ocean to land-based facilities. The hybrid tank was successfully optimized by changing the size of the tank and adding irradiance to the tank. Optimization also included making changes to the sampling protocol associated with the hybrid tank.

Decreasing the size of the tank, while maintaining the L/D ratio, significantly improved temperature control in the tank. Since there was no mixing in the tank, there was an uneven distribution of heat in the initial hybrid tank. This meant that the temperature probe was accurate to a certain part of the tank resulting in noticeable changes in the ice depth as ice continuously melted and froze during transportation. Decreasing the size of the tank reduced the ice depth fluctuations that occurred in the initial hybrid tank to between 10 and 15mm as opposed to nearly 100mm in the initial tank.

Irradiance conditions experienced by the phytoplankton at the MIZ sampling site in the SO were measured using handheld par sensors. The measured irradiance values were incorporated into the hybrid tank. This was done to simulate the irradiance conditions experienced in the MIZ in the hybrid tank. The irradiance was provided by LED strip lights attached to the lid of the hybrid tank. Par sensors were also fitted at the bottom of the tanks to track the light intensity of the provided irradiance during the transportation of samples from the Southern Ocean to land-based facilities.

The combined effects of reducing the size of the hybrid tank, incorporating irradiance, and refining the sampling protocol resulted in microscopy analysis demonstrating an increase in the cell concentration of phytoplankton species within the hybrid tank, in comparison to starting concentrations, and solid and liquid transport (Figure 4-8). Solid transport exhibited a decrease in cell concentration attributed to brine loss, while liquid transport displayed a significant decline in

cell concentration possibly due to inadequate aeration and nutrient scarcity. Consequently, liquid transport proved incomparable to both solid and hybrid transport methods and warrants modification. It was anticipated that changes in phytoplankton concentrations would occur during hybrid transport, as the design of the hybrid system aimed to promote growth by alleviating nutrient and light limitations. The documented increase in cell concentration in the hybrid tanks, as illustrated in Figure 4-9 and Figure 4-10, underscores the effectiveness of the optimized hybrid tank in preserving phytoplankton species. Thus, the optimized hybrid tank not only promotes the survival of diverse phytoplankton species but also facilitates their preservation.

Additionally, it's important to acknowledge the limitations of the hybrid tank. Full control over all *in situ* environmental conditions found in the Southern Ocean is not possible in the hybrid tank. Waves and snow cover could not be added to the tank. The hybrid tank however in its form is sufficient for the transportation of different phytoplankton species and possibly experimentation on the phytoplankton species.

Before experimentation on the obtained phytoplankton species could commence, an environmental chamber had to be constructed for housing aquaria where phytoplankton species would reside during experimentation. A tabletop environmental chamber was successfully constructed. The environmental chamber houses 4 aquaria and offers temperature and light intensity control. A cooling plate receiving coolant from a chiller is used to regulate temperature in the EC. The functional chamber as in Figure 5-1, was tested for temperature control and proved to have a maximum temperature deviation of +1°C. The environmental chamber, however, has to be temperature regulated for 8 hours before experimentation can begin. The environmental chamber was designed with perforations on the side for aeration and it has been designed such that an aquarium filled with water constantly has to be in the chamber to provide humidity. The environmental chamber makes use of an LED light whose light intensity can be adjusted by using shade filters. Light intensity is tracked with par sensors sitting at the bottom of the aquaria in the chamber. The chamber has been designed only for liquid bath experimentation on sea ice phytoplankton.

Post construction of the environmental chamber, phytoplankton species were introduced into the aquaria and irradiance and temperature experiments conducted on them. For an irradiance variation at 5°C, the light intensities used were $200\mu\text{molm}^{-2}\text{s}^{-1}$, $42\mu\text{molm}^{-2}\text{s}^{-1}$ and $0\mu\text{molm}^{-2}\text{s}^{-1}$. All the diatom species experimented on were photo inhibited at $200\mu\text{molm}^{-2}\text{s}^{-1}$ with only *Navicula spp*, *Cylindrotheca closterium* and the unidentified pennates showing limited cell concentration at the end of the experiment. Microscopy also showed that *Navicula spp*, *Cylindrotheca closterium*

and the unidentified pennates survived irradiances of up to $42\mu\text{molm}^{-2}\text{s}^{-1}$. This study thus demonstrates the resilience of *Navicula spp*, *Cylindrotheca closterium*, and unidentified pennates for a light intensity range $0\text{-}200\mu\text{molm}^{-2}\text{s}^{-1}$. All other diatom species examined in this study can be tentatively classified as shade-adapted, indicating that further investigations into their irradiance requirements are warranted, particularly within the range of 0 to $42\mu\text{molm}^{-2}\text{s}^{-1}$ at 8°C . In addition to irradiance experiments, a temperature comparison revealed that the diatom species experimented on favor warmer temperatures, in this case 8°C to 5°C .

The death of phytoplankton led to the release of nutrients into the aquaria. As depicted in Figure 6-9, there was a continual increase in phosphate levels throughout the experiment, coinciding with a decrease in chlorophyll A in vivo. This rise in phosphate indicates an overall increase in nutrient levels within the aquaria. Tyagi, Ahmad, and Malik (2022) have demonstrated that excess nitrogen in aquatic systems can be harmful, leading to the depletion of dissolved oxygen and consequent marine life mortality. Additionally, Natarajan (1970) found that ammonia concentrations exceeding those typical of natural environments are toxic to marine diatoms. To prevent nutrient concentrations from reaching toxic levels for the phytoplankton species, it is imperative to monitor not only phosphate but ammonium and silicate levels as well, the latter being a vital diatom nutrient (Thomas and Dieckmann, 2009), throughout the duration of the experiment.

A limitation of this study was agitation only being conducted twice a week during sampling. Agitation was achieved by gently stirring the aquaria with a clean rod before sampling, and it was limited to twice a week to prevent shredding of phytoplankton species. However, due to cells adhering to the walls of the aquaria, attributed to the lack of vertical stability, more frequent agitation is necessary to keep cells in suspension. Ensuring cells remain in suspension is crucial to avoid nutrient limitation within the system.

Ardyna *et al.* (2020) argue that for ice algae to be mass released into the water column, a meteorological event would have happened, suggesting that ice phytoplankton do not do well in free waters. Guglielmo *et al.* (2000) studied the bottom-ice algal communities in the Terra Nova Bay and discovered that they were dominated by species not found in free waters. Due to their sticky nature, ice algae aggregate in ice and, as such have a lower residence time in column waters (Meiners *et al.*, 2008). This is a major limitation when culturing phytoplankton whether from the Southern Ocean or the Arctic waters, and partly why Vancoppenolle and Tedesco (2016) and Ryan *et al.* (2011) advocate for in-situ studies.

It is inherently difficult to grow phytoplankton species because of the strict environmental requirements that are virtually impossible to recreate. Nonetheless, the experiments conducted in this study demonstrate the feasibility of culturing phytoplankton species capable of surviving transportation, and obtaining responses comparable to those observed *in situ*. However further improvements in the culturing methods can be made to mimic *in situ* conditions. Addressing factors such as the lack of continuous agitation, nutrient limitation towards the end of the six-week experiments due to batch culturing, and the potential presence of grazers are areas that warrant attention and improvement. This study highlights that culturing phytoplankton species can provide valuable insights into their responses to environmental changes, and with enhancements to the Environmental Chamber, this avenue of research should be pursued further.

8 CONCLUSIONS AND RECOMMENDATIONS

8.1 Conclusions

The overall aim of this study was to investigate response of phytoplankton species to different temperatures and irradiances. The overall conclusions of this work are as below:

- The previously designed hybrid tank was successfully optimized via reduction in size of the tank and inclusion of irradiance in the tank. Optimization also included improvements to the previously used sampling protocol. The tank was successfully used to bring phytoplankton from the Marginal Ice Zone of the Southern Ocean to land based facilities at the University of Cape Town. The optimized tank promotes survival of the different phytoplankton species which is particularly important for experimentation. The tank also results in an increase in cell concentration of phytoplankton during transportation.
- A table-top environmental chamber housing four aquariums was successfully designed and constructed. The environmental chamber regulates temperature and radiation. The chamber was successfully used in performing experiments on phytoplankton.
- The diatom species from the Marginal Ice Zone of the Southern Ocean were successfully experimented on.
 - The diatom species investigated in this study are mostly shade adaptative, being photo inhibited at irradiances between 42 and 200 $\mu\text{molm}^{-2}\text{s}^{-1}$, with the exception of *Navicula spp*, *Cylindrotheca closterium* and the unidentified pennates.
 - Surviving diatom species favor warmer temperatures, in this case 8°C over 5°C.

8.2 Recommendations

The hybrid system designed in this work was successful in increasing phytoplankton cell concentration and preserving species. However, only one tank was a success. It is therefore recommended that the hybrid tanks be tested again in spring with three hybrid tanks being used to obtain cores per station. Spring offers a greater chance of coring from multiple stations favoring both consolidated and open drift stations. Furthermore, it is advised that the original protocol of melting tanks in different time intervals be followed i.e., one week, 6 weeks, and 12 weeks post-cruise.

The designed environmental chamber only allows for liquid culturing of a few phytoplankton species and has considerable potential

- It is recommended that agitation be incorporated in future work. Cells tended to stick to the walls of the aquaria, therefore it can be concluded that stirring with a rod twice a week was not enough to keep cells in suspension. The EC thus has to be optimized such that gentle automatic agitation is incorporated.
- The EC can be retrofitted to perform ice experiments. A cold finger can be designed and together with the aquaria in the environmental chamber, be used for ice experiments. The EC will prove beneficial for initial ice experiments as it provides an enclosure with temperature control.
- It is also recommended that PAR and temperature measurements conducted when testing the EC, be conducted with artificial seawater as opposed to milli Q water. The EC is designed for experimentation with phytoplankton in seawater and, as such the solutes in the artificial seawater impact these measurements.

The initial liquid culturing of phytoplankton gave preliminary data, however more work still has to be conducted for more accurate results.

- Species can be isolated and their response to irradiation changes and temperature measured. This will determine if certain species are indeed photo-inhibited at certain irradiances or if other species-species interactions are at play.
- Phytoplankton responses to irradiances between 0 and $42\mu\text{molm}^{-2}\text{s}^{-1}$ should be measured. This study already showed that most species are shade-adaptive. This will help determine the exact irradiances at which the shade adaptive species are photo-inhibited.
- At low irradiances, phytoplankton should be investigated in ice, to determine whether vertical stability will still influence cell concentration as would have been discovered in liquid culturing.
- Batch culturing results in nutrient limitation towards the end of the experiment. This has been shown in this study and it is thus recommended that for a six-week experiment, nutrients be supplemented mid-experiment i.e., after three weeks of starting the experiment. Furthermore, it is recommended that the impact of sample removal on temperature, salinity, and nutrients be tested on seawater when the EC is tested for control of PAR and temperature.

- In addition to phosphate measurements, it is also recommended that nitrate and silicate measurements be conducted. As a result of the death of phytoplankton, nitrogen dynamics would have changed in the aquaria. This would also have to be accounted for as nitrogen is not the preferred nutrient of diatoms.
- Before experimental analysis, grazers were not removed. Grazers not being accounted for in the experiments means their influence on the experiments and certain species is unknown. This should be considered in future work.

REFERENCES

- Ackley, S. and Weeks, W. (1990) 'Sea Ice Properties and Processes. Proceedings of the W. F. Weeks Sea Ice Symposium Held In San Francisco, California on December 1988', p. 296.
- Ackley, S. and Sullivan, C.W. (1994) 'Physical controls on the development and characteristics of Antarctic Sea ice biological communities— a review and synthesis', *Deep Sea Research Part I: Oceanographic Research Papers*, 41(10), pp. 1583–1604. Available at: [https://doi.org/10.1016/0967-0637\(94\)90062-0](https://doi.org/10.1016/0967-0637(94)90062-0).
- Aletsee, L. and Jahnke, J. (1992) 'Growth and productivity of the psychrophilic marine diatoms *Thalassiosira antarctica* and *Nitzschia frigida* Grunow in batch cultures at temperatures below the freezing point of sea water', *Polar Biology*, 11, pp. 643–647. Available at: doi: 10.1007/BF00237960.
- Andreoli, C., Moro, I. La Rocca, N. Valle, L. D. Masiero, L. Rascio, N. and Vecchia, F. D. (2000) 'Ecological, physiological, and biomolecular surveys on microalgae from Ross Sea (Antarctica)', *Italian Journal of Zoology*, 67(sup1), pp 147–156. Available at: <https://doi.org/10.1080/11250000009356370>.
- Ardyna, M., Mundy, C.J. Mayot, N. Matthes, L. Oziel, O. Horvat, C. Leu, E. Assmy, P. Hill, V. Matrai, P. Gale, M. Melnikov, I.A. and Arrigo, K. (2020) 'Under-Ice Phytoplankton Blooms: Shedding Light on the “Invisible” Part of Arctic Primary Production', *Frontiers in Marine Science*, 7. Available at: <https://doi.org/10.3389/fmars.2020.608032>
- Ardyna, M., Gosselin, M. Michel, C. Poulin, M. and Tremblay, J. (2011) 'Environmental forcing of phytoplankton community structure and function in the Canadian High Arctic: contrasting oligotrophic and eutrophic regions', *Marine Ecology Progress Series*, 442, pp 37-57. Available at: doi: 10.3354/meps09378.
- Arrigo, K.R., Worthen, D.L. Lizotte, M.P. Dixon, P. and Dieckmann, G. (1997) 'Primary Production in Antarctic Sea Ice', *Science*, 276(5311), pp. 394–397. Available at: <https://doi.org/10.1126/science.276.5311.394>.
- Arrigo, K.R. (2016) 'Sea ice as a habitat for primary producers', in *Sea Ice*. Chichester, UK: John Wiley & Sons, Ltd, pp. 352–369. Available at: <https://doi.org/10.1002/9781118778371.ch14>.

Arrigo, K.R. and Sullivan, C.W. (1992) 'The influence of salinity and temperature covariation on the photophysiological characteristics of Antarctic Sea ice microalgae¹', *Journal of Phycology*, 28(6), pp. 746–756. Available at: <https://doi.org/10.1111/j.0022-3646.1992.00746.x>.

Arrigo, K.R. and Thomas, D.N. (2004) 'Large scale importance of sea ice biology in the Southern Ocean', *Antarctic Science*, 16(04), pp 471-486. Available at: <http://dx.doi.org/10.1017/S0954102004002263>

Arrigo, K.R., van Dijken, G.L. Alderkamp, A.C. Erickson, Z.K. Lewis, K.M. Lowry, K.E. van de Poll, W. (2017) 'Early Spring phytoplankton dynamics in the western Antarctic Peninsula', *Journal of Geophysical Research: Oceans*, 122, pp 9350–9369. Available at: <https://doi.org/10.1002/2017JC013281>

Ashton, G. D. (1989) 'Thin ice growth', *Water Resources Research*, 25(3), pp. 564–566. Available at: <https://doi.org/10.1029/WR025i003p00564>.

Aulicino, G. Cotroneo, Y. Ansorge, I. van den Berg, M. Cesarano, C. Rivas, M.B. and Casal, E.O. (2018) 'Sea surface salinity and temperature in the southern Atlantic Ocean from South African icebreakers, 2010–2017', *Earth Syst. Sci. Data*, 10(3), pp. 1227–1236. Available at: <https://doi.org/10.5194/essd-10-1227-2018>.

Barcelos e Ramos, Schulz, K.G. Voss, M. Narciso, A. Muller, M.N. Reis, F.V. Cachao, M. and Azevedo, E.B. (2017) 'Nutrient-specific responses of a phytoplankton community: a case study of the North Atlantic Gyre, Azores', *Journal of Plankton Research*, 39(4), pp. 744–761. Available at: <https://doi.org/10.1093/plankt/fbx025>.

Brits Nonwoven, P.L. (2015) *Isotherm Product Specifications*. Available at: <https://www.isotherm.co.za/isotherm/product-specifications>.

Bowman, J.S. and Deming, J.W. (2017) 'Wind-driven distribution of bacteria in coastal Antarctica: evidence from the Ross Sea region', *Polar Biology*, 40, pp 25–35. Available at: <https://doi.org/10.1007/s00300-016-1921-2>.

Bowman, J.S. and Ducklow, H.W. (2015) 'Microbial Communities Can Be Described by Metabolic Structure: A General Framework and Application to a Seasonally Variable, Depth-Stratified Microbial Community from the Coastal West Antarctic Peninsula', *PLoS ONE* 10(8). Available at: e0135868. <https://doi.org/10.1371/journal.pone.0135868>.

Campbell, K., Mundy, C.J. Juhl, A.R. Dalman, L.A. Michel, C. Galley, R.J. Else, B.E. Geilfus, N.X and Rysgaard, S. (2019) 'Melt Procedure Affects the Photosynthetic Response of Sea Ice Algae', *Frontiers in Earth Science*, 7. Available at: <https://doi.org/10.3389/feart.2019.00021>.

Campbell Scientific Africa (2019) *Campbell Scientific Africa*. Available at: <https://www.campbellsci.co.za>.

Castellani, G., Schaafsma, F. L. Arndt, S. Lange, B. A. Peeken, I. Ehrlich, J. David, C. Ricker, R. Krumpfen, T. Hendricks, S. Schwegmann, S. Massicotte, P. and Floures, H. (2020) 'Large-scale variability of physical and biological sea-ice properties in polar oceans', *Frontiers in Marine Science*, 7(536). Available at: doi: 10.3389/fmars.2020.00536.

Chapman, C.C., Lea, M. Meyer, A. Sallée, J. and Hindell, M. (2020). 'Defining Southern Ocean fronts and their influence on biological and physical processes in a changing climate', *Nature Climate Change*, 10, pp. 209-219. Available at: <https://doi.org/10.1038/s41558-020-0705-4>.

Charlson, R.J., Lovelock, J.E. Andreae, M.O. and Warren, S.G. (1987) 'Oceanic phytoplankton, atmospheric sulphur, cloud albedo and climate', *Nature*, 326(6114), pp. 655–661. Available at: <https://doi.org/10.1038/326655a0>.

Cota, G.F. and Smith, R.E.H. (1991) 'Ecology of bottom ice algae: II. Dynamics, distributions and productivity', *Journal of Marine Systems*, 2(3–4), pp. 279–295. Available at: [https://doi.org/10.1016/0924-7963\(91\)90037-U](https://doi.org/10.1016/0924-7963(91)90037-U).

Cox, G.F.N. and Weeks, W.F. (1986) 'Changes in the Salinity and Porosity of Sea-Ice Samples During Shipping and Storage', *Journal of Glaciology*, 32(112), pp. 371–375. Available at: <https://doi.org/10.3189/S0022143000012065>.

Cumulus Insulation (2019) *Cumulus Insulation*. Available at: <https://www.cumulus.co.za>

Darehshouri, S., Michelsen, N. Schüth, C. and Schulz, S. (2020) 'A low-cost environmental chamber to simulate warm climatic conditions', *Vadose Zone J.* Available at: <https://doi.org/10.1002/vzj2.20023>.

Dawson, H.M., Heal, K. Boysen, A. Carlson, L. Ingalls, A. and Young, J. (2020). 'Potential of temperature- and salinity-driven shifts in diatom compatible solute concentrations to impact biogeochemical cycling within sea ice', *Elementa: Science of the Anthropocene*, 8(25). Available at: <https://doi.org/10.1525/elementa.421>.

- Deppeler, S.L. and Davidson, A.T. (2017) 'Southern Ocean Phytoplankton in a Changing Climate', *Frontiers in Marine Science*, 4. Available at: <https://doi.org/10.3389/fmars.2017.00040>.
- Dugdale, R.C. and Wilkerson, F.P. (1991) 'Low Specific Nitrate Uptake Rate: A Common Feature of High-Nutrient, Low-Chlorophyll Marine Ecosystems', *Limnology and Oceanography*, 36, pp 1678-1688. Available at: <https://doi.org/10.4319/lo.1991.36.8.1678>
- Duncan, R.J. and Petrou, K. (2022) 'Biomolecular Composition of Sea Ice Microalgae and Its Influence on Marine Biogeochemical Cycling and Carbon Transfer through Polar Marine Food Webs', *Geosciences*, 12(1), p. 38. Available at: <https://doi.org/10.3390/geosciences12010038>.
- Ewert, M. and Deming, J. (2013) 'Sea Ice Microorganisms: Environmental Constraints and Extracellular Responses', *Biology*, 2(2), pp. 603–628. Available at: <https://doi.org/10.3390/biology2020603>.
- Ezike, S., Alabi, A.B. Ossai, A.N. and Aina A.O. (2018) 'A Low-Cost Temperature-Controlled Chamber Fabricated for Materials Testing', *Designs*, 2(3), p. 25. Available at: <https://doi.org/10.3390/designs2030025>.
- Fiala, M. and Oriol, L. (1990) 'Light-temperature interactions on the growth of Antarctic diatoms', *Polar Biology*, 10(8), pp. 629–636. Available at: <https://doi.org/10.1007/BF00239374>.
- Forsythe, W.C., Rykiel Jr, E. Stahl, R.S. Wu, H. and Schoolfield, R.M. (1995) 'A model comparison for daylength as a function of latitude and day of year', *Ecological Modelling*, 80(1), pp. 87–95. Available at: [https://doi.org/10.1016/0304-3800\(94\)00034-F](https://doi.org/10.1016/0304-3800(94)00034-F).
- Franklin, J. (1998) 'Plant Growth Chamber Handbook USA', *New Phytologist*, 138(4), pp. 743–750. Available at: <https://doi.org/DOI: 10.1046/j.1469-8137.1998.00149-7.x>.
- Fripiat, F., Meiners, K.M. Vancoppenolle, M. Papadimitriou, S. Thomas, D.N. Ackley, S.F. Arrigo, K. Gauthier, C. Stefano, C. Delille, B. Dieckmann, G.S. Dunbar, R.B. Fransson, A. Kattner, G. Kennedy, H. Lannuzel, D. Munro, D.R. Nomura, D. Rintala, J.M. Schoemann, V. Stefels, J. Steiner, N. and Tison, J.N. (2017) 'Macro-nutrient concentrations in Antarctic pack ice: Overall patterns and overlooked processes', *Elementa: Science of the Anthropocene*, 5. Available at: <https://doi.org/10.1525/elementa.217>.
- Garrison, D.L., Close, A.R. and Reimnitz, E. (1989) 'Algae concentrated by frazil ice: evidence from laboratory experiments and field measurements', *Antarctic Science*, 1(4), pp. 313–316. Available at: <https://doi.org/10.1017/S0954102089000477>.

Gleitz, M. and Thomas, D. (1993) 'Variation in phytoplankton standing stock, chemical composition and physiology during sea-ice formation in the southeastern Weddell Sea, Antarctica', *Journal of experimental Marine Biology and Ecology*, 173(2), pp. 211-230. Available at: [https://doi.org/10.1016/0022-0981\(93\)90054-R](https://doi.org/10.1016/0022-0981(93)90054-R).

Golden, K.M., Ackley, S.F. and Lytle, V.I. (1998) 'The Percolation Phase Transition in Sea Ice', *Science*, 282(5397), pp. 2238–2241. Available at: <https://doi.org/10.1126/science.282.5397.2238>.

Gradinger, R. (2009) 'Sea-ice algae: Major contributors to primary production and algal biomass in the Chukchi and Beaufort Seas during May/June 2002', *Deep Sea Research Part II: Topical Studies in Oceanography*, 56(17), pp. 1201–1212. Available at: <https://doi.org/10.1016/j.dsr2.2008.10.016>.

Grant, W.S. and Horner, R.A. (1976) 'Growth responses to salinity variation in four arctic ice diatoms', *Journal of Phycology*, 12(2), pp. 180–185. Available at: <https://doi.org/10.1111/j.1529-8817.1976.tb00498.x>.

Greenspan, S. E., Morris, W. Warburton, R. Edwards, L. Duffy, R. Pike, D. A. Alford, R.A. (2016) 'Low-cost fluctuating-temperature chamber for experimental ecology', *Methods in Ecology and Evolution*, 7, pp 1567–1574. Available at: <https://doi.org/10.1111/2041-210X.12619>

Grenfell, T.C. and Perovich, D.K. (1981) 'Radiation absorption coefficients of polycrystalline ice from 400–1400 nm', *Journal of Geophysical Research*, 86(C8), p. 7447. Available at: <https://doi.org/10.1029/JC086iC08p07447>.

Gugliemo, L. ,Carrada, G.C. Catalano, G. Dell'Anno, A. Fabiano, M. Lazzara, L. Mangoni, O. Pusceddu, A. and Saggiomo, V. (2000) 'Structural and functional properties of sympagic communities in the annual sea ice at Terra Nova Bay (Ross Sea, Antarctica)', *Polar Biology*, 23(2), pp. 137-146. Available at: <https://doi.org/10.1007/s003000050019>.

Hallegraeff, G.M. Anderson, D.M. and Cembella, A.D. (2004) 'Manual on Harmful Marine Microalgae'. Available at: <http://unesdoc.unesco.org/images/0013/001317/131711e.pdf>.

Hambrock, M., Rampai, T. and Walker, D. (2021) *Exploring the effects of single and dual phase culturing on the concentrations of Southern Ocean sea-ice algae and transporting living sea-ice*

algae from the Southern Ocean to land-based research facilities. Dissertation. University of Cape Town.

Hancke, K., Lund-Hansen, L.C. Lamare, M.L. Pedersen, S.H. King, M.D Per Anderson, and Sorrell, B.K. (2018) 'Extreme Low Light Requirement for Algae Growth Underneath Sea Ice: A Case Study From Station Nord, NE Greenland', *Journal of Geophysical Research: Oceans*, 123(2), pp. 985–1000. Available at: <https://doi.org/10.1002/2017JC013263>.

Harada, N. (2016) 'Potential catastrophic reduction of sea ice in the western Arctic Ocean: its impact on biogeochemical cycles and marine ecosystems', *Global and Planetary Change*, 135, pp. 1–17. Available at: doi: 10.1016/j.gloplacha.2015.11.005.

Hayes, P.K., Whitaker, T.M. and Fogg, G.E. (1984) 'The distribution and nutrient status of phytoplankton in the Southern Ocean between 20° and 70° W', *Polar Biology*, 3(3), pp. 153–165. Available at: <https://doi.org/10.1007/BF00442647>.

Hop, H., Vihtakari, M. Bluhm, B.A. Assmy, P. Poulin, M. Gradinger, R. Peeken, I. von Quillfeldt, C. Olsen, L.M. Zhitina, L. and Melnikov, I.A. (2020) 'Changes in sea-ice protist diversity with declining sea ice in the Arctic Ocean from the 1980s to 2010s', *Frontiers in Marine Science*, 7 (243). Available at: <https://doi.org/10.3389/fmars.2020.00243>.

Horner, R., Ackley, S.F. Dieckmann, G.S. Gulliksen, B. Hoshiai, T. Legendre, L. Melnikov, I.A. Reeburgh, W.A. Spindler, M. and Sullivan, C. (1992) 'Ecology of sea ice biota', *Polar Biology*, 12(3–4). Available at: <https://doi.org/10.1007/BF00243113>.

Horvat, C., Bisson, K. Seabrook, S. Cristi, A. and Matthes, L. (2022) 'Evidence of phytoplankton blooms under Antarctic Sea ice', *Frontiers in Marine Science*, 9. Available at: <https://doi.org/10.3389/fmars.2022.942799>.

Huang, B.J., Liao, Y.C. and Kuo, T.C. (2007) 'Study of a new environmental chamber design', *Applied Thermal Engineering*, 27(11–12), pp. 1967–1977. Available at: <https://doi.org/10.1016/j.applthermaleng.2006.12.010>.

Huisman, J., Arrayas, M. Ebert, U. and Sommeijer, B. (2002) 'How Do Sinking Phytoplankton Species Manage to Persist?', *The American Naturalist*, 159(3), pp. 245-254. Available at: <http://dx.doi.org/10.1086/338511>.

Installed Building Products (2017) *Installed Building Contacts*. Available at: <https://www.ibpportland.com>.

IQS Manufacturer Directory (2019) *Industrial Quick Search Manufacturer Directory*. Available at: <https://www.iqsdirectory.com/articles/environmental-chamber.html>.

Junge, K., Imhoff, T. Deming, J.W. (2002) 'Phylogenetic diversity of numerically important Arctic sea-ice bacteria cultured at subzero temperature', *Microbiology Ecology*, 43, pp 315-328. Available at: 10.1007/s00248-001-1026-4.

Kaartokallio, H., Kuosa, H. Thomas, D.N. Granskog, M.A. and Kivi, A. (2006) 'Biomass, composition and activity of organism assemblages along a salinity gradient in sea ice subjected to river discharge in the Baltic Sea', *Polar Biology*, 30(2), pp. 183–197. Available at: <https://doi.org/10.1007/s00300-006-0172-z>.

Kattner, G. Thomas, D.N. Haas, C. Kennedy, H. and Dieckmann, G. (2004) 'Surface ice and gap layers in Antarctic Sea ice: highly productive habitats', *Marine Ecology Progress Series*, 277, pp. 1–12. Available at: <https://doi.org/10.3354/meps277001>.

Kauko, H. M. Olsen, L. M. Duarte, P. Peeken, I. Granskog, M. A. Johnsen, G. Fernandez-Mendez, M. Pavlov, A.K. Mundy, C.J. and Assmy, P. (2018). 'Algal colonization of young Arctic sea ice in spring', *Frontiers in Marine Science*, 5(199). Available at: doi: 10.3389/fmars.2018.00199.

Kottmeier, S.T. and Sullivan, C.W. (1988) 'Sea ice microbial communities (SIMCO)', *Polar Biology*, 8(4), pp. 293–304. Available at: <https://doi.org/10.1007/BF00263178>.

Lancelot, C., Mathot, S. Veth, C. and Hein de Baar. (1993) 'Factors controlling phytoplankton ice-edge blooms in the marginal ice-zone of the northwestern Weddell Sea during sea ice retreat 1988: Field observations and mathematical modelling', *Polar Biology*, 13(6), pp. 377–387. Available at: <https://doi.org/10.1007/BF01681979>.

Learnz. (2021) 'Virtual Experiences - Field Trips for Aotearoa Schools'. Available at: <https://www.learnz.org.nz/scienceonice144/bg-standard-f/antarctic-food-webs>.

Lefcourt, A.M., Buell, B. and Tasch, U. (2001) 'Large environmental chamber: Design and operating characteristics', *Applied Engineering in Agriculture*, 17(5). Available at: <https://doi.org/10.13031/2013.6915>.

Lifferth, S.O. (2009) *Design and construction of a new psychrometric chamber*. Dissertation. Oklahoma State University.

Lizotte, M. and Sullivan, C. (1991) 'Photosynthesis-irradiance relationships in microalgae associated with Antarctic pack ice: evidence for *in situ* activity', *Marine Ecology Progress Series*, 71, pp. 175–184. Available at: <https://doi.org/10.3354/meps0711175>.

Lizotte, M. and Sullivan, C. (1992) 'Biochemical composition and photosynthate distribution in sea ice microalgae of McMurdo Sound, Antarctica: evidence for nutrient stress during the spring bloom', *Antarctic Science*, 4, pp. 23–30. Available at: <https://doi.org/10.1017/S0954102092000063>.

Lizotte, M.P. (2003) 'The Microbiology of Sea Ice', in *Sea Ice*. Oxford, UK: Blackwell Science Ltd, pp. 184–210. Available at: <https://doi.org/10.1002/9780470757161.ch6>.

Louw S.D.V, Walker D.R. and Fawcett, S.E. (2022) 'Factors influencing sea-ice algae abundance, community composition, and distribution in the marginal ice zone of the Southern Ocean during winter', *Deep Sea Res. Part I: Oceanogr. Res. Pap*, 185. Available at: 103805. doi: 10.1016/j.dsr.2022.103805.

Maizey Engineering Plastic Products (2021) *Maizey Engineering Plastic Products*. Available at: <https://www.maizey.co.za/>.

Malone, T.C. (1980) 'Size fractionated primary productivity of marine phytoplankton', *Primary productivity in the sea*, P. G. Falkowski, editor, Plenum Press, New York, pp. 301-3 19.

Margalef, R. (1978) 'Life-forms of phytoplankton as survival alternatives in an unstable environment', *Oceanologica Acta*, 1, pp. 493–509.

McMinn, A. and Hegseth, E.N. (2007) 'Sea ice primary productivity in the northern Barents Sea, spring 2004', *Polar Biology*, 30(3), pp. 289–294. Available at: <https://doi.org/10.1007/s00300-006-0182-x>.

McMinn, A., Hattori, H. Hirawike, T. and Iwamoto, A. (2008) 'Preliminary investigation of Okhotsk Sea ice algae; taxonomic composition and photosynthetic activity', in *Polar Biology*, 31(8), pp. 1011-1015. Available at: <https://doi.org/10.1007/s00300-008-0433-0>.

McMinn, A., Martin, A. and Ryan, K. (2010) 'Phytoplankton and sea ice algal biomass and physiology during the transition between winter and spring (McMurdo Sound, Antarctica)', *Polar Biology*, 33(11), pp. 1547–1556. Available at: <https://doi.org/10.1007/s00300-010-0844-6>.

Meiners, K. M., Krembs, C. and Gradinger, R. (2008) 'Exopolymer particles: microbial hotspots of enhanced bacterial activity in Arctic fast ice (Chukchi Sea)', *Aquat. Microb. Ecol.* 52, pp. 195–207. Available at: doi: 10.3354/ame01214.

Meiners, K.M. and Michel, C. (2016) 'Dynamics of nutrients, dissolved organic matter and exopolymers in sea ice', in *Sea Ice*. Chichester, UK: John Wiley & Sons, Ltd, pp. 415–432. Available at: <https://doi.org/10.1002/9781118778371.ch17>.

Mikkelsen, D.M. and Witkowski, A. (2010) 'Melting sea ice for taxonomic analysis: a comparison of four melting procedures', *Polar Research*, 29, pp. 451-454. Available at: <https://doi.org/10.1111/j.1751-8369.2010.00162.x>

Miller, L.A., Fripiat, F. Else, B.G.T. Bowman, J.S. Brown, K.A. Collins, E.R. Ewert, M. Fransson, A. Gosselin, M. Lannuzel, D. Meiners, K.A. Michel, K. Nishioka, J. Nomura, D. Papadimitriou, S. Russell, L.M. Sørensen, L. Thomas, D.N. Tison, J.N. Van Leeuwe, M.A. Vancoppenolle, M. Wolff, E.W. and Zhou, J. (2015) 'Methods for biogeochemical studies of sea ice: The state of the art, caveats, and recommendations', *Elementa: Science of the Anthropocene*, 3. Available at: <https://doi.org/10.12952/journal.elementa.000038>.

Mock, T. and Thomas, D.N. (2005) 'Recent advances in sea-ice microbiology', *Environmental Microbiology*, 7(5), pp. 605–619. Available at: <https://doi.org/10.1111/j.1462-2920.2005.00781.x>.

Mundy, C.J., Gosselin, M. Ehn, J.K. Belzile, C. Poulin, M. Alou, E. Roy, S. Hop, H. Lessard, S. Papakyriakou, T.N. Barber, D.G. and Stewart, J. (2011) 'Characteristics of two distinct high-light acclimated algal communities during advanced stages of sea ice melt', *Polar Biology*, 34, pp. 1869–1886. Available at: <https://doi.org/10.1007/s00300-011-0998-x>.

Natarajan, K. (1970) 'Toxicity of Ammonia to Marine Diatoms', *Journal (Water Pollution Control Federation)*, 42(5), pp. 184-190. Available at: <https://www.jstor.org/stable/25036590>.

Nelson, D.M. and Smith, W.O. (1986) 'Phytoplankton bloom dynamics of the western Ross Sea ice edge—II. Mesoscale cycling of nitrogen and silicon', *Deep Sea Research Part A. Oceanographic Research Papers*, 33(10), pp. 1389–1412. Available at: [https://doi.org/10.1016/0198-0149\(86\)90042-7](https://doi.org/10.1016/0198-0149(86)90042-7).

Palmisano, A. and Sullivan, C. (1982) 'Physiology of Sea ice diatoms. I. Response of three polar diatoms to a stimulated summer-winter transition', *Journal of Phycology*, 18(4), pp. 489-498. Available at: <https://doi.org/10.1111/j.1529-8817.1982.tb03215.x>

Palmisano, A., SooHoo, J. and Sullivan, C. (1985) 'Photosynthesis-irradiance relationships in Sea ice microalgae from McMurdo Sound, Antarctica 1', *Journal of Phycology*, 21(3), pp. 341-346. Available at: <https://doi.org/10.1111/j.0022-3646.1985.00341.x>

Petrou, K., Hill, R. Doblin, M.A. McMinn, A. Johnson, R. Wright, S.W and Ralph, P.J. (2011) 'Photoprotection of sea-ice microalgal communities from the east Antarctic pack ice1', *Journal of Phycology*, 47(1), pp. 77–86. Available at: <https://doi.org/10.1111/j.1529-8817.2010.00944.x>.

Post, A., Meijers, A.J.S. Fraser, A.D. Meiners, K.M. Ayers, J. Bindoff, N. Griffiths, H.J Van de Putte, A. O'Brien, P.E. Swadling, K.M and Raymond, B. (2014) 'Environmental Setting', in *Biogeographic Atlas of the Southern Ocean*, pp. 46–64.

Le Quéré, C., Rodenbeck, C. Buitenhuis, E.T. Conway, T.J. Langenfelds, R. Gomez, A. Labuschagne, C. Ramonet, M. Nakazawa, T. Metzl, N. Gillet, N and Heimann, M. (2007) 'Saturation of the Southern Ocean CO₂ Sink Due to Recent Climate Change', *Science*, 316(5832), pp. 1735–1738. Available at: [10.1126/science.1136188](https://doi.org/10.1126/science.1136188)

Le Quéré, C., Andrew, R. M. Canadell, J. G. Sitch, S. Korsbakken, J. I. Peters, G. P. Manning, A. C. Boden, T. A. Tans, P. P. Houghton, R. A. Keeling, R. F. Alin, S. Andrews, O. D. Anthoni, P. Barbero, L. Bopp, L. Chevallier, F. Chini, L. P. Ciais, P. Currie, K. Delire, C. Doney, S. C. Friedlingstein, P. Gkritzalis, T. Harris, I. Hauck, J. Haverd, V. Hoppema, M. Klein Goldewijk, K. Jain, A. K. Kato, E. Körtzinger, A. Landschützer, P. Lefèvre, N. Lenton, A. Lienert, S. Lombardozi, D. Melton, J. R. Metzl, N. Millero, F. Monteiro, P. M. S. Munro, D. R. Nabel, J. E. M. S. Nakaoka, S. O'Brien, K. Olsen, A. Omar, A. M. Ono, T., Pierrot, D., Poulter, B., Rödenbeck, C., Salisbury, J., Schuster, U., Schwinger, J., Séférian, R. Skjelvan, I. Stocker, B. D. Sutton, A. J. Takahashi, T. Tian, H. Tilbrook, B. Van der Laan-Luijkx, I. T. Van der Werf, G. R. Viovy, N., Walker, A. P. Wiltshire, A. J. and Zaehle, S. (2016) 'Global Carbon Budget 2016', *Earth System Science Data*, 8(2), pp. 605–649. Available at: <https://doi.org/10.5194/essd-8-605-2016>.

Ralph, P. J. Ryan, K. G. Martin, A. and Fenton, G. (2007) 'Melting out of sea ice causes greater photosynthetic stress in algae than freezing in', *Journal of Phycology*, 43, pp 948–956. Available at: [doi: 10.1111/j.1529-8817.2007.00382.x](https://doi.org/10.1111/j.1529-8817.2007.00382.x).

Rintala, JM., Piiparinen, J. Blomster, J. Majaneva, M. Muller, S. Uusikivi, J. and Riitta, A. (2014) 'Fast direct melting of brackish sea-ice samples results in biologically more accurate results than slow buffered melting', *Polar Biol*, 37, pp 1811–1822. Available at: <https://doi.org/10.1007/s00300-014-1563-1>.

Ryan, K.G., Ralph, P. and McMinn, A. (2004) 'Acclimation of Antarctic bottom-ice algal communities to lowered salinities during melting', *Polar Biology*, 27, pp. 679–686. Available at: <https://doi.org/10.1007/s00300-004-0636-y>.

Ryan, K.G, Tay, M.L. Martin, A. McMinn, A. and Davy, S.K. (2011) 'Chlorophyll fluorescence imaging analysis of the responses of Antarctic bottom-ice algae to light and salinity during melting', *Journal of Experimental Marine Biology and Ecology*, 399(2), pp. 156–161. Available at: <https://doi.org/10.1016/j.jembe.2011.01.006>.

Schlie, C. and Karsten, U. (2016) 'Growth of the Antarctic Sea ice diatom *Navicula* cf. *normaloides* Cholnoky at different temperatures and salinities', *Algological Studies*, 151–152, pp. 39–49. Available at: [10.1127/algol_stud/2016/0271](https://doi.org/10.1127/algol_stud/2016/0271).

Smetacek, V., Scharek, R. and Nöthig, E.-M. (1990) 'Seasonal and Regional Variation in the Pelagial and its Relationship to the Life History Cycle of Krill', in *Antarctic Ecosystems*. Berlin, Heidelberg: Springer Berlin Heidelberg, pp. 103–114. Available at: https://doi.org/10.1007/978-3-642-84074-6_10.

Smith Jr, W.O., Nelson, D. and Mathot, S. (1999) 'Phytoplankton growth rates in the Ross Sea, Antarctica, determined by independent methods: temporal variations', *Journal of Plankton Research*, 21(8), pp 1519–1536. Available at: <https://doi.org/10.1093/plankt/21.8.1519>.

Smith, W.O., Marra, J. Hiscock, M.R. and Barber, R. (2000) 'The seasonal cycle of phytoplankton biomass and primary productivity in the Ross Sea, Antarctica', *Deep Sea Research Part II: Topical Studies in Oceanography*, 47(15–16), pp. 3119–3140. Available at: [https://doi.org/10.1016/S0967-0645\(00\)00061-8](https://doi.org/10.1016/S0967-0645(00)00061-8).

Sugie, K., Fujiwara, A. Nishino, S. Kameyama, S. and Harada, N. (2020) 'Impacts of Temperature, CO₂, and Salinity on Phytoplankton Community Composition in the Western Arctic Ocean', *Frontiers in Marine Science*, 6 (821). Available at: <https://doi.org/10.3389/fmars.2019.0082>.

Thomas, D.N. (ed.) (2017) *Sea Ice*. Wiley. Available at: <https://doi.org/10.1002/9781118778371>.

Thomas, D.N. and Dieckmann, G.S. (eds) (2009) *Sea Ice*. Wiley. Available at: <https://doi.org/10.1002/9781444317145>.

Timco, G.W. and Weeks, W.F. (2010) 'A review of the engineering properties of sea ice', *Cold Regions Science and Technology*, 60(2), pp. 107–129. Available at: <https://doi.org/10.1016/j.coldregions.2009.10.003>.

Torstensson, A., Jiménez, C. Nilsson, A.K. and Wulff, A. (2019) 'Elevated temperature and decreased salinity both affect the biochemical composition of the Antarctic sea-ice diatom *Nitzschia lecointei*, but not increased pCO₂', *Polar Biol* 42, pp. 2149–2164. Available at: <https://doi.org/10.1007/s00300-019-02589-y>

Tyagi, J., Ahmad, S. and Malik, M. (2022) 'Nitrogenous fertilizers: impact on environment sustainability, mitigation strategies, and challenges', *Int. J. Environ. Sci. Technol*, 19, pp. 11649–11672. Available at: <https://doi.org/10.1007/s13762-022-04027-9>.

Van Leeuwe M., Tedesco L, Arrigo K, Assmy P, Campbell K, Meiners K, Rintala J, Selz V, Thomas D, Stefels J and Deming J. (2018) 'Microalgal community structure and primary production in Arctic and Antarctic sea ice: A synthesis', *Elementa Science of the Anthropocene*, 6(4), pp 1-25. Available at: <https://doi.org/10.1525/elementa.267>.

Wadhams, P., Lange, M.A. and Ackley, S.F. (1987) 'The ice thickness distribution across the Atlantic sector of the Antarctic Ocean in midwinter', *Journal of Geophysical Research*, 92(C13), pp. 14535. Available at: <https://doi.org/10.1029/JC092iC13p14535>.

Williams, G. P. (1963) 'Heat transfer coefficients for natural water surfaces', *International Association of Scientific Hydrology*, 62, pp. 203–212.

Yan, D., Yoshida, K. Nishioka, J. Ito, M. Toyota, T. and Suzuki, K. (2020) 'Response to Sea Ice Melt Indicates High Seeding Potential of the Ice Diatom *Thalassiosira* to Spring Phytoplankton Blooms: A Laboratory Study on an Ice Algal Community From the Sea of Okhotsk', *Frontiers in Marine Science*, 7. Available at: <https://doi.org/10.3389/fmars.2020.00613>

APPENDICES

Appendix A: Optimization of the Hybrid Tank

A1: Determination of daylight hours

Table A. 1: Calculation of Daylight hours at sampling sites

Sample	1
Day of the year	205
Revolution angle	2.094

Declination Angle	-0.2
Latitude	-59.1649
P	0.000
Daylight Hours	6.97

Table A. 2: Day length definitions defined by the position of the sun with respect to the horizon (Forsythe et al., 1995)

Day length definitions (With and Without Twilight)	P (degrees)
Sunrise/Sunset is when the center of the sun is even with the horizon	0.000
Sunrise/Sunset is when the top of the sun is even with the horizon	0.267
Sunrise/Sunset is when the top of the sun is apparently even with the horizon	0.833
With Civil twilight	6.000
With nautical twilight	12.000
With astronomical twilight	18.000

This value is the summation of the radius of the sun (in degrees as seen from Earth) plus the adopted value for the refraction of the light through the atmosphere of 34 minutes (Astronomical Almanac 1992)

A2: Additional images and figures



Figure A. 1: On deck coring of pancake



Figure A. 2: Setup of hybrid tank with open insulation during transportation

Table A. 3: Additional information on cores collected during the SCALEWIN 2022 in the marginal sea ice zone of the Southern Ocean

Station Number	
Station Type	Open Drift Station
Date	24/07/2022
Opening time	7:30 am
Closing time	11:00 am
Time of extraction	9:00 am
Processing duration	00:30
Core depths (mm)	400
Latitude	-59.1649
Longitude	0.85777
Temperature (°C)	-2.0

Table A. 4: Microscopic cell concentration per mL for all taxonomic groups for the different transport systems

Species	Immediate preservation	Hybrid Tank 1	Solid transport	Liquid Transport
Navicula	782	1612	1098	9
Cylindrotheca	610	1158	520	4
Pseudo Nitzschia	538	501	558	13
Fragilariopsis kerguelensis	691	1015	208	355
Asterionellopsis glacialis	0	2	0	1
Striatella unipunctata	50	101	12	4
Unidentified Pennates	64	239	81	63
Total Pennates	2735	4628	2477	449
Unidentified Centrics	165	370	45	3
Dactyliosolen	198	329	70	0
Dactyliosolen antarctica	519	455	114	8
Chaetoceros	446	859	163	1
Asteromphalus	0	32	0	0
Total Centrics	1328	2045	392	12
Dinoflagellates	3	5	1	0

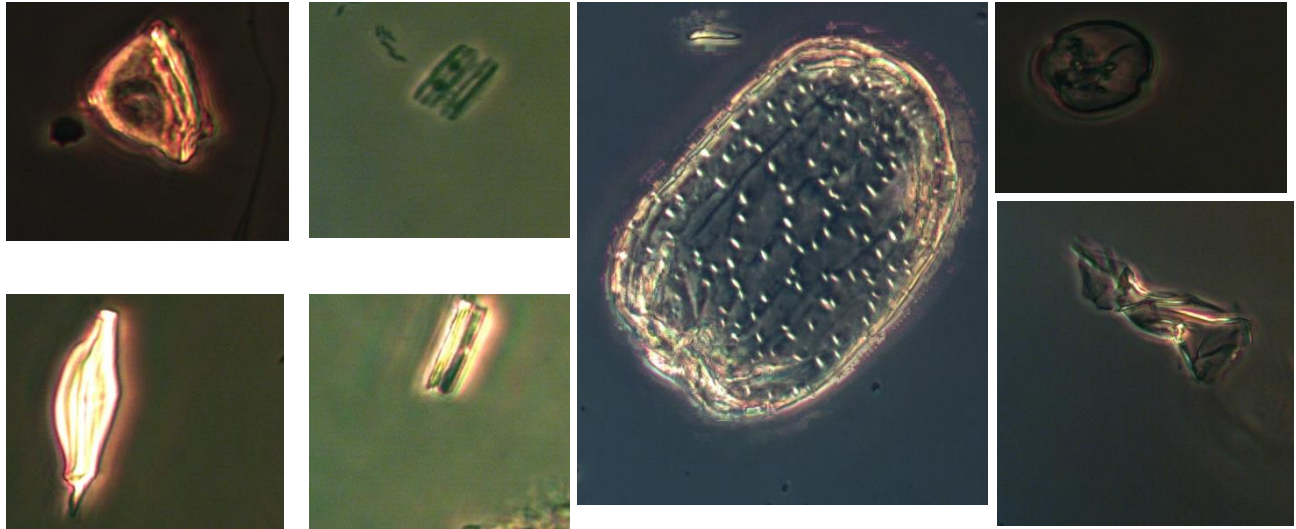


Figure A. 3: Unidentified pennates as per Hambrock, Rampai and Walker (2021) studies.

Table A. 5: Microscopic cell concentration per Hambrock, Rampai and Walker (2021) studies for hybrid tank 1 sampled -59.3248S, 0.066617E in the marginal ice zone of the Southern Ocean

	Baseline	Hybrid tank 1	Liquid culturing	Species Growth
Unidentified pennates 1	34256.41	47958.97	12430.77	40%
Cylindrotheca closterium	1435.897	5743.589744	0	300%
Pseudo-nitzschia	396.5812	1483.760684	82.05128205	274%
Navicula	82.05128	1100.854701	0	1242%
fragilariopsis kerguelensis	205.1282	574.3589744	0	180%
unidentified pennate 2	0	47.86324786	0	100%
unidentified pennate 3	22	0	0	-100%
unidentified pennate 4	13.67521	0	0	-100%
unidentified pennate 5	65	0	0	-100%
unidentified pennate 6	27	0	0	-100%
unidentified pennate 7	218.8034	622.2222222	0	184%
unidentified centrics	12745.3	984.6153846	54.7008547	-92%
Odontella	1039.316	519.6581197	0	-50%
Dactyliosolen	656.4103	273.5042735	0	-58%
dactyliosolen phuketensis (2)	0	259.8290598	0	100%
dactyliosolen phuketensis (1)	5811.966	15316.23932	0	164%
dactyliosolen antarctica	656.4103	13.67521368	0	-98%

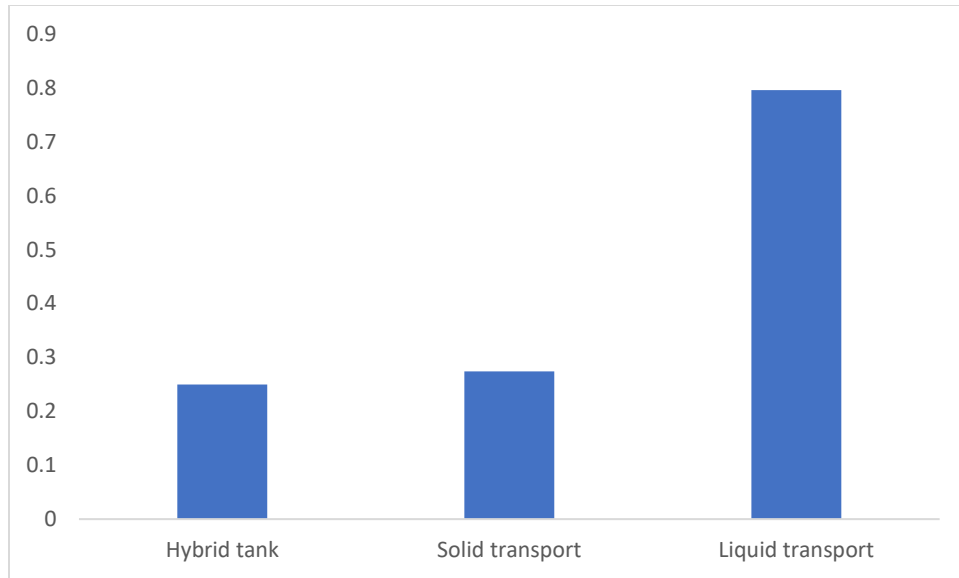


Figure A. 4: Bray Curtis Dissimilarity for all modes of transportation in comparison with baseline count.

Appendix B: Environmental Chamber

B1: Insulation calculations for the EC.

Perspex and expanded polystyrene thicknesses used were per the smallest cuts provided by the supplier. The first step was to investigate the ratio of internal resistance to external resistance, internal resistance being conduction and external resistance being convection. This was done by analyzing the Biot Modulus (Carnahan, et al., 1969). The ratio was calculated for the external

layer, the Perspex layer. It was assumed that air in the lab is under forced convection due to presence of air conditioning and thus h was taken as $250 \text{ Wm}^{-2}\text{K}^{-1}$ (Carnahan, et al., 1969).

$$Bi = \frac{h\left(\frac{V}{A}\right)}{k} = \frac{250\left(\frac{0.84 \times 0.52 \times 0.56}{0.84 \times 0.56 \times 2}\right)}{0.18} = 361 > 10$$

Since the Biot number was >10 , convection was therefore termed negligible, and conduction determined to be the main heat transfer mechanism in the system. The Outside temperature of the EC was therefore assumed to be the same as the room temperature i.e., 18°C . Radiation was assumed negligible as the EC is indoors (Coulson & Richardson, 2002)

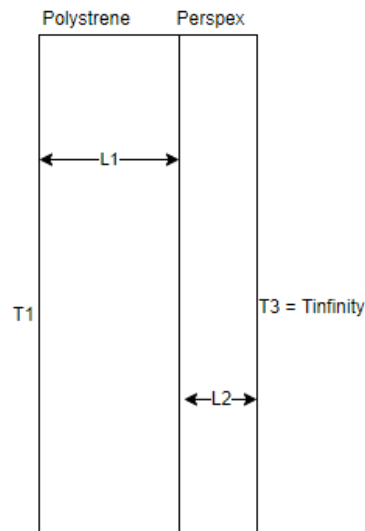


Figure B. 1 : illustration of heat transfer for the EC

For the EC, heat loss is considered greatest from the wall opposite the cooling plate. Heat loss via conduction is considered thermal conduction and Fourier's rate equation is applied in 1D for a plane wall. (Coulson & Richardson, 2002). Wall is composed of 2 layers i.e., expanded polystyrene layer (L1) and the Perspex layer (L2) (Figure B1). Assuming EC is set at 8°C .

$$\begin{array}{lll} L1 = 50 \text{ mm} = 0.05\text{m} & k1 = 0.035 \text{ Wm}^{-1}\text{k}^{-1} & T1 = 281\text{K} \\ L2 = 5 \text{ mm} = 0.005\text{m} & k2 = 0.18 \text{ Wm}^{-1}\text{k}^{-1} & T3 = 291\text{K} \end{array}$$

$$R1 = \frac{L1}{k1A1} = \frac{0.05}{0.035 \times 0.83 \times 0.51} = 3.37\text{K/W}$$

$$R2 = \frac{L2}{k2A2} = \frac{0.005}{0.18 \times 0.84 \times 0.52} = 0.064 \text{ K/W}$$

Assuming steady state within the walls

$$q = \frac{T1 - T3}{R1 + R2} = \frac{281 - 291}{3.37 + 0.064} = -46.4W$$

Bearing in mind that the greatest heat loss is from the wall opposite the cooler then assuming that all walls have the same heat loss, the total heat loss from the chamber upon cooling the EC to 8°C would be 185.6W. The EC thus makes use of a 600W chiller, as per supplier limitation to provide any chiller with power less than 600W.

B2: Temperature and Light mapping within the EC.

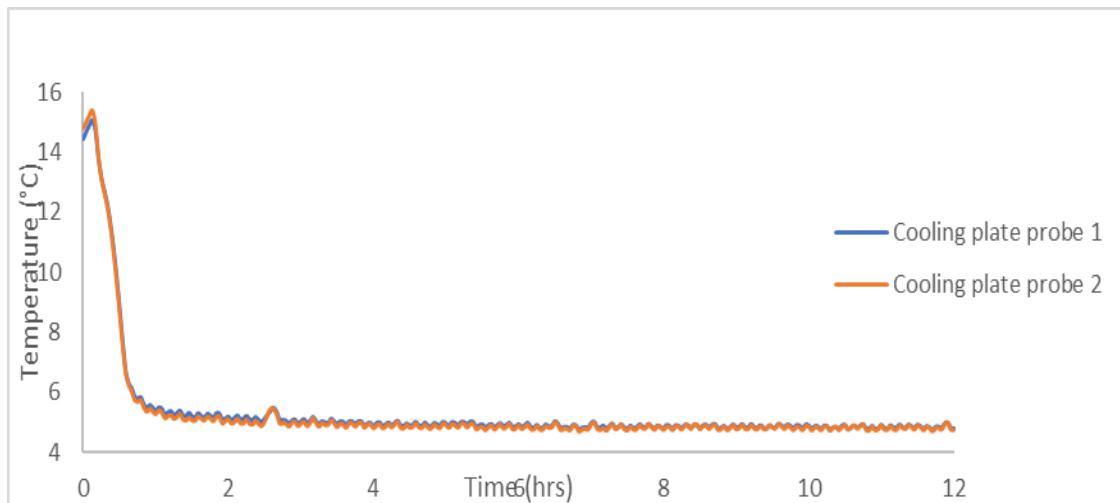


Figure B. 2: Temperature mapping within EC at 5°C focusing on the cooling plate.

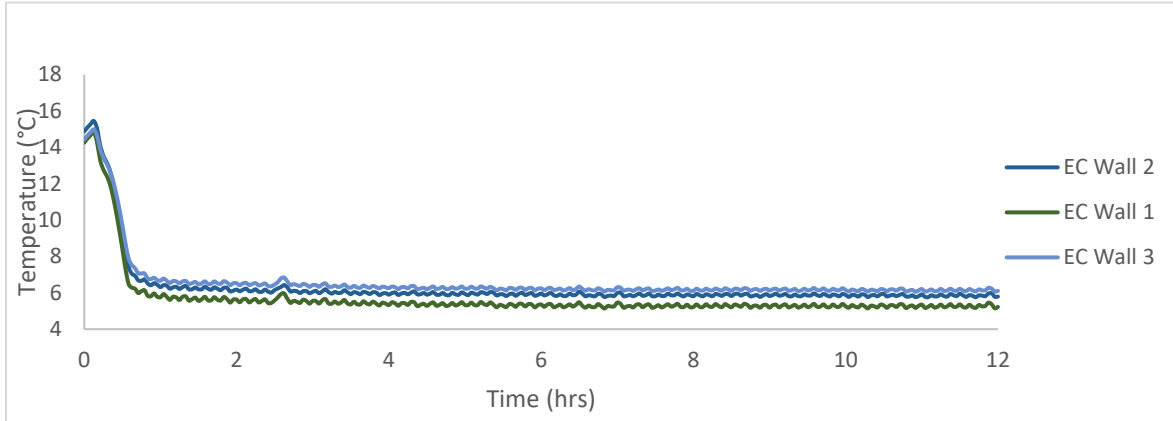


Figure B. 3: Temperature mapping at 5°C within EC focusing on the EC walls

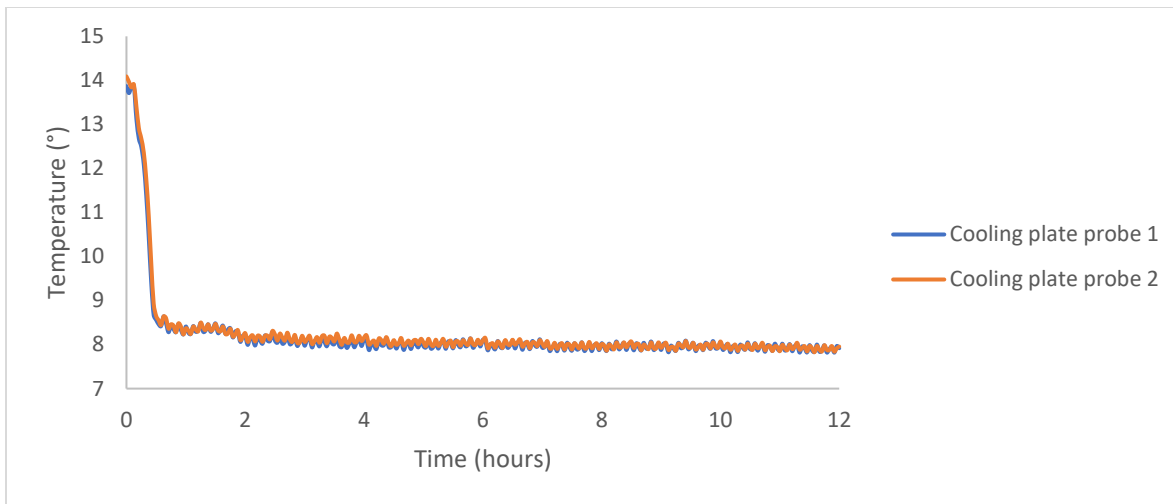


Figure B. 4: Temperature mapping at 8°C within the EC focusing on the cooling plate

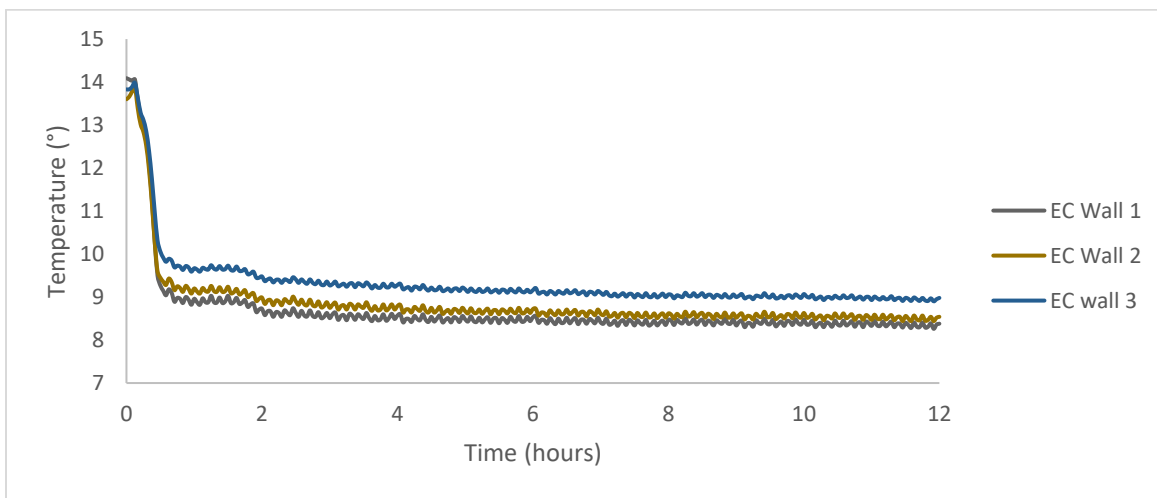


Figure B. 5: Temperature mapping at 8°C within the EC.

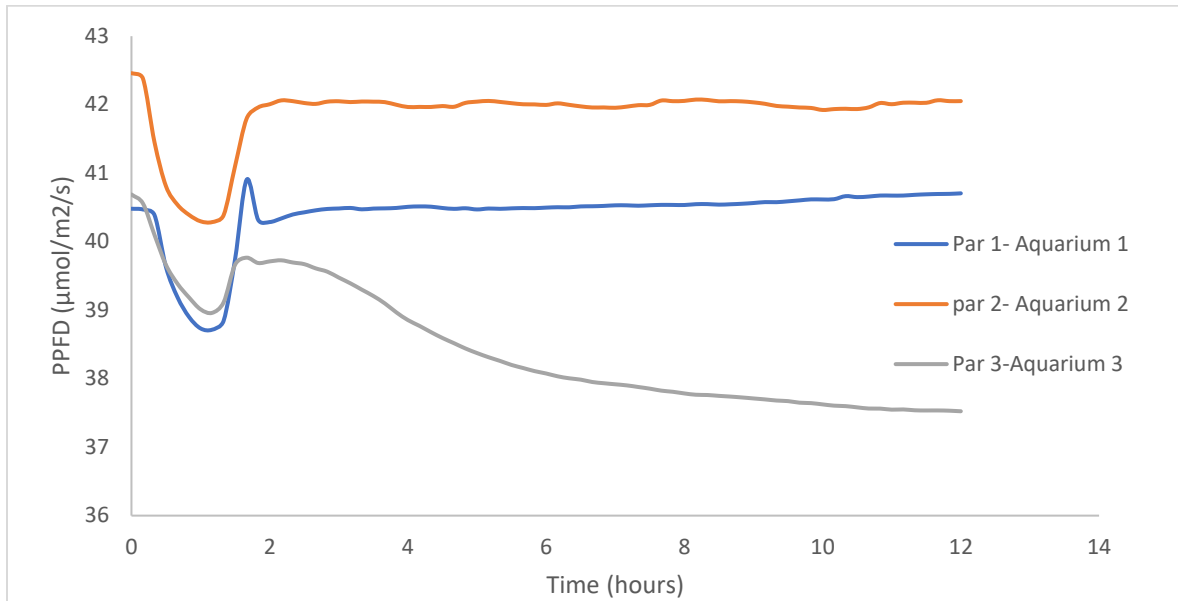


Figure B. 6: Par readings for light mapping in the EC when a shade filter is applied

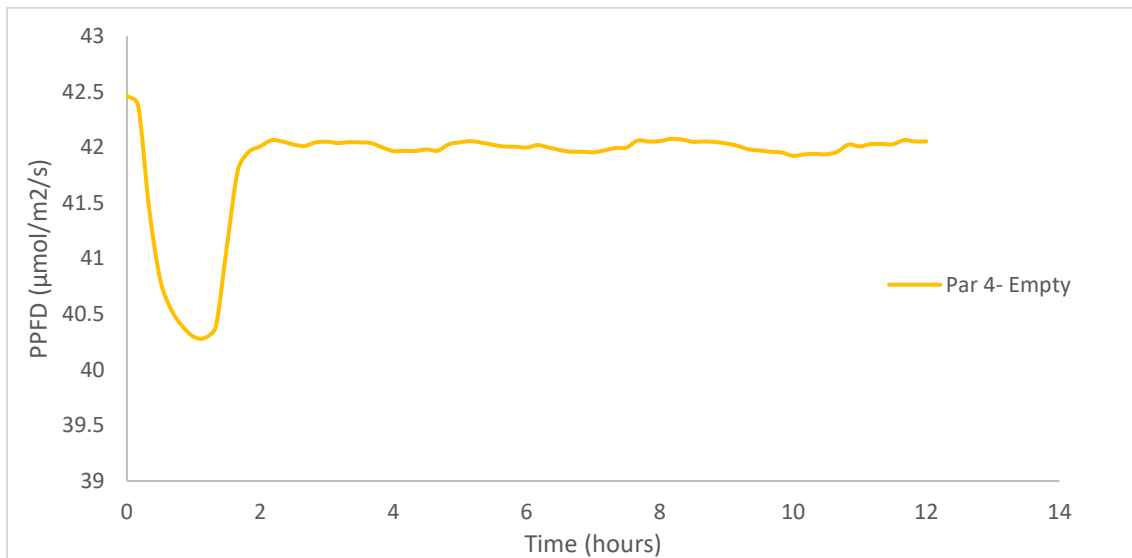


Figure B. 7: Par readings for light mapping in the EC when a shade filter is applied

B3: Additional drawings and pictures of the EC

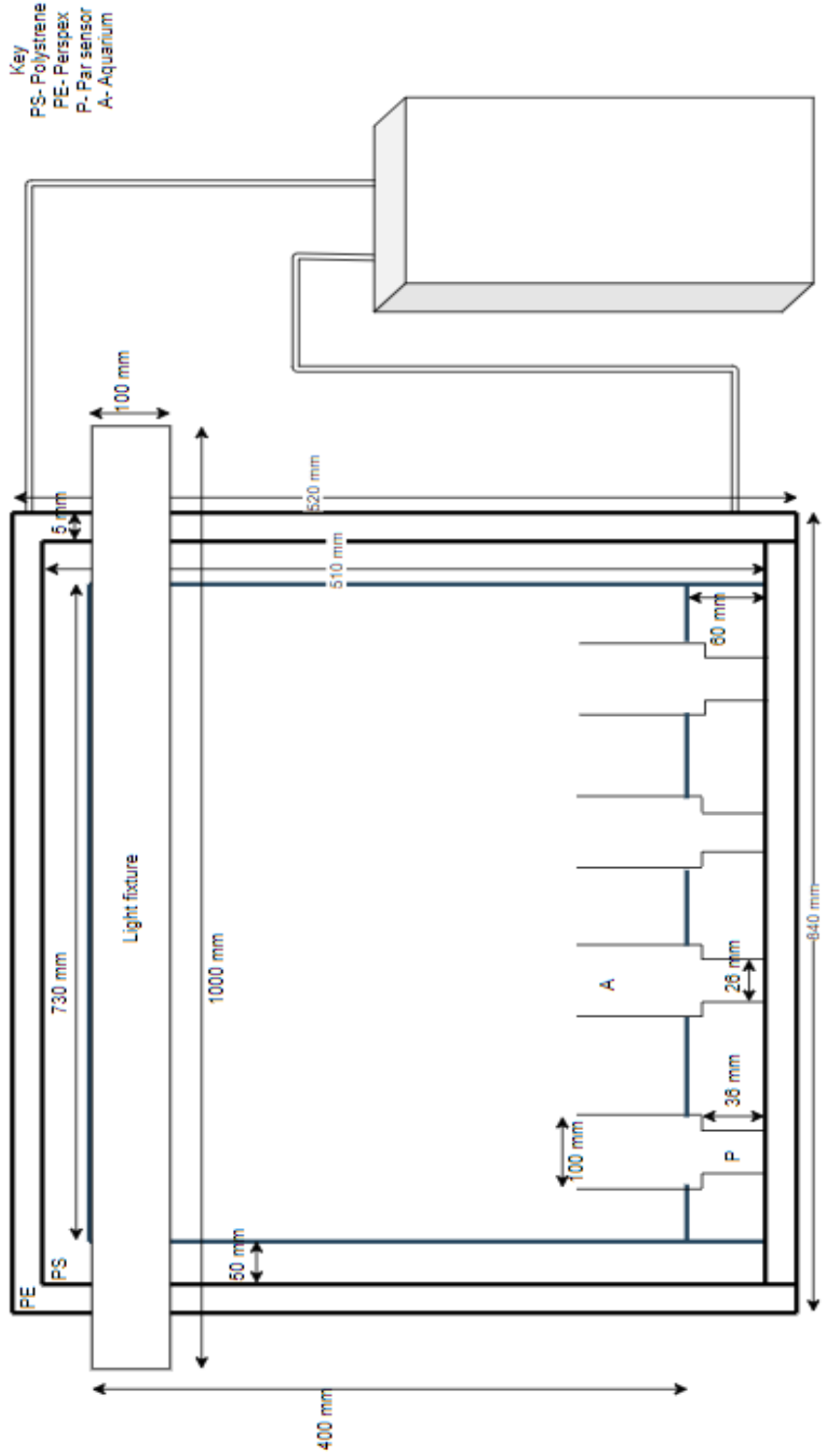


Figure B. 8: Front view of EC with its dimensions

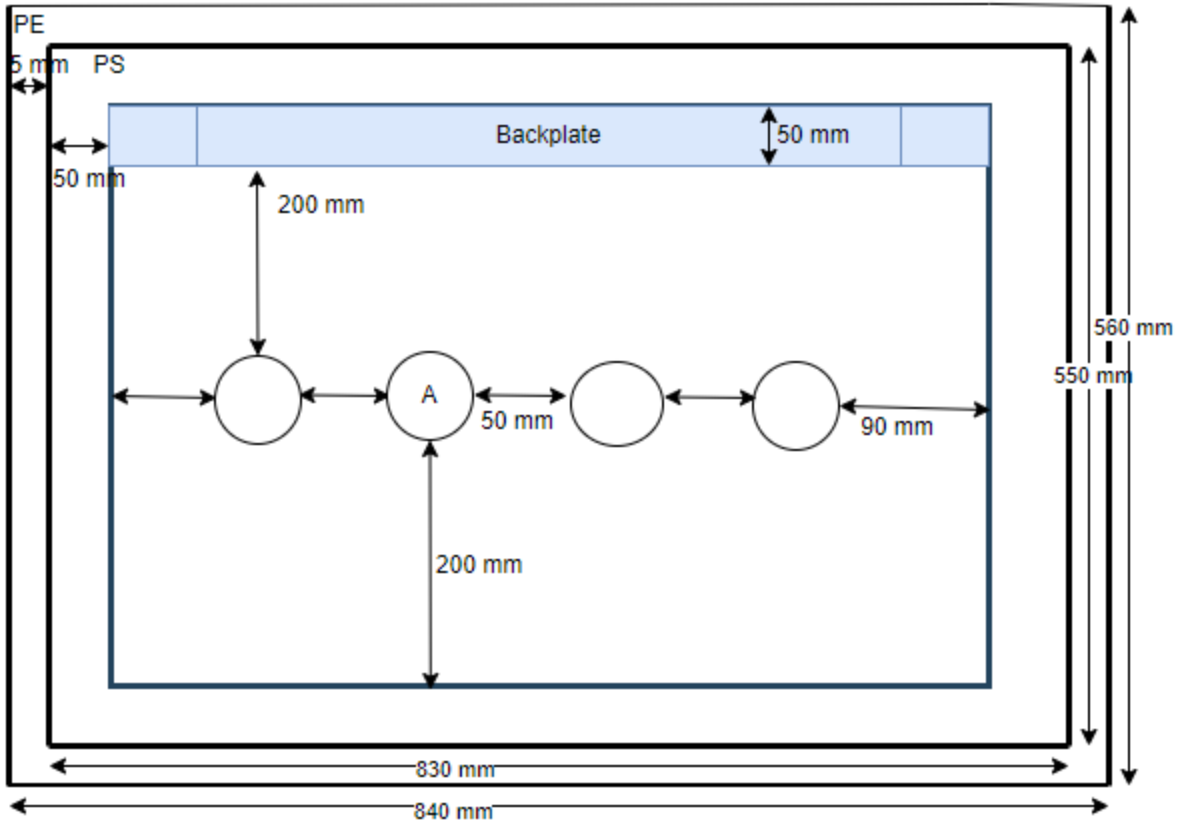


Figure B. 9: Top view of EC and its associated dimensions making use of key given in front view figure

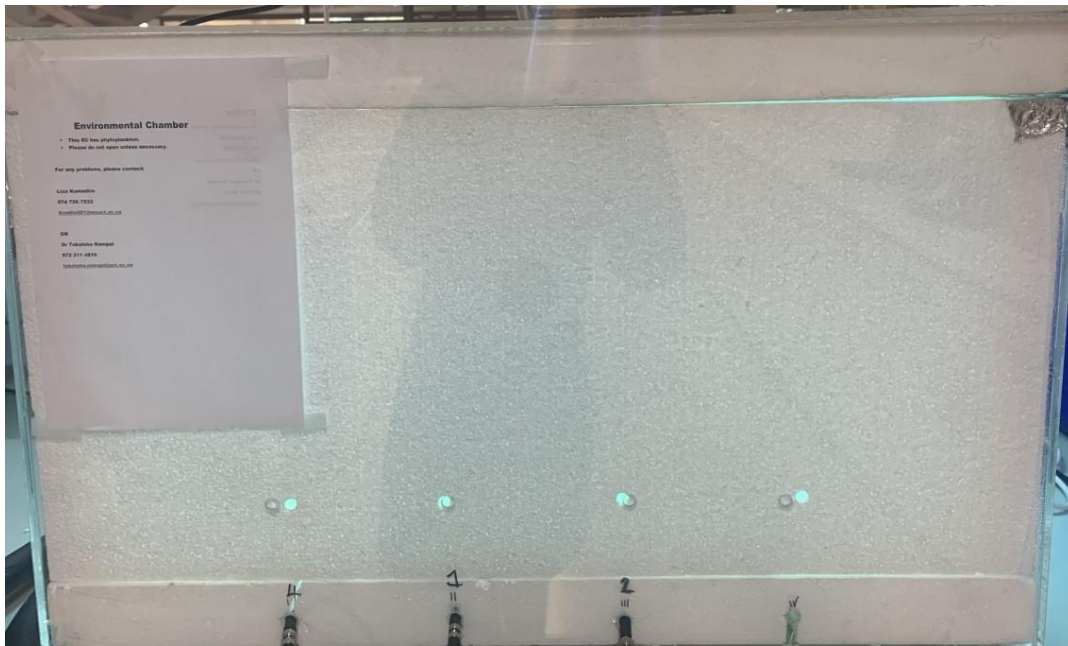


Figure B. 10: Front pictorial view of the EC



Figure B. 11: Side pictorial view of EC to show perforation.

Appendix C: Nutrient solution

Synthetic Ocean Water (SOW)

Component	Stock Solution	Quantity	Molar Concentration in Final Medium
Anhydrous Salts			
NaCl	---	24.5400 g	$4.20 \times 10^{-1} \text{ M}$
Na ₂ SO ₄	---	4.0900 g	$2.88 \times 10^{-2} \text{ M}$
KCl	---	0.7000 g	$9.39 \times 10^{-3} \text{ M}$
NaHCO ₃	---	0.2000 g	$2.38 \times 10^{-3} \text{ M}$
KBr	---	0.1000 g	$8.40 \times 10^{-4} \text{ M}$
H ₃ BO ₃	---	0.0030 g	$4.85 \times 10^{-5} \text{ M}$
NaF	---	0.0030 g	$7.15 \times 10^{-5} \text{ M}$
Hydrous Salts			
MgCl ₂ ·6H ₂ O	---	11.1000 g	$5.46 \times 10^{-2} \text{ M}$
CaCl ₂ ·2H ₂ O	---	1.5400 g	$1.05 \times 10^{-2} \text{ M}$
SrCl ₂ ·6H ₂ O	---	0.0170 g	$6.38 \times 10^{-5} \text{ M}$

Major Nutrients

The major nutrients may be prepared separately as stock solutions and 1 mL of each added to SOW to prepare 1 liter of medium. Alternatively, 10⁻³ of the stock solution may be mixed directly with the SOW salts.

Component	Stock Solution	Quantity	Molar Concentration in Final Medium
NaH ₂ PO ₄ ·H ₂ O	1.38 g L ⁻¹ dH ₂ O	1 mL	$1.00 \times 10^{-5} \text{ M}$
NaNO ₃	8.50 g L ⁻¹ dH ₂ O	1 mL	$1.00 \times 10^{-4} \text{ M}$
Na ₂ SiO ₃ ·9H ₂ O	28.40 g L ⁻¹ dH ₂ O	1 mL	$1.00 \times 10^{-4} \text{ M}$

Component	Stock Solution	Quantity	Molar Concentration in Final Medium
EDTA	---	29.200 g	$1.00 \times 10^{-4} \text{ M}$
FeCl ₃ .6H ₂ O	---	0.270 g	$1.00 \times 10^{-6} \text{ M}$
ZnSO ₄ .7H ₂ O	---	0.023 g	$7.97 \times 10^{-8} \text{ M}$
MnCl ₂ .4H ₂ O	---	0.0240 g	$1.21 \times 10^{-7} \text{ M}$
CoCl ₂ .6H ₂ O	---	0.0120 g	$5.03 \times 10^{-8} \text{ M}$
Na ₂ MoO ₄ .2H ₂ O	---	0.0242 g	$1.00 \times 10^{-7} \text{ M}$
CuSO ₄ .5H ₂ O	4.9 g L ⁻¹ dH ₂ O	1 mL	$1.96 \times 10^{-8} \text{ M}$
Na ₂ SeO ₃	1.9 g L ⁻¹ dH ₂ O	1 mL	$1.00 \times 10^{-8} \text{ M}$

Mixed Vitamin Stock Solution

To prepare, first make separate stock solutions of cyanocobalamin and biotin by dissolving the indicated amounts into 1 liter of highest quality de-ionized water (e.g., MilliQ). To prepare the mixed vitamin stock solution, begin with 950 mL of high quality de-ionized water, add 1 mL of the cyanocobalamin stock solution, 1 mL of the biotin stock solution and 100 mg of thiamine. Bring the final volume to 1 liter with de-ionized water. After completely dissolved, filter sterilize the solution and dispense into small containers (e.g., 1-10 mL aliquots) and freeze. Use 1 mL of the mixed vitamin stock solution for each liter of Aquil* medium.

Component	Stock Solution	Quantity	Molar Concentration in Final Medium
Thiamine (Vit. B ₁)	---	100 mg	$2.97 \times 10^{-7} \text{ M}$
Biotin (Vit. H)	5.0 g L ⁻¹ dH ₂ O	1 mL	$2.25 \times 10^{-9} \text{ M}$
cyanocobalamin (Vit. B ₁₂)	5.5 g L ⁻¹ dH ₂ O	1 mL	$3.70 \times 10^{-10} \text{ M}$

Appendix D: Phosphate measurement protocol

Background:

Phosphate (PO_4^{3-}) concentrations are measured colourimetrically following the method of Strickland and Parsons, 1968.

Reagents:

- 1) *Ammonium molybdate solution* – 7.5 g of analytical grade ammonium paramolybdate ($(\text{NH}_4)_6\text{Mo}_7\text{O}_{24} \cdot 4\text{H}_2\text{O}$) in 250 mL DI water. Store in a plastic bottle away from direct sunlight.
- 2) *Sulfuric acid solution* – Add 70 mL of concentrated analytical reagent grade sulphuric acid to 450 mL of DI water. Allow the solution to cool and store in a glass bottle. **Make this solution in the fume hood and add the sulphuric acid to the DI water over time, this is an exothermic reaction!**
- 3) *Ascorbic acid solution* – Dissolve 13.5 g of ascorbic acid in 250 mL of DI water. Store the solution in a plastic bottle frozen solid in the freezer. Ascorbic acid solution can only be kept at room temperature for ~ one week, discard if brown in colour.
- 4) *Potassium antimonyl-tartrate solution* – Dissolve 0.34 g of potassium antimonyl-tartrate in 250 mL DI water, warming if necessary. Store in a glass or plastic bottle.
- 5) *Mixed reagent* (enough for 100 samples) – mix together 10 mL of ammonium molybdate, 25 mL of sulphuric acid, 10 mL of ascorbic acid, and 5 mL of potassium antimonyl-tartrate. **NB:** mix the reagents together in order.
- 6) *Mother 10 mM (10000 μM) phosphate stock* – 1.3609g of Potassium phosphate monobasic salt (H_2KPO_4) in 1 L of MilliQ. Store in a 1 L glass bottle.
- 7) *Primary 50 μM phosphate standard* – 0.5ml of mother stock (10 mM) in 100 mL of DIW. Store in 250 mL glass bottle. This is to be made daily with the standards.

Collection protocol:

- 1) On the log sheet, assign each numbered centrifuge tube (50 mL; blue lids) to a corresponding depth (and Niskin bottle). Note the date, time, latitude and longitude, cast number, etc. on the log sheet. (You can use the same tube that you use for nitrite).

- 2) At the CTD, rinse each centrifuge tube three times with sample water, including the lids, and fill to the ~45 mL line with sample water. Replace the lids.
- 3) These samples should be stored in the fridge if you are going to measure them within 12 hours of collection or in the freezer at -20°C.

Analysis protocol:

- 1) Standard preparation: a new standard curve must be prepared and measured every day along with the samples. The standards are prepared as follows:
*it is better to use the same pipette for all standards if possible

- a) Using the 50 µM primary phosphate standard, prepare eight phosphate standards via dilution with Milli-Q water using 50 mL glass volumetric flasks. The table below indicates the volumes of mother stock that should be added (using the *correct*) pipettes to make the standards.
- b) Rinse the pipette tips three times in Milli-Q and once with mother stock. Pipette the desired volume of primary standard into each volumetric flask and then fill to the line with Milli-Q. Even though the volumetric flasks should be rinsed with Milli-Q after analysis, you should still use the same volumetric flask for the same concentration standard each day. Shake the flasks well.

Table D. 1: Phosphate concentrations and appropriate volumes used

Secondary standard concentration (µM)	PO ₄ ³⁻	Volume of primary PO ₄ ³⁻ standard (mL) – 50 mL	Pipette to use (for 50ml volumetric)
0		0	-
0.25		0.25	100-1000 µl
0.5		0.5	100-1000 µl
0.75		0.75	100-1000 µl
1.0		1.0	100-1000 µl
1.5		1.5	100-1000 µl
2.0		2.0	500-5000 µl
3		3	500-5000 µl

2. Sample preparation: Absorption measurement.

- a) Transfer 5 mL of each standard, blank and samples into individually labelled test tube using a 5 mL pipette (remember to make duplicates). Ensure you rinse the pipette three times with Milli Q between samples and shake the centrifuge tubes vigorously before decanting the sample.
- b) Add 0.5 mL of mixed reagent into each test tube and vortex.
- c) Allow to react for a minimum of 5 minutes and a maximum of 2-3 hours.
- d) Zero the spectrophotometer with a test tube filled only with DI water (no added reagent).
- e) Read the absorbances at 885 nm. Each standard (and blank) should be measured three times. Record the absorbances in the log sheet.

Note: Turn the spectrophotometer on 30 minutes before you start measuring to allow the bulb to heat up.

Appendix E: Phytoplankton based experiments

Experiments carried out at 8°C

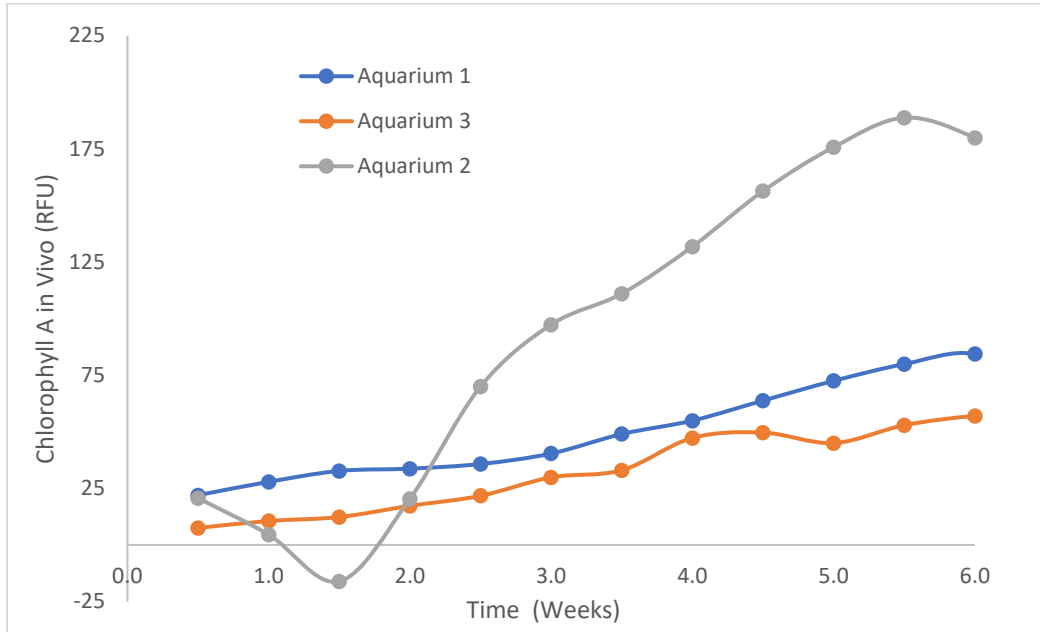


Figure E. 1: Chlorophyll A in Vivo for experiments carried out at 8°C for an irradiance of 0 $\mu\text{mol}/\text{m}^2/\text{s}$

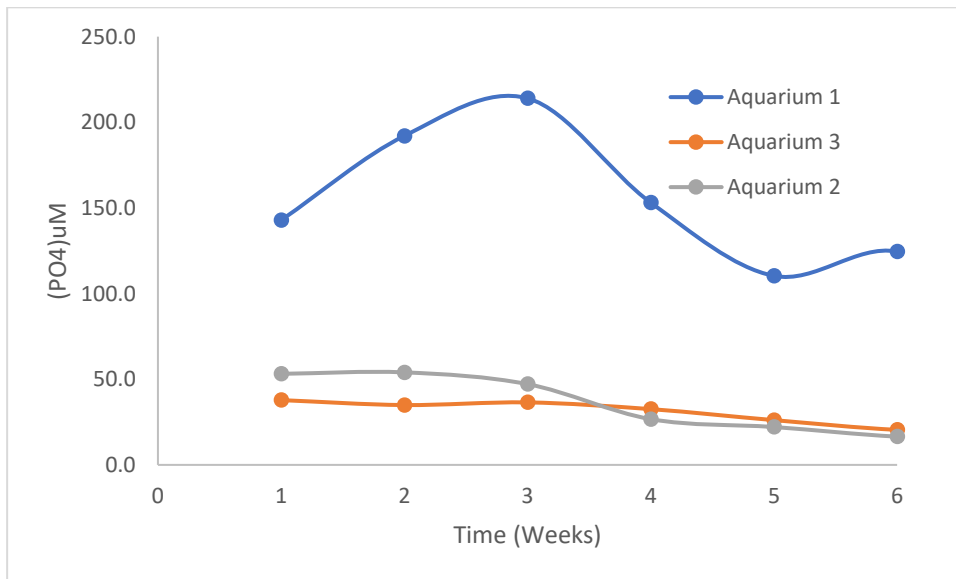


Figure E. 2: Phosphate measurements for experimentation at 8°C with an irradiance of 0 $\mu\text{mol}/\text{m}^2/\text{s}$

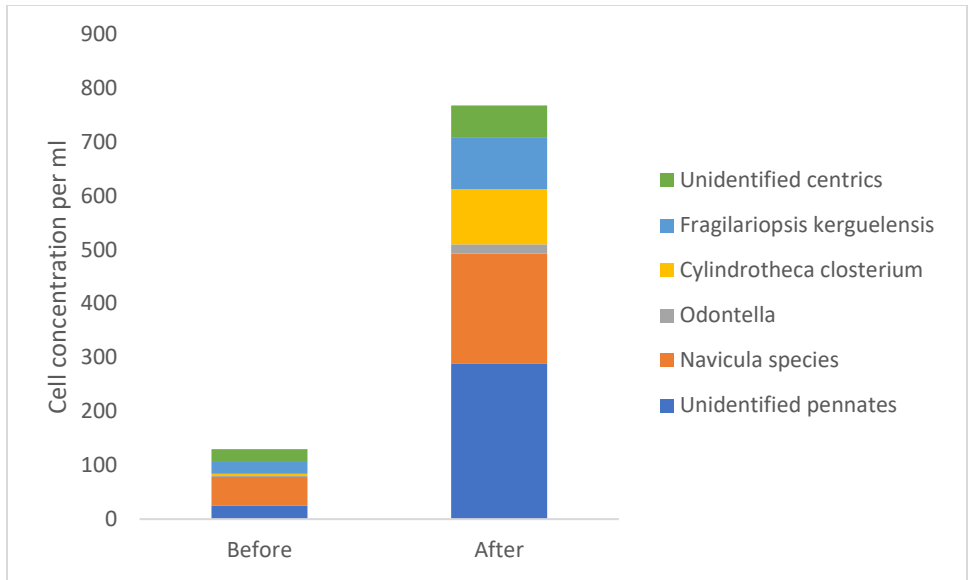


Figure E. 3: Cell concentration per ml before and after experimentation for aquarium 1 at 8°C and with an irradiance of 0 $\mu\text{mol}/\text{m}^2/\text{s}$

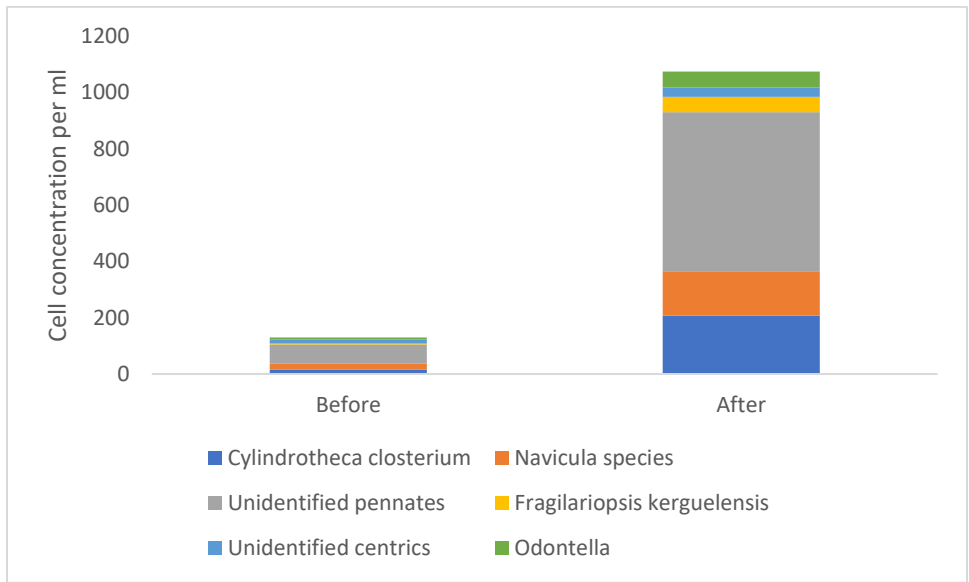


Figure E. 4: Cell concentration per ml before and after experimentation for aquarium 2 at 8°C and with an irradiance of 0 $\mu\text{mol}/\text{m}^2/\text{s}$

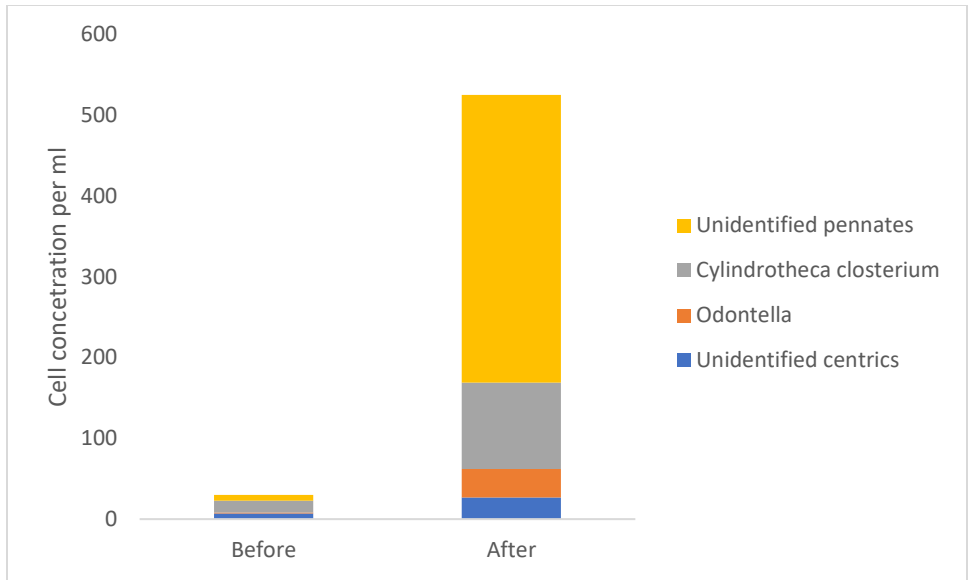


Figure E. 5: Cell concentration per ml before and after experimentation for aquarium 3 at 8°C and with an irradiance of 0 $\mu\text{mol}/\text{m}^2/\text{s}$

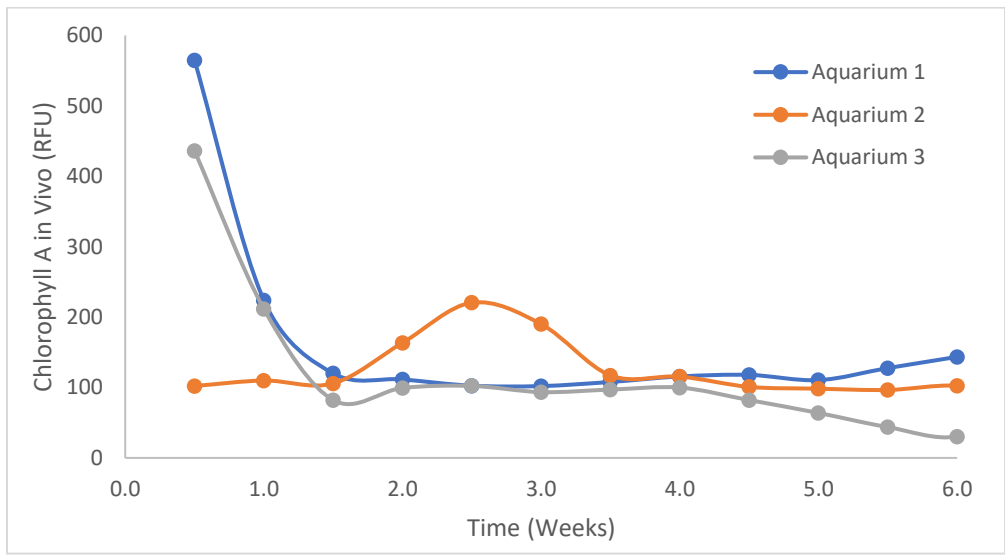


Figure E. 6: Chlorophyll A in Vivo for experiments carried out at 8°C for an irradiance of 42 $\mu\text{mol}/\text{m}^2/\text{s}$

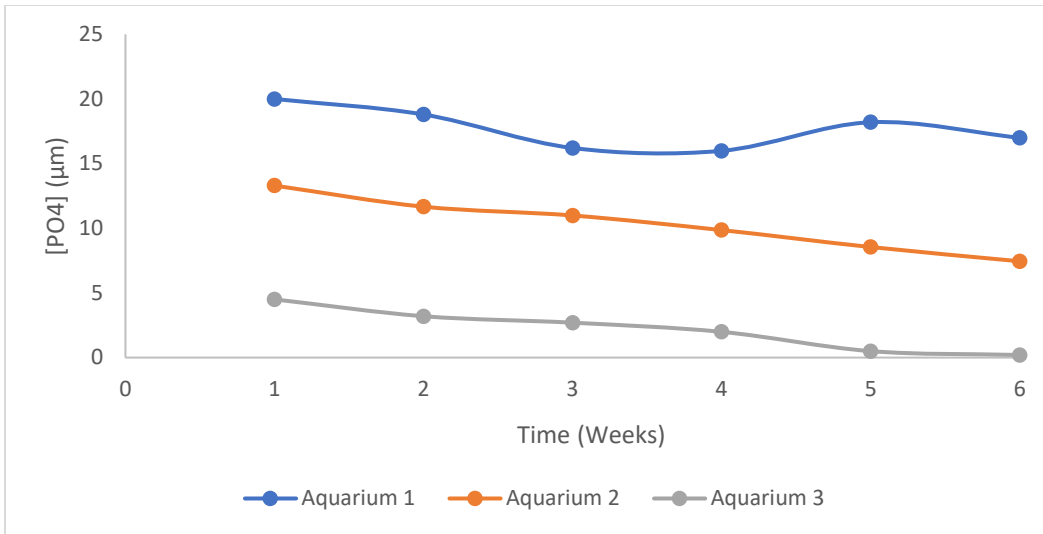


Figure E. 7: Phosphate measurements for experimentation at 8°C with an irradiance of 42 μmol/m²/s

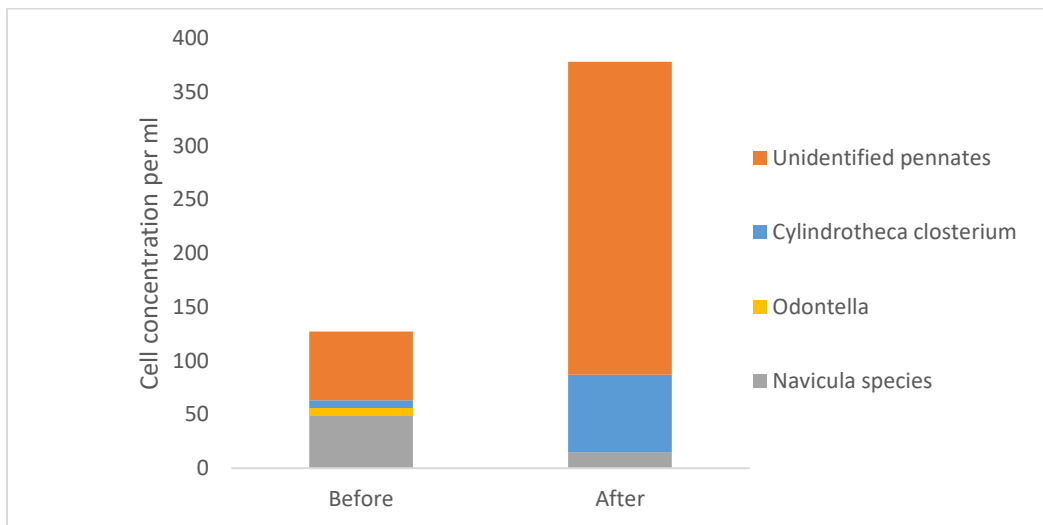


Figure E. 8: Cell concentration per ml before and after experimentation for aquarium 1 at 8°C and with an irradiance of 42 μmol/m²/s

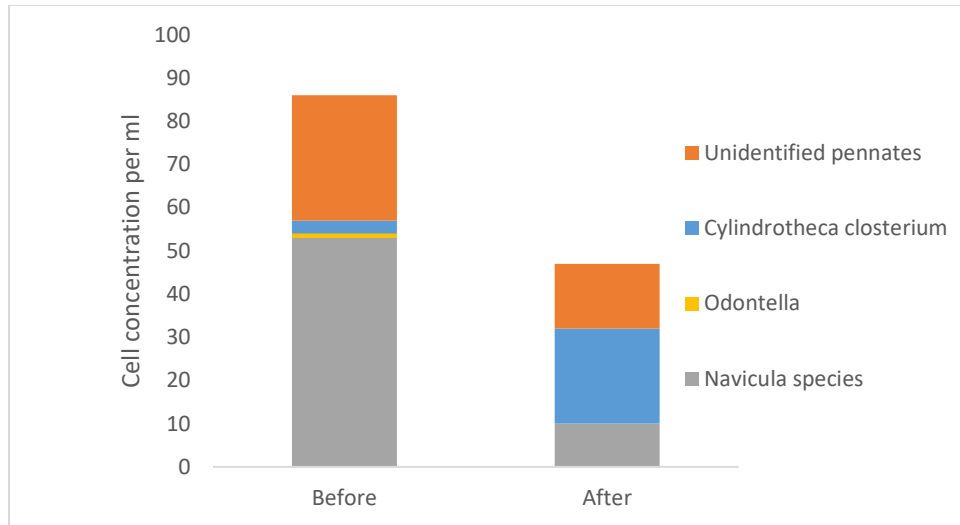


Figure E. 9: Cell concentration per ml before and after experimentation for aquarium 2 at 8°C and with an irradiance of 42 $\mu\text{mol}/\text{m}^2/\text{s}$

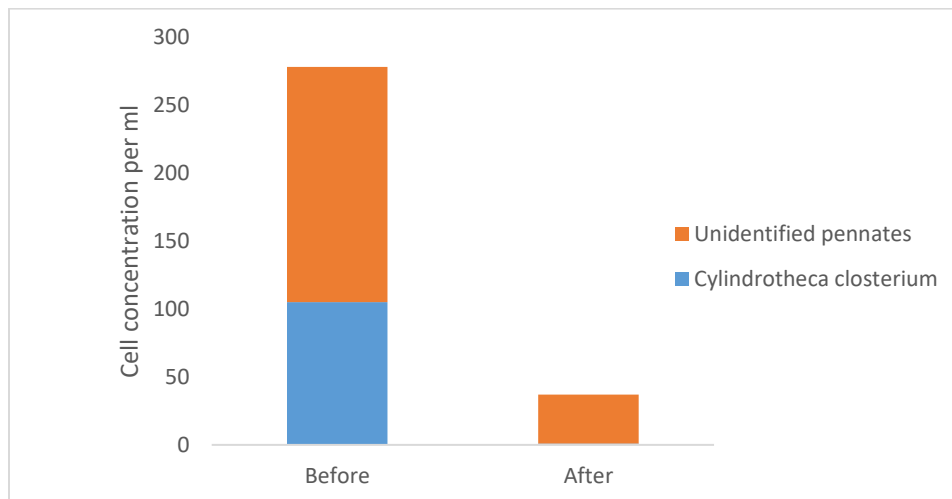


Figure E. 10: Cell concentration per ml before and after experimentation for aquarium 3 at 8°C and with an irradiance of 42 $\mu\text{mol}/\text{m}^2/\text{s}$

Experiments carried out at 5°C

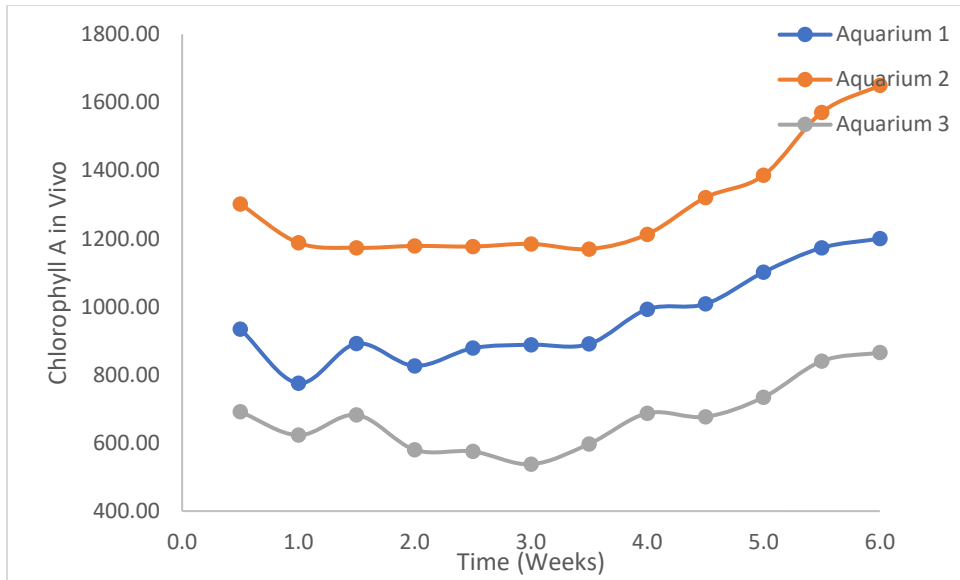


Figure E. 11: Chlorophyll A in Vivo for experiments carried out at 5°C for an irradiance of 0 $\mu\text{mol}/\text{m}^2/\text{s}$

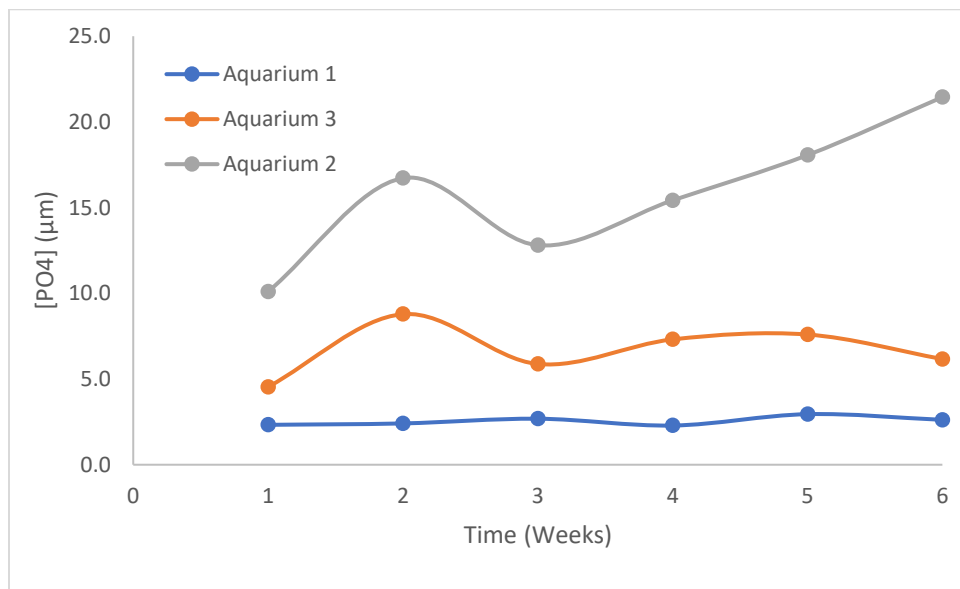


Figure E. 12: Phosphate measurements for experimentation at 5°C with an irradiance of 0 $\mu\text{mol}/\text{m}^2/\text{s}$

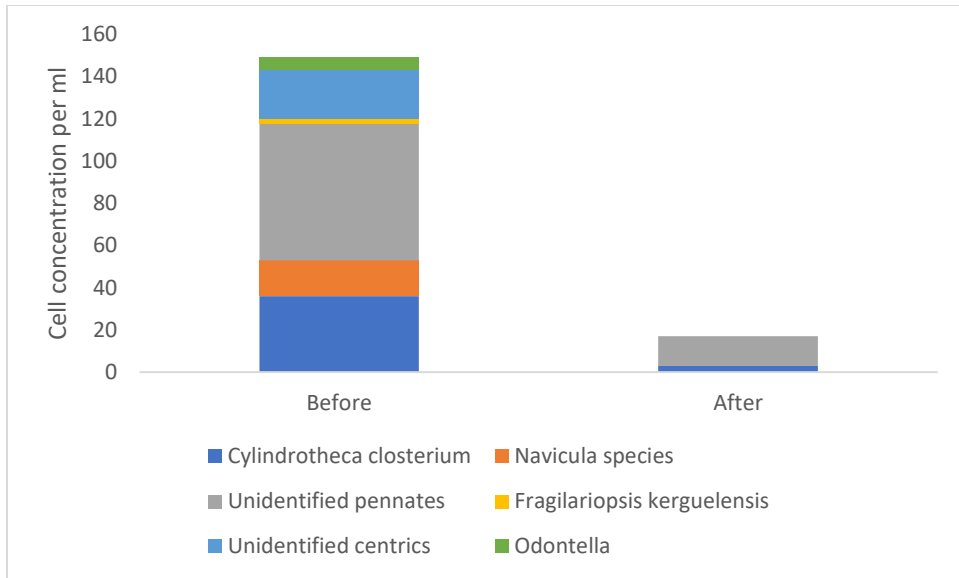


Figure E. 13: Cell concentration per ml before and after experimentation for aquarium 1 at 5°C and with an irradiance of 0 $\mu\text{mol}/\text{m}^2/\text{s}$

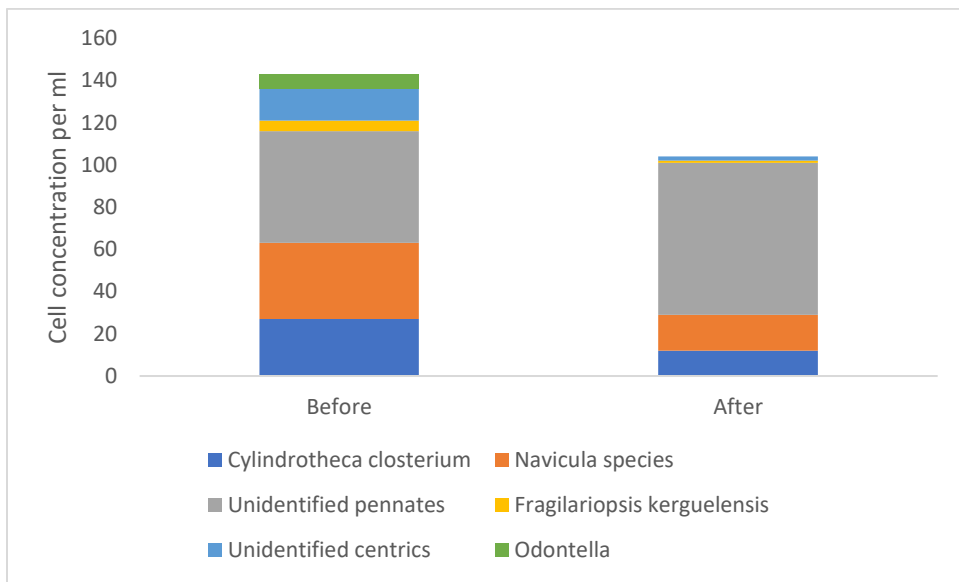


Figure E. 14: Cell concentration per ml before and after experimentation for aquarium 2 at 5°C and with an irradiance of 0 $\mu\text{mol}/\text{m}^2/\text{s}$

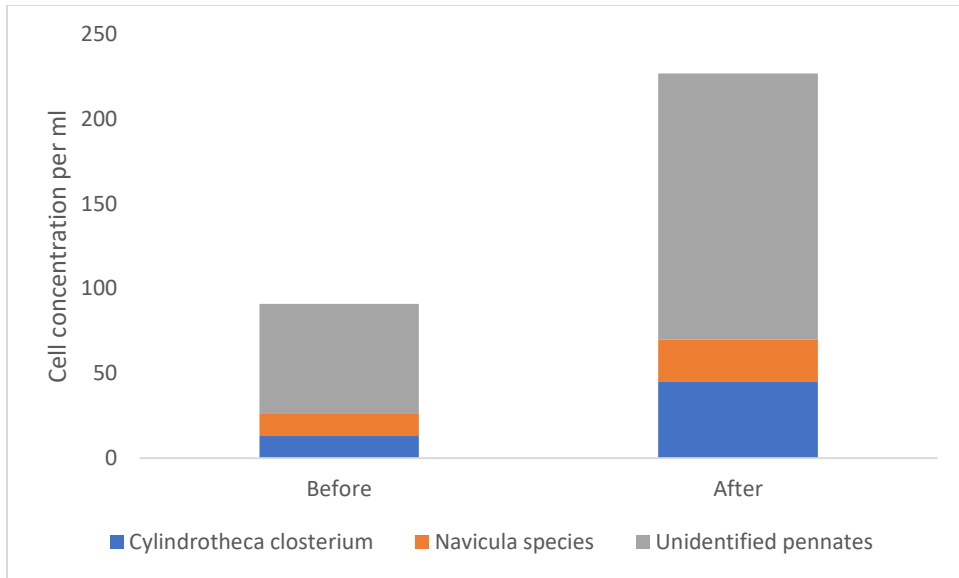


Figure E. 15: Cell concentration per ml before and after experimentation for aquarium 3 at 5°C and with an irradiance of 0 $\mu\text{mol}/\text{m}^2/\text{s}$

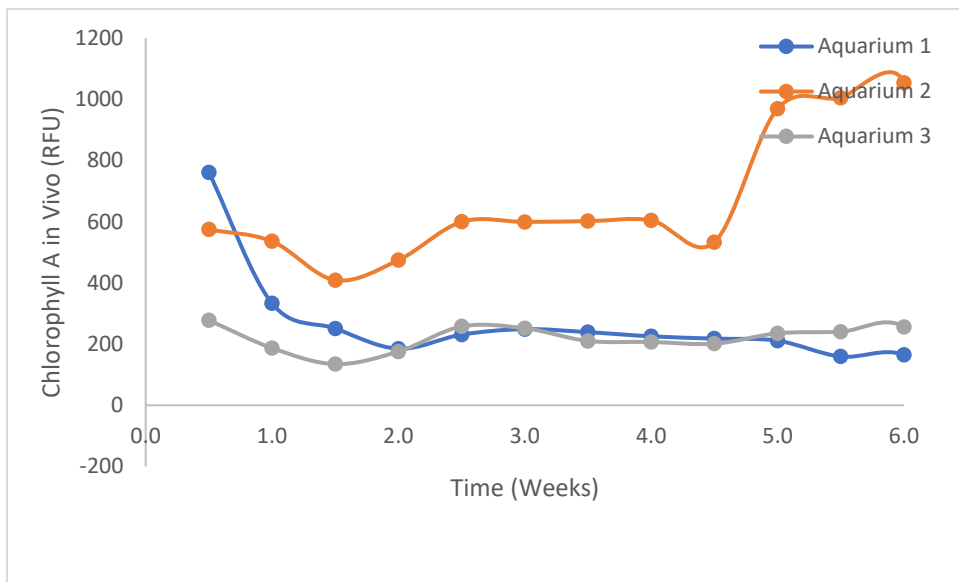


Figure E. 16: Chlorophyll A in Vivo for experiments carried out at 5°C for an irradiance of 42 $\mu\text{mol}/\text{m}^2/\text{s}$

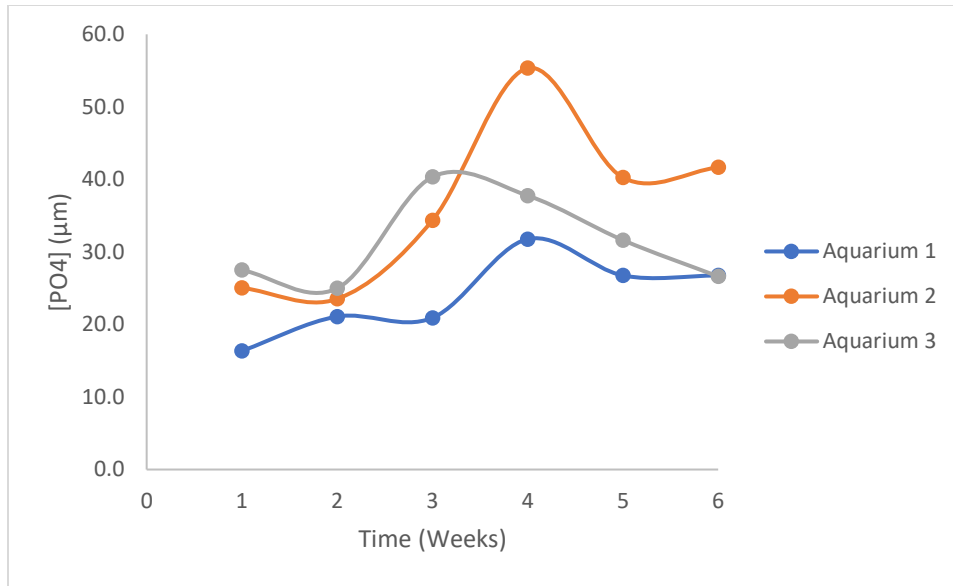


Figure E. 17: Phosphate measurements for experimentation at 5°C with an irradiance of 42 µmol/m²/s

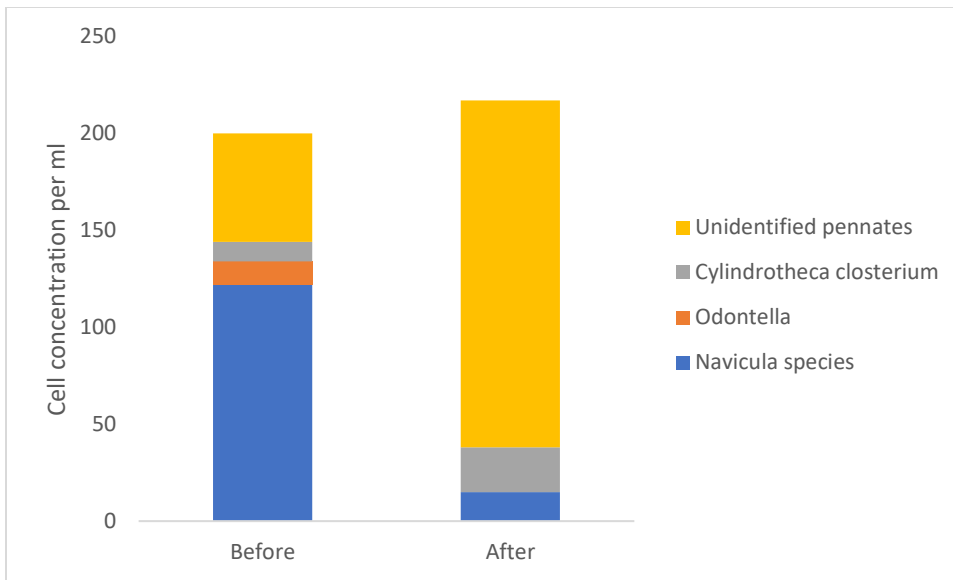


Figure E. 18: Cell concentration per ml before and after experimentation for aquarium 1 at 5°C and with an irradiance of 42 µmol/m²/s

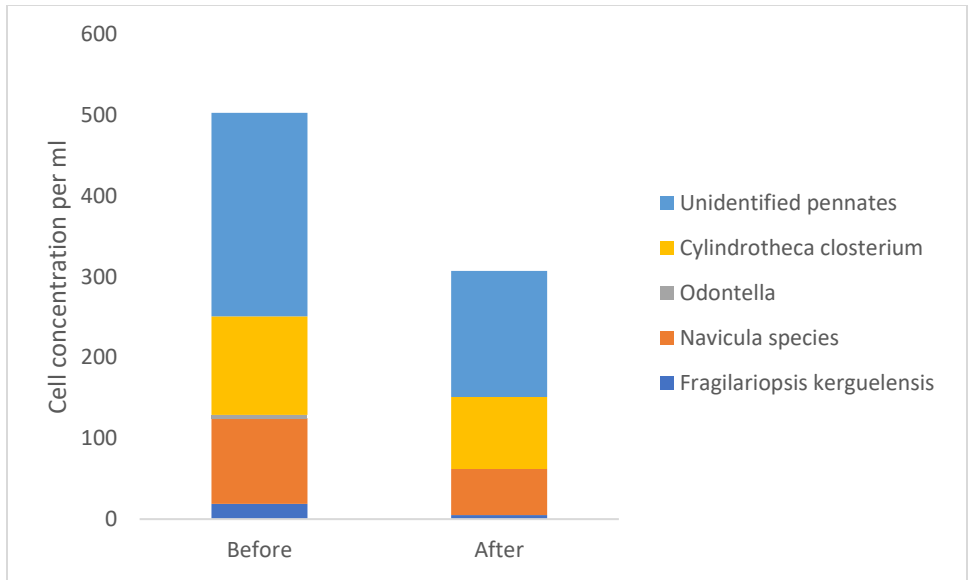


Figure E. 19: Cell concentration per ml before and after experimentation for aquarium 2 at 5°C and with an irradiance of 42 $\mu\text{mol}/\text{m}^2/\text{s}$

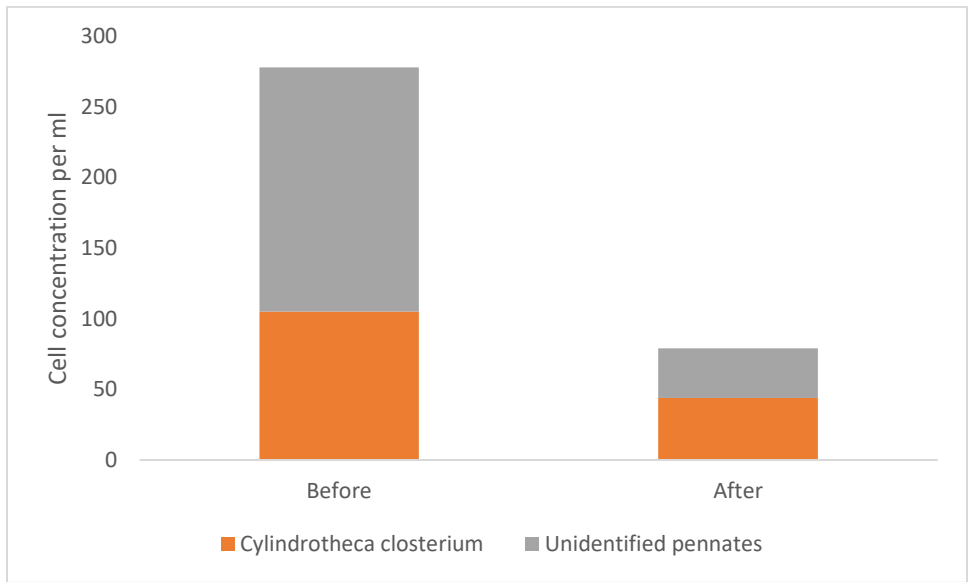


Figure E. 20: Cell concentration per ml before and after experimentation for aquarium 3 at 5°C and with an irradiance of 42 $\mu\text{mol}/\text{m}^2/\text{s}$

ETHICS APPLICATION FORM

Please Note:

Any person planning to undertake research in the Faculty of Engineering and the Built Environment (EBE) at the University of Cape Town is required to complete this form before collecting or analysing data. The objective of submitting this application prior to embarking on research is to ensure that the highest ethical standards in research, conducted under the auspices of the EBE Faculty, are met. Please ensure that you have read, and understood the EBE Ethics in Research Handbook (available from the UCT EBE, Research Ethics website) prior to completing this application form: <http://www.ebe.uct.ac.za/eberesearchethics/>

APPLICANT'S DETAILS	
Name of principal researcher, student or external applicant	
Department	
Preferred email address of applicant:	
If Student	Your Degree: e.g., MSc, PhD, etc.
	Credit Value of Research: e.g., 60/120/180/240 etc.
	Name of Supervisor (if supervised):
If this is a research contract, indicate the source of funding/sponsorship	
Project Title	

I hereby undertake to carry out my research in such a way that:

- there is no apparent legal objection to the nature or the method of research; and
- the research will not compromise staff or students or the other responsibilities of the University;
- the stated objective will be achieved, and the findings will have a high degree of validity;
- limitations and alternative interpretations will be considered;
- the findings could be subject to peer review and publicly available; and
- I will comply with the conventions of copyright and avoid any practice that would constitute plagiarism.

APPLICATION BY	Full name	Signature	Date
Principal Researcher/ Student/External applicant	Lisa T. Kumadino		14/01/2020

SUPPORTED BY	Full name	Signature	Date
Supervisor (where applicable)	Tobaloba Rumpai		17/01/2021

APPROVED BY	Full name	Signature	Date
HOD (or delegated nominee) Final authority for all applicants who have answered NO to all questions in Section 1; and for all Undergraduate research (Including Honours).	Elaine Opitz		14/06/2021
Chair: Faculty EIR Committee For applicants other than undergraduates students who have answered YES to any of the questions in Section 1.			